UNIVERSITY OF HAWAII
LIBRARY
APR 14 '61

Journal of MOLECULAR BIOLOGY

EDITOR-IN-CHIEF: J. C. KENDREW

Volume III, Number 1, February 1961

ACADEMIC PRESS LTD., LONDON
ACADEMIC PRESS INC., NEW YORK

JOURNAL OF MOLECULAR BIOLOGY

EDITOR-IN-CHIEF

J. C. KENDREW, Peterhouse, Cambridge, England

EDITORIAL BOARD

P. DOTY, Department of Chemistry, Harvard University, Cambridge, Mass., U.S.A.
A. F. HUXLEY, Department of Physiology, University College, London, England.
R. L. SINSHEIMER, Division of Biology, California Institute of Technology, Pasadena, Cal., U.S.A.
J. D. WATSON, Biological Laboratories, Harvard University, Cambridge, Mass., U.S.A.
M. H. F. WILKINS, Physics Department, King's College, London, England.

ADVISORY BOARD

S. BENZER, Purdue University, U.S.A.
M. CALVIN, University of California, Berkeley, U.S.A.
F. H. C. CRICK, University of Cambridge, England.
J. F. DANIELLI, King's College, London, England.
A. ENGSTRÖM, Karolinska Institutet, Stockholm, Sweden.
A. D. HERSHEY, Carnegie Institute, Cold Spring Harbor, U.S.A.
F. JACOB, Pasteur Institute, Paris, France.
A. KORNBERG, Stanford University, Stanford, California, U.S.A.
C. LEVINTHAL, Massachusetts Institute of Technology, Cambridge, Mass., U.S.A.
S. E. LURIA, Massachusetts Institute of Technology, Cambridge, Mass., U.S.A.
D. MAZIA, University of California, Berkeley, U.S.A.
P. B. MEDAWAR, University College, London, England.
L. E. ORGEL, University of Cambridge, England.
M. F. PERUTZ, University of Cambridge, England.
R. D. PRESTON, University of Leeds, England.
G. N. RAMACHANDRAN, University of Madras, India.
A. RICH, Massachusetts Institute of Technology, Cambridge, Mass., U.S.A.
G. SCHRAMM, Max-Planck Institut, Tübingen, Germany.
F. S. SJØSTRAND, Karolinska Institutet, Stockholm, Sweden.
I. WATANABE, Institute for Virus Research, Kyoto University, Japan.
R. C. WILLIAMS, University of California, Berkeley, U.S.A.

Published by Academic Press Inc. (London) Limited

Volume III, 1961: 128*s.* 6*d.* ($18.00)

Subscription orders should be sent to Academic Press Inc. (London) Limited, 17 Old Queen Street, London, S.W.1, with the exception of those originating in the U.S.A., Canada, Central America, and South America; these should be sent to Academic Press Inc., 111 Fifth Avenue, New York 3, N.Y.

Copyright © 1961, by Academic Press Inc. (London) Limited

F00659

J. Mol. Biol. (1961) **3**, 1–10

5857-32
QH301
J73
V. 3

Correlation of Structure with Function in *Spinacea oleracea* Chloroplasts†

Roderic B. Park and Ning G. Pon

Lawrence Radiation Laboratory and Department of Chemistry, University of California, Berkeley, California, U.S.A.

(*Received 16 July 1960*)

Spinach chloroplasts, isolated in isotonic sucrose medium, were sonically ruptured and separated by differential centrifugation into three main fractions: a green precipitate, a colourless supernatant and a yellow, low density lipid-containing layer. These fractions were analyzed for their physical, chemical and biochemical properties.

Comparison of a thin section of an isolated osmium-stained chloroplast with a thin section of osmium-stained green precipitate, by electron microscopy, shows that the particles in the green precipitate correspond both in thickness and lateral dimensions to the lamellar structure of the isolated chloroplast. Heavy metal shadowing of both air-dried and lyophilized green precipitate demonstrates the presence of lamellar structures from 10,000 to 20,000 Å in diameter. The lamellar structure, totaling 160 Å in thickness, is composed of two layers; each layer is made up of granular subunits 100 Å thick. Chlorophyll to nitrogen weight ratios are fairly constant for green lamellar structures from 800 to 20,000 Å in diameter, indicating that chlorophyll is uniformly distributed throughout the lamellar structure of the chloroplast. The similarity of relative photosynthetic pigment concentrations over the visible region, of the Hill reaction activity and of the carbon dioxide fixation capacities for the various sized particles in the green precipitate suggests that the smallest lamellar fragments used in these experiments are large in comparison with the smallest fragment which converts electromagnetic to chemical energy. A model for chloroplast lamellar structure is proposed on the basis of the results obtained.

The supernatant, by electron microscopy, is seen to consist principally of oblately spherical particles, 100 Å thick and 200 Å in diameter. These particles are indistinguishable from the main water-soluble protein of the chloroplast with sedimentation coefficient 16 (Fraction I protein). About 90% of the total carboxydismutase activity is associated with the supernatant proteins. In addition, these proteins are able to convert fructose-6-phosphate into other photosynthetic carbon cycle intermediates. This supernatant must be added to the green precipitate in order to obtain maximum carbon dioxide fixation rates.

Electron micrographs of unfractionated osmium-fixed chloroplast sonicate show large osmium-stained spherical objects corresponding in size and staining properties to the osmiophyllic granules observed in thin sections of osmium-stained chloroplast in the intact leaf. Similar granules, 500 to 1500 Å in diameter, were obtained when the yellow, low density lipid layer was fixed with osmium and then shadowed.

1. Introduction

Green plant photosynthesis is generally considered to consist of two component processes, light reactions and dark reactions. The light reactions convert electromagnetic energy into chemical potential necessary for oxygen production, reduction

†The work described in this paper was sponsored by the United States Atomic Energy Commission.

of CO_2 and formation of adenosine triphosphate (ATP). The dark reactions fix CO_2 and regenerate CO_2 acceptor from the first products of photosynthesis. Studies on isolated chloroplasts have shown that both the light and dark reactions of photosynthesis in higher plants are associated with this cytoplasmic plastid (Arnon, Whatley & Allen, 1954). Trebst, Tsujimoto & Arnon (1958) first showed that it was possible to fractionate isolated chloroplasts in such a way that the light and dark reactions of photosynthesis became physically separated. Trebst found that the colourless supernatant obtained by centrifuging osmotically swollen spinach chloroplasts carried out the dark reactions of photosynthesis, CO_2 fixation and regeneration of CO_2 acceptor from photosynthetic products. The green precipitate obtained from the centrifugation carried out the light reactions of photosynthesis, production of oxygen, reducing power and ATP. The physical separation of the two major series of photosynthetic reactions obtained by Trebst suggests the possibility of correlating the chemical, physical and enzymatic properties of the separated particles with structures observed by electron microscopy of an intact chloroplast.

Spinacea oleracea leaves were washed with cold tap water and allowed to drain as completely as possible. All operations were carried out at, or near, 0°C. Leaves (125 g) were homogenized in 250 ml. of 0·5 M-sucrose, 0·1 M-potassium phosphate buffer, pH 7·4, and 0·01 M-versenol titrated to pH 7·4, in a blender operated at full speed for 30 sec. The green homogenate was filtered through 8 layers of cheesecloth.

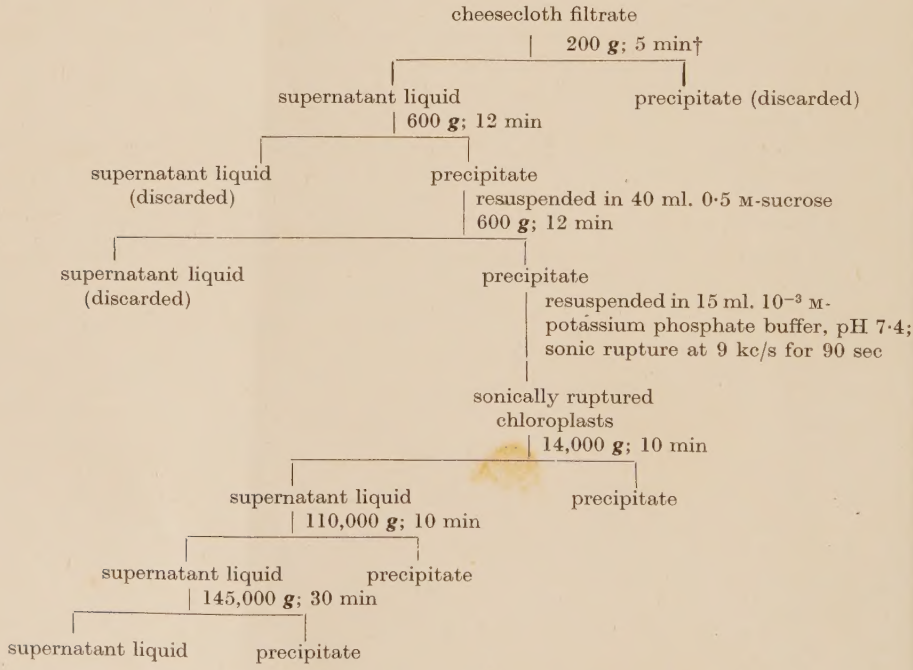

FIG. 1. Typical flow sheet for the preparation of chloroplast fragments.
†The accelerations due to gravity (*g*) are maximum values.

Such a correlation study would require a wide size spectrum of chloroplast particles from very simple units to the more complex structure. Recent work in this laboratory showed that sonic rupture of isolated spinach chloroplasts produces a photosynthetic system in which $^{14}CO_2$ fixation rates are comparable to the CO_2 fixation rates for

intact chloroplasts on a unit chlorophyll basis (Park, Pon, Louwrier & Calvin, 1960). A wide spectrum of particle sizes is present in this sonically ruptured system. By observing the chemical, enzymatic, centrifugal and electron microscopic properties of the various types of particles separated from a sonically ruptured suspension of spinach chloroplasts, we are now able to attribute specific functions and chemical properties to some of the structures seen in an electron micrograph of a thin section of spinach chloroplasts.

2. Experimental

(a) *Preparation of chloroplasts and chloroplast fragments*

Chloroplasts were isolated from *Spinacea oleracea* leaves using a method similar to that of Holm-Hansen, Pon, Nichida, Moses & Calvin (1959). The precipitated whole chloroplasts obtained by this procedure were resuspended in 10^{-3} M-potassium phosphate buffer pH 7·4. This suspension was sonically ruptured for 90 sec in a 9 kc/s Raytheon 100 watt magnetostriction oscillator operated at full voltage. Following sonication the fragmented chloroplasts were subjected to fractional centrifugation. This general scheme is outlined in Fig. 1.

(b) *Enzyme assays*

The organic cofactors and metal cofactors used in the photosynthetic reactions were prepared separately from one another and titrated to pH 7·4 (see Table 1). The photo-

TABLE 1

Reaction mixture used for studying $^{14}CO_2$ fixation by chloroplast fragments

Compound	μM	Compound	μM
$MgSO_4$	4·0	Thiamine pyrophosphate	1·4
$MnCl_2$	1·6	Ascorbate	2·5
Adenosine diphosphate	1·0	$NaH^{14}CO_3$	4·0 (100 μc)
Triphosphopyridine nucleotide	0·02	Glutathione	1·3
Diphosphopyridine nucleotide	0·2	Phosphate (pH 7·4)	1·0

Each flask contained 1 mg of chlorophyll as chloroplast material in 1·2 ml. total volume. Incubation time: 30 min at 24°C.

synthetic reactions were run at 24°C at a light intensity of 1000 ft candles in airtight 35 ml. flasks. The total reaction mixture volume was about 1·2 ml. and contained about 1 mg of chlorophyll. After 30 min incubation, the enzymatic reaction was stopped by adding 4 ml. ethanol to the reaction mixture. The precipitate was then extracted with 20% ethanol, 100% ethanol and water. The extracts were pooled. A small portion was acidified and placed on an aluminum planchet for assay of the total radioactivity in the reaction mixture. Another portion was applied to the origin of a paper chromatogram. Two-dimensional chromatography of the photosynthetic products and counting of the radioactive areas on the chromatograms was carried out according to the methods described by Bassham & Calvin (1957).

The carboxydismutase assay used in these experiments is described by Park *et al.* (1960).

(c) *Ultracentrifugal analysis*

The sedimentation rates of Fraction I protein were studied in a Spinco ultracentrifuge model E (serial number 1). The Fraction I protein was dissolved in pH 7·25 potassium maleate buffer, ionic strength 0·2, at a concentration of 10 mg/ml. Centrifugation was performed at 49,330 rev/min at an average temperature of 17·4°C. In the Fraction I run, the calculation of $S_{20,w}$ (the sedimentation coefficient in water at 20°C) from S_{obs} (the observed sedimentation coefficient) was made by using the specific viscosity of sodium succinate and density of potassium tartrate, respectively.

(d) *Nitrogen analysis*

Nitrogen was determined according to the usual Kjeldahl method except that $SeOCl_2$ was used as a catalyst instead of $HgSO_4$. The reproducibility of the method was tested on plant tissues by digesting the algae, *Chlorella pyrenoidosa* and *Scenedesmus obliquus*, under a variety of conditions, e.g. varying amounts of digestion mixture and varying digestion times. The results of this test showed that the method was reproducible to within $\pm$ 0·3%.

(e) *Chlorophyll analysis*

Chlorophyll concentrations were determined spectrophotometrically in 80% acetone according to the method of Arnon (1949).

(f) *Electron microscopy*

The electron microscopic observations were performed with an RCA EMU-2 instrument. The sectioned material was fixed and embedded according to the methods outlined by Farquhar (1950). Shadowing for particle work was done with a gold, palladium and platinum alloy, or nichrome wire from a tungsten filament at a pressure of less than 0·1 μ. The frozen dried specimens were prepared following the procedure of Williams (1953).

3. Results and Discussion

Leyon (1954), Steinmann & Sjostrand (1955), von Wettstein (1958), Hodge (1959) and others have used electron microscopic observations to describe the principal features of higher plant chloroplast structure. Electron microscopic observations of osmium-stained chloroplast-containing material have shown that the plastid is surrounded by an outer membrane. Within the chloroplast membrane there is a series of lamellar structures. Thickened areas on the lamellae are called grana, while the structures surrounding the grana are called stroma. Heavily stained spherical objects 500 Å to 1500 Å in diameter are also seen in thin sections of chloroplast material. These structures have been termed "osmiophyllic granules" in the literature (Leyon (1954)).

The principal features of chloroplast structure described above are seen in the electron micrographs of spinach chloroplasts shown in Plates III and IV. The tissues in Plates III and IV were fixed at 0°C for 30 min in buffered 2% osmium tetroxide and 0·5% potassium permanganate respectively. It is seen that the dimensions of the structures within chloroplasts as viewed in the electron microscope are quite dependent on the fixation method used. The dimensions used in this paper are taken primarily from the permanganate-fixed material since this tissue is relatively less disrupted than that fixed in osmium.

Our experiments were designed to obtain direct evidence for the functions and chemistry of the chloroplast structures described above and shown in Plates III and IV.

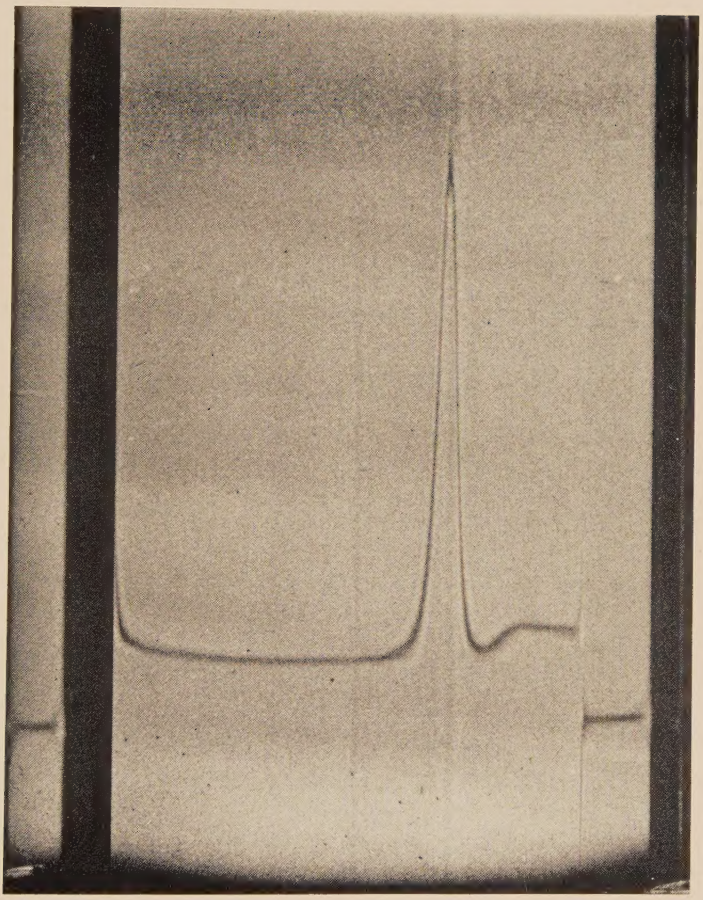

PLATE I. Schlieren pattern of Fraction I protein ($S_{20,w} = 16$) in Spinco model E ultracentrifuge. Sedimentation is from right to left.

[*To face page* 4

(a)

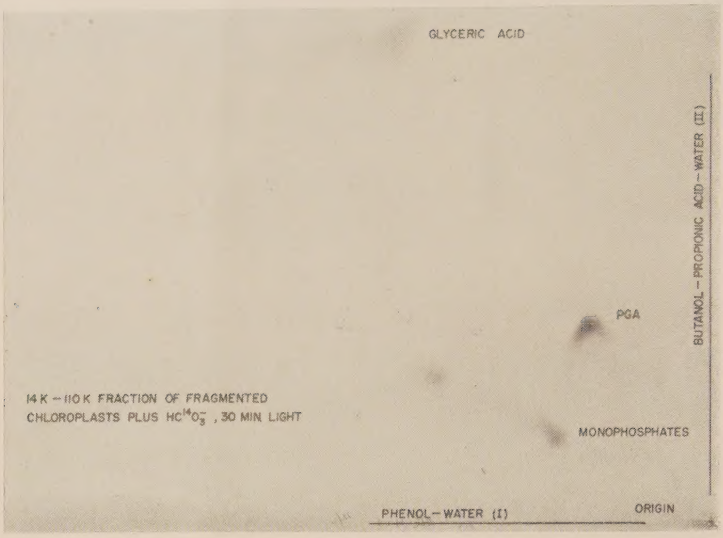

(b)

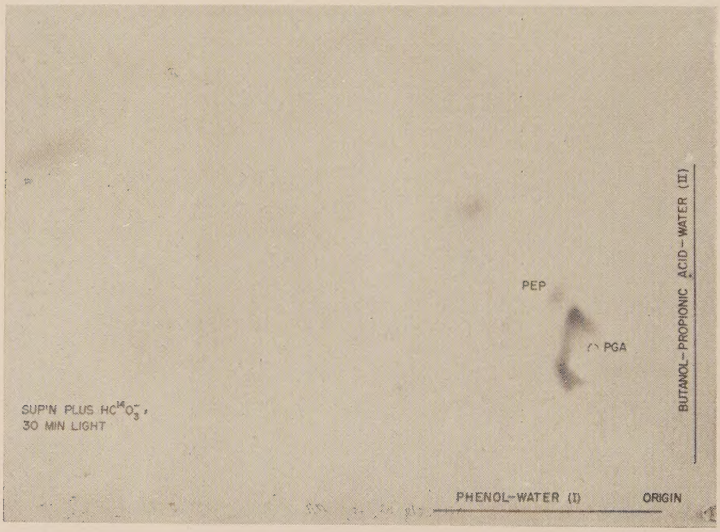

(c)

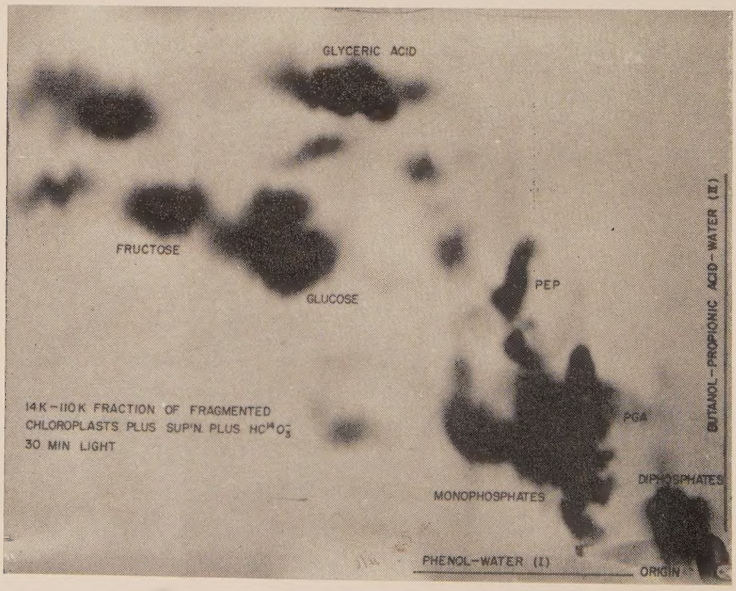

PLATE II. Comparison among the products of $^{14}CO_2$ fixation by green precipitate, supernatant and green precipitate plus supernatant in light.

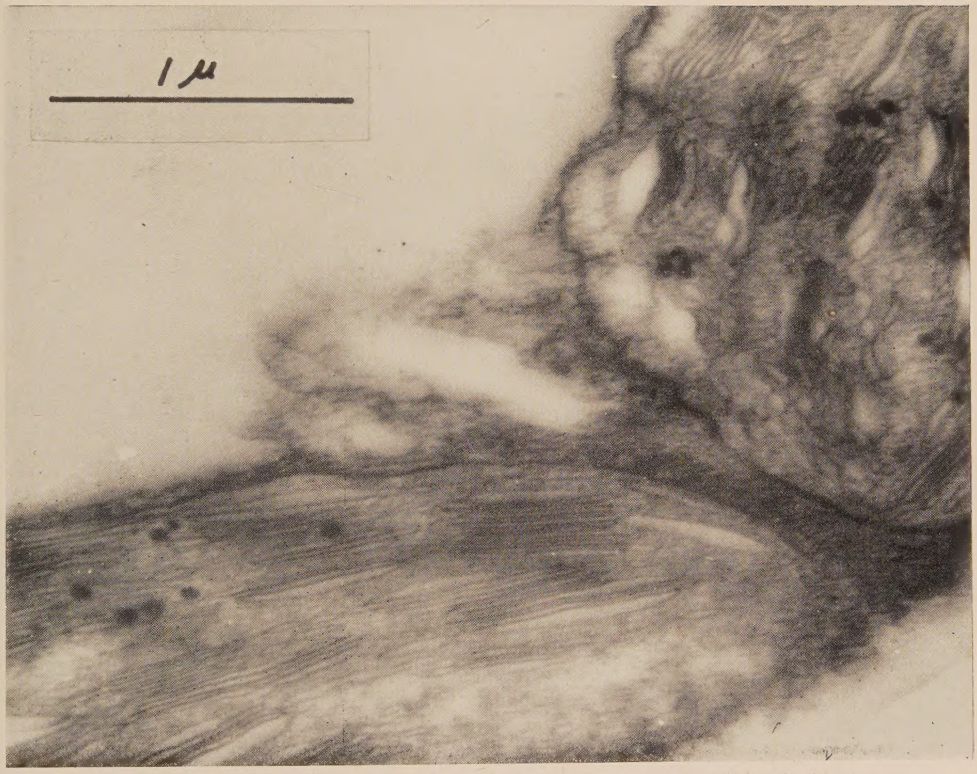

PLATE III. Thin section of spinach leaf showing chloroplasts. Fixed in buffered 2% OsO_4.

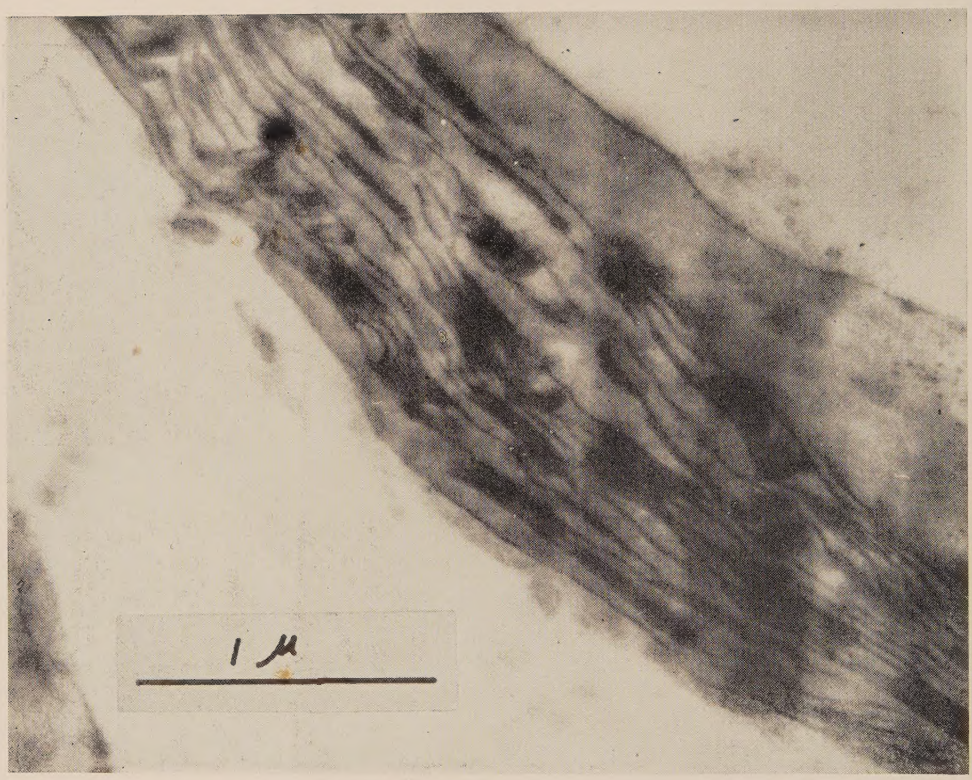

PLATE IV. Thin section of spinach leaf showing chloroplasts. Fixed in 0·5% $KMnO_4$.

PLATE V. Comparison between thin sections of buffered 2% osmium fixed (a) chloroplasts, and (b) 20,000 to 40,000 *g* precipitate of chloroplast sonicate.

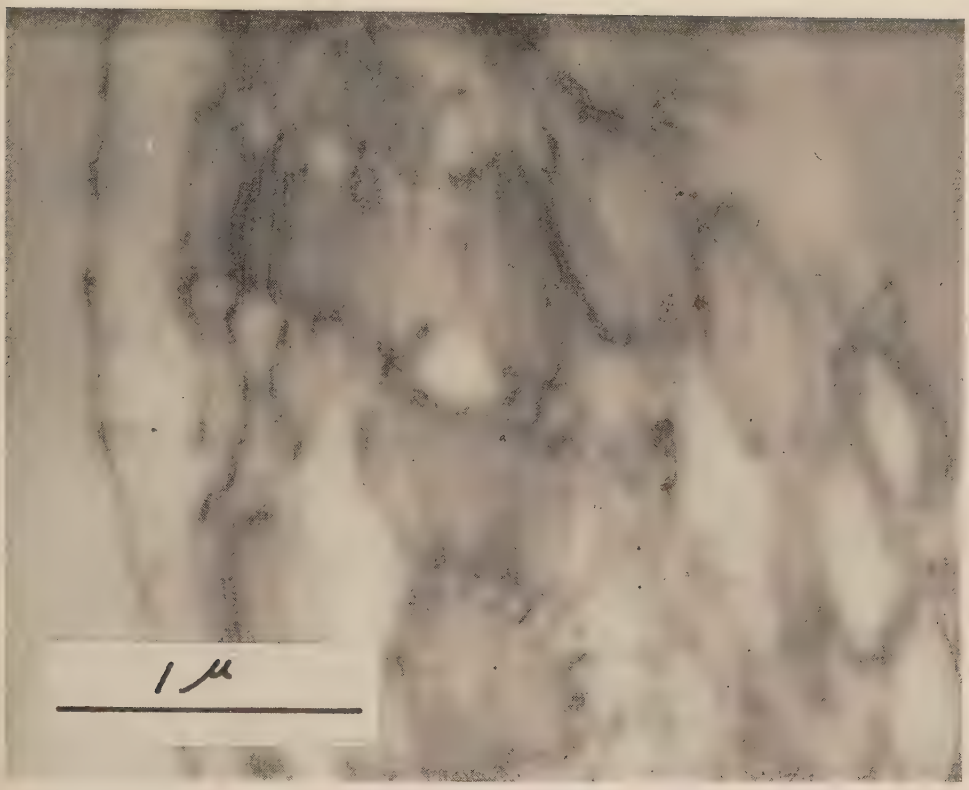

(a)

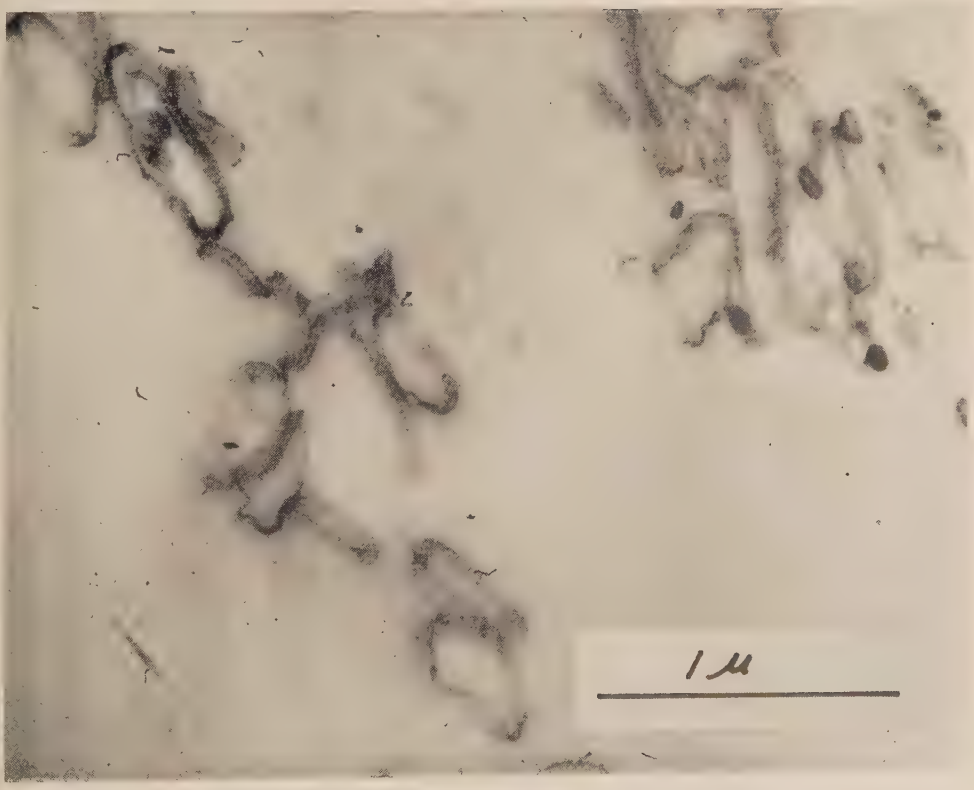

(b)

PLATE V. (*see facing page*)

PLATE VI. 5,000 to 10,000 *g* precipitate of spinach chloroplast sonicate. 880 Å diameter polystyrene latex (PSL) marker molecules.

PLATE VII. 5,000 to 10,000 *g* precipitate of frozen dried spinach chloroplast sonicate. 880 Å diameter PSL marker molecules.

PLATE VIII. 5,000 to 10,000 *g* precipitate of spinach chloroplast sonicate. 880 Å diameter PSL marker molecules.

Chloroplasts were isolated from spinach leaf tissue following the scheme in Fig. 1. The isolated chloroplasts were placed in dilute buffer, and sonically ruptured. The sonically ruptured chloroplast preparation was then fractionated by centrifugation. High speed centrifugation of a chloroplast sonicate in dilute buffer yields three principal fractions: a green precipitate, a colourless supernatant and a layer of lipid-containing material which rises to the surface of the tube during centrifugation. The electron microscopic, chemical and enzymatic properties of these three separate fractions are considered below. The enzymology of the recombined fractions is also described and a correlation is made between the isolated fractions and structures observed in a whole chloroplast.

Green precipitate

Plate V is a comparison between a thin section of an isolated chloroplast stained with osmium in isotonic sucrose and a thin section of osmium stained 20,000 to 40,000 ***g*** green precipitate. The green precipitate corresponds both in thickness and lateral dimension to the lamellar structures of the isolated chloroplast. The lamellar structures in the green precipitate contain a number of closely spaced osmium-staining particles in the outer surface which are not evident in the isolated chloroplasts. The two preparations have comparable enzymatic activities. Whether the particles are a result of the sonic treatment, excessive swelling of the lamellar structure or are an artifact is not known. A comparison between Plates V(a) and III shows that either the chloroplast is considerably disrupted during the isolation procedure or it becomes less resistant to distortion during fixation in the isolated state.

If the 5,000 to 10,000 ***g*** green precipitate is metal shadowed rather than sectioned, micrographs such as those shown in Plates VI and VII are obtained. Plate VI is an electron micrograph of green material precipitated between 5,000 and 10,000 ***g*** which was air-dried and shadowed with gold, palladium and platinum alloy. Plate VII is an electron micrograph of the same fraction, but frozen dried and shadowed with chromium. Both figures show a lamellar structure from 10,000 to 20,000 Å in diameter. The complete lamella is about 160 Å in thickness. The 200 Å diameter particles seen on the background in Plates VI and VII are contaminating supernatant proteins which are described in the next section. In Plate VI two layers are evident within the lamellar structure: an upper smooth layer and a lower granular layer which can be seen through the depressions on the lamellar structure. This suggests that at least two layers are present in the lamellar structure. The frozen dried preparation in Plate VII also indicates that at least two layers are present. A number of thickness measurements have shown that the lamellar structures seen in Plates VI and VII are made of two layers of equal thickness (100 Å). The total thickness of the lamellar structure is about 160 Å, or less than twice the thickness of the two individual layers from which it is made. Apparently the granular surfaces are packed in such a way as to allow a reduction of overall thickness. The inner surfaces of the two layers appear more granular than the outer surfaces when observed in the electron microscope. That the layers of the granular subunits run throughout the lamellar structure is indicated in Plate VIII. Here apparently solid structures are seen breaking down into particles along their length. This has never been observed in the frozen dried preparations, suggesting that the forces of surface tension are responsible for releasing the subunits from the layers.

Chlorophyll-to-nitrogen weight ratios (Table 2) for green lamellar structures from 20,000 Å to 800 Å in diameter are fairly constant though precipitation of colourless supernatant protein at high *g* values reduces the ratio slightly. The large lamellar structures such as those seen in Plate VI appear to be stripped of grana. These structures have chlorophyll-to-nitrogen ratios similar to the precipitates obtained at higher *g* values which contain grana. This fact can be interpreted to mean that chlorophyll is uniformly distributed throughout the lamellar structure of the chloro-

TABLE 2

Chlorophyll-to-nitrogen weight ratios of spinach leaves, chloroplasts, and chloroplast fragments

Fraction	$\frac{\text{Chlorophyll (mg)}}{\text{Nitrogen (mg)}}$	Particle size (μ)
Leaves	0·32	
Whole chloroplasts	1·06	4
600 to 5,000 ***g*** precipitate	1·91	
5,000 to 10,000 ***g*** precipitate	1·80	
10,000 to 20,000 ***g*** precipitate	2·07	1 to 2
20,000 to 40,000 ***g*** precipitate	1·99	
40,000 to 145,000 ***g*** precipitate	1·82	
145,000 ***g*** precipitate (30 min)	1·37	$< 0{\cdot}1$
145,000 ***g*** supernatant	0·52	

plast. Chlorophyll may be more evident in the grana regions of a chloroplast when observed by a light or fluorescence microscope primarily because of the increased amount of chlorophyll-containing lamellar structure present in the grana areas. That grana are not essential to photosynthesis is indicated by electron micrographs of algal chloroplasts. Grana are absent from algal chloroplasts, though the lamellar structures are still present.

Spectrophotometric examination of 80% acetone extracts of different sizes of lamellar fragments has shown that relative photosynthetic pigment concentrations within the fragments are similar over the range 400 to 700 mμ. The Hill reaction rates of the various green precipitates, assayed manometrically with $Fe(CN)_6^{3-}$ as the oxidant, were uniform over the particle size range studied. The $^{14}CO_2$ fixation capacities of these particles are also similar (Table 4). These results all indicate that the smallest lamellar structures we have used (800 Å in diameter) are large in comparison to the smallest lamellar fragment which will convert electromagnetic energy to chemical potential.

The model for chloroplast lamellar structure presented in Fig. 2 is in accord with our results. The model for a lamella consists of two layers of 100 Å maximum thickness with an overall thickness of 160 Å. The outer surfaces of the layers represent the osmium-staining material of the lamellar structure seen in Plates III, IV and V. The layers are made of subunits 100 Å in thickness and 200 Å in diameter which are osmiophyllic over the outer surface. The rounder inner side of such subunits are evident in Plate VII. The granular layers in the depressions in the lamellar structure of

Plates VI and VII would represent the inner surface of the lower layer in this model, while the smooth upper layer would represent the outside surface of the upper layer. This model combines features previously proposed by Frey-Wyssling & Steinmann (1953) and Steinmann & Sjostrand (1955).

The model predicts that the top or bottom layer of a stack of grana should consist of a single 30 Å thick osmium-staining layer. This prediction is verified in a number of instances in Plate III. The swelling of the lamellar structures in Plate V indicates that the bond between the two lamellar layers is fairly weak. The weakness of this bond compared with the bond between the osmium-staining layers could explain the

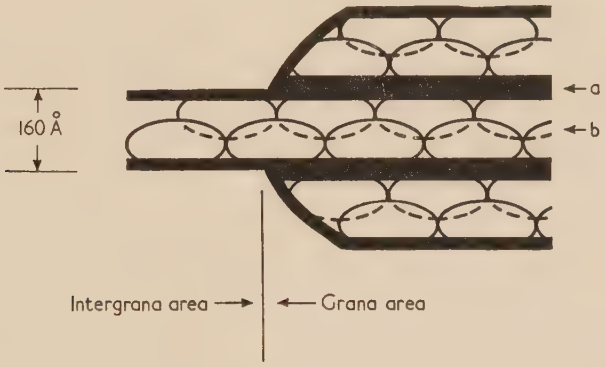

FIG. 2. Model for the lamellar structure within a spinach chloroplast

(a) Osmium-staining layer of the lamellar structure. Thickness 30 Å in the intergrana regions and 60 Å in the grana regions.

(b) Particles forming the granular inner surface of the two layers making up the lamellar structure. The packing of oblate spheres would not be as simple as illustrated in the figure since the central axis of both layers would not be in the same vertical plane shown here.

depressions in the lamellar surface in Plate VI if these areas had been the site of grana which had been sheared away from the large lamellar structure during sonication. The subunits 100 Å in height and 200 Å in diameter correspond in size to Fraction I molecules described in the next section. Smith & Kupke (1956) report that extracted protochlorophyll holochrome has a sedimentation coefficient typical of Fraction I protein. It will be interesting to find whether Smith & Kupke's extracted holochrome corresponds to the lamellar subunit in an early stage of development.

Supernatant

Plate IX is an electron micrograph of frozen dried supernatant from a 145,000 ***g*** centrifuge run for one hour's duration. This material is nearly colourless and therefore differs from the subunits described above. The supernatant in Plate IX is seen to consist principally of oblately spherical proteins about 200 Å in diameter and 100 Å in height. An ultracentrifugal analysis of this preparation shows that about half of the protein has an $S_{20,w}$ of 16. The remaining components are slower moving. The similarity between this sedimentation coefficient and that of Fraction I protein (Eggman, Singer & Wildman, 1953), as prepared by Lyttleton & Ts'o (1958) suggested that the 200 Å protein particles seen in Plate IX are actually Fraction I protein. To test this hypothesis Fraction I protein was prepared from spinach chloroplasts according to the method of Lyttleton & Ts'o. This preparation having an $S_{20,w}$ of 16 (see

Plate I), when observed under the electron microscope (Plate X), was indistinguishable from the 200 Å particles shown in Plate IX. The oblately spherical 200 Å supernatant proteins seen in Plate IX are apparently Fraction I protein.

Our analysis of the distribution of carboxydismutase activity in various centrifugal fractions from sonically ruptured chloroplasts is given in Table 3. About 90%

TABLE 3

Distribution of the carboxydismutase activity in various chloroplast fractions

Fraction	Activity in % of total
0 to 20,000 ***g*** supernatant	100†
20,000 to 40,000 ***g*** precipitate	3
40,000 to 145,000 ***g*** precipitate	6
40,000 to 145,000 ***g*** supernatant	90

†In another experiment 96% of the total carboxydismutase activity was present in this fraction. The remaining 4% was in the 0 to 20,000 ***g*** precipitate. Carboxydismutase activity was determined by mixing together in the order listed, in μM: $NaH^{14}CO_3$, 1·34 (20 μC); RuDP *ca.* 0·1; tris 15 (pH 8·3); $MgCl_2$, 2; and enzyme fraction 24 to 31 μg. Water was added to make 200 μl. final volume. Incubation was for 10 min at 25°C. Reaction was stopped by adding 50 μl. of 6 N-acetic acid. One-tenth of this mixture was plated and counted.

of the total carboxydismutase activity is associated with the colourless supernatant protein from the centrifugation. Incubation of ^{14}C-labeled fructose-6-phosphate with the supernatant protein yielded a number of radioactive photosynthetic carbon cycle intermediates (Turner, private communication) which also confirms Trebst's observation (Trebst *et al.*, 1958) that the dark reactions of photosynthesis are associated with the colorless supernatant from a centrifuged chloroplast preparation. Our observation that this preparation is largely Fraction I protein could be interpreted to mean that Fraction I protein contains a number of enzymatic sites of the photosynthetic cycle. The possibility of adsorption of small enzymes to the surface of this large (200 Å) protein cannot, however, be excluded by these experiments.

$^{14}CO_2$ fixation in green precipitate and supernatant

The difference between $^{14}CO_2$ fixation by precipitated green fragments resuspended in 1 ml. 10^{-3} M-phosphate (pH 7·4) and those resuspended in 1 ml. of supernatant from the 145,000 ***g*** centrifugation is presented in Table 4. The cofactors (Table 1) and $H^{14}CO_3^-$ were added to the system which was then incubated for 30 min in the light or dark at 24°C. Apparently, supernatant must be added to the chloroplast fragments to obtain high $^{14}CO_2$ fixation rates. The green fragments in the 145,000 ***g*** precipitate average 800 Å in diameter and were as active in CO_2 fixation on a unit chlorophyll basis as the largest fragments. Actually the calculated size for a photosynthetic unit of 600 chlorophyll molecules is considerably smaller than the 800 Å particles used in these experiments. Diminution of fixation rate owing to the preparation of incomplete photosynthetic units would not be expected until the green particles were reduced to a size of 200 Å (Thomas, Blaauw & Duysens, 1953). The relatively high light fixation rates of the 110,000 to 145,000 ***g*** precipitate resuspended in 10^{-3} M-phosphate is appar-

PLATE IX. 145,000 ***g*** supernatant of chloroplast sonicate. 1880 Å diameter PSL marker molecules.

[*To face page* 8

PLATE X. Purified Fraction I protein. Frozen dried. 880 Å diameter PSL marker molecules.

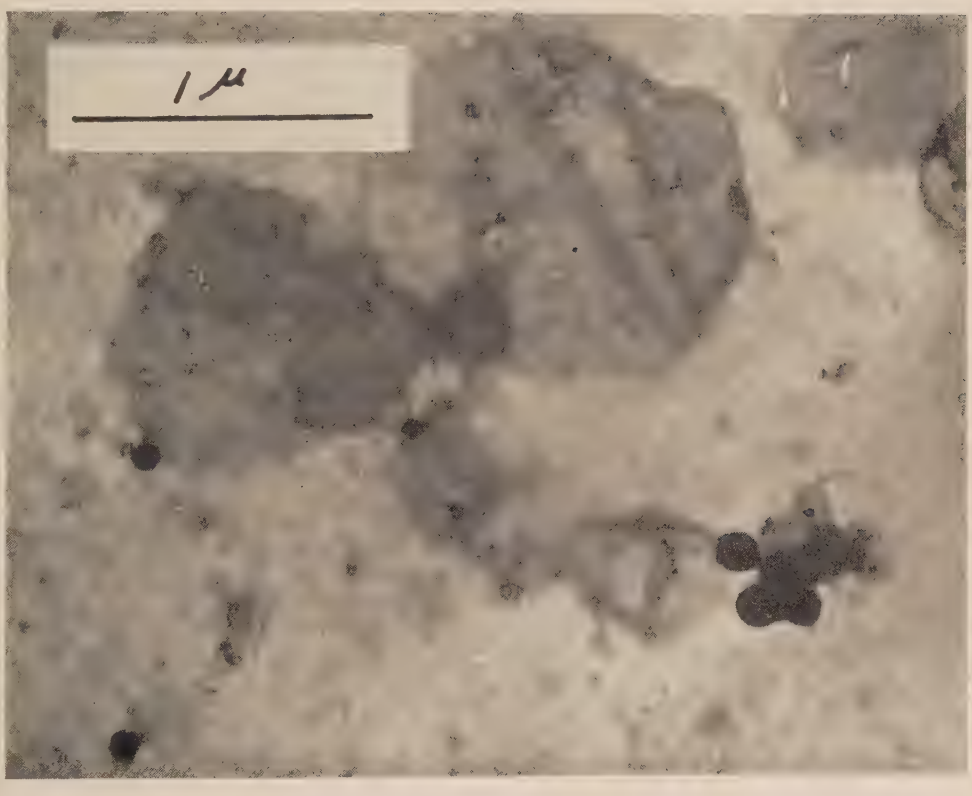

PLATE XI. Spinach chloroplast sonicate. Fixed in buffered 2% OsO_4. Not shadowed.

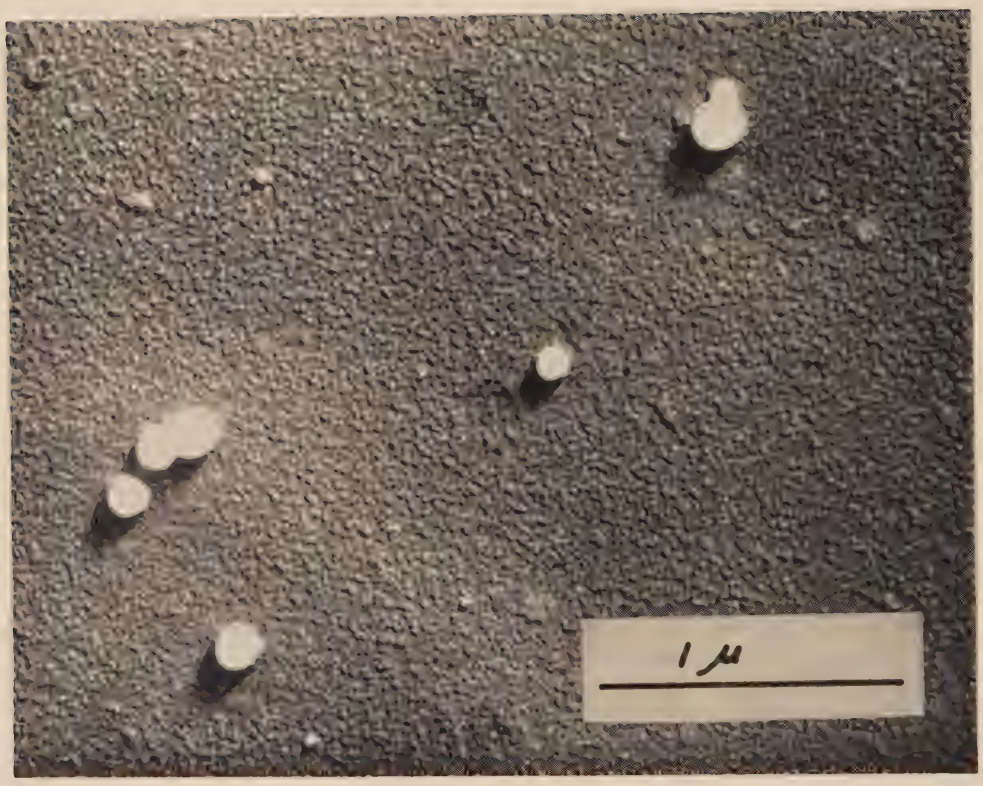

PLATE XII. Isolated osmiophyllic granules. Fixed in buffered 2% OsO_4. No PSL present.

ently due to the precipitation of some of the supernatant protein along with the green particles at this high *g* value. Chromatograms of ethanol extracts from the 14,000 to 110,000 *g* precipitate, 145,000 *g* supernatant and 14,000 to 110,000 *g* precipitate plus 145,000 *g* supernatant after incubation with $^{14}CO_2$ are given in Plate II. Although a small amount of reduction is carried out by the green fragments alone, it is evident that this effect is enormously enhanced by addition of supernatant protein, which contains the photosynthetic carbon cycle enzymes, to the reaction mixture.

TABLE 4

Fixation of $^{14}CO_2$ by various fractions from sonically fragmented chloroplasts

Fraction	Counts/min/mg of chlorophyll	
	Light	Dark
Total sonicate	2,100,000	40,000
0 to 14,000 *g* precipitate	76,000	9,000
0 to 14,000 *g* plus supernatant	3,300,000	28,000
14,000 to 110,000 *g* precipitate	18,000	4,200
14,000 to 110,000 *g* plus supernatant	3,000,000	22,000
110,000 to 145,000 *g* precipitate	210,000	—
110,000 to 145,000 *g* plus supernatant	2,500,000	22,000
Supernatant alone, 1 ml.	30,000	53,000

Details of the preparation of these fractions are given in Fig. 1. Supernatant refers to the supernatant liquid obtained from 145,000 *g* centrifugation in Fig. 1. A fixation rate of 3×10^6 counts/min/mg chlorophyll/30 min is equivalent to 1 micromole of CO_2 fixed/mg chlorophyll/hr.

Lipid layer

Plate XI is an electron micrograph of unfractionated osmium-fixed chloroplast sonicate which has undergone no further treatment. The large osmium-stained spherical objects in this micrograph correspond in size and osmium staining properties to the osmiophyllic granules seen in Plate III. These osmiophyllic granules are not evident in the preparation unless osmium staining is carried out (Hayes, Murchio, Lindgren & Nichols, 1959). If the lipid layer obtained upon centrifugation is osmium-fixed and shadowed, a picture such as Plate XII is obtained. It is seen that some of the lipid materials are very similar in dimensions to the osmiophyllic granules of Plates III and XI, and are very probably identical with them. These large lipid granules do not acquire ^{14}C-label rapidly during photosynthesis by the chloroplast sonicate. For example during a 30-minute incubation, less than 1% of the fixed carbon is associated with the lipid granules. This, of course, may not be the case in the intact leaf. That these granules might be reservoirs for some interesting lipids associated with photosynthesis, such as diglycerol phosphate (Benson, Wintermans & Wiser, 1959), is an interesting possibility.

4. Conclusions

From the electron microscopic, ultracentrifugal, enzymological and chemical data presented in the preceding sections we can correlate certain structures and functions in spinach chloroplasts. The light reactions of photosynthesis are associated with the

pigment-containing lamellar structures within the chloroplast. The lamellae are made of two layers of subunits. The layers are osmiophyllic on the outer surface. On the inner surface the granular appearance of the subunits is evident. Chlorophyll-to-nitrogen ratio studies on the lamellar structures may be interpreted to mean that the localization of chlorophyll in the grana of spinach plants is due to the greater number of chlorophyll-containing lamellar structures in this area of the spinach chloroplast rather than to localization of chlorophyll exclusively in the grana area. Small fragments of the lamellar structures are capable of Hill reaction though not capable of rapid light-dependent CO_2 fixation without addition of stroma protein. The stroma proteins within which the lamellar structures lie contain the enzymes associated with the dark reaction of photosynthesis and are largely Fraction I protein. The dimensions of Fraction I protein were determined from frozen dried preparations. Fraction I protein appeared as oblate spheres 100 Å in height and 200 Å in diameter.

Osmiophyllic granules ranging in size from 500 to 1500 Å in diameter have been isolated from the chloroplasts by nature of their low density. Presumably these structures are lipid in character.

The authors wish to thank Dr. Thomas Hayes of the University of California Donner Laboratory, both for the use of his electron microscope and for his many helpful suggestions during the course of this work.

REFERENCES

Arnon, D. I. (1949). *Plant Physiol.* **24**, 1.
Arnon, D. I., Whatley, F. R. & Allen, M. B. (1954). *J. Amer. Chem. Soc.* **76**, 6324.
Bassham, J. A. & Calvin, M. (1957). *The Path of Carbon in Photosynthesis.* Englewood Cliffs, New Jersey: Prentice-Hall, Inc.
Benson, A. A., Wintermans, J. F. G. M. & Wiser, R. (1959). *Plant Physiol.* **34**, 315.
Eggman, L., Singer, S. J. & Wildman, S. A. (1953). *J. Biol. Chem.* **205**, 969.
Farquhar, M. G. (1950). *Lab. Investigation,* **5**, 317.
Frey-Wyssling, A. & Steinmann, E. (1953). *Vjschr. Naturf. Ges., Zurich,* **98**, 20.
Hayes, T. L., Murchio, J. C., Lindgren, F. T. & Nichols, A. V. (1959). *J. Mol. Biol.* **1**, 297.
Hodge, A. J. (1959). *Rev. Mod. Phys.* **31**, 331.
Holm-Hansen, O., Pon, N. G., Nishida, K., Moses, V. & Calvin, M. (1959). *Physiol. Plant.* **12**, 475.
Leyon, H. (1954). *Exp. Cell Res.* **7**, 265.
Lyttleton, J. W. & Ts'o, P. O. P. (1958). *Arch. Biochem. Biophys.* **73**, 120.
Park, R. B., Pon, N. G., Louwrier, K. P. & Calvin, M. (1960). *Biochim. biophys. Acta,* **42**, 27.
Smith, J. H. C. & Kupke, D. W. (1956). *Nature,* **178**, 751.
Steinmann, E. & Sjostrand, F. S. (1955). *Exp. Cell. Res.* **8**, 15.
Thomas, J. B., Blaauw, O. H. & Duysens, L. N. M. (1953). *Biochim. biophys. Acta,* **10**, 230.
Trebst, A. V., Tsujimoto, H. Y. & Arnon, D. I. (1958). *Nature,* **182**, 351.
von Wettstein, D. (1958). *Brookhaven Symp. Biol.* **11**, 138.
Williams, R. C. (1953). *Exp. Cell. Res.* **4**, 188.

J. Mol. Biol. (1961) **3**, 11–17

The Ultraviolet Spectrum of Deoxyribonucleic Acids and their Constituents

E. Fredericq, A. Oth and F. Fontaine

Institute of Physical Chemistry and Anti-Cancer Centre, University of Liège, Belgium

(*Received 25 July 1960*)

The spectra of deoxyadenylic, deoxyguanylic, deoxycytidylic and thymidylic acids are given at pH 1, 2, 3, 5 and 7, from 220 to 310 mμ. The spectrum of thymus DNA denatured in 0·1 N-acetic acid at pH 3, at low concentration, is almost identical to the calculated spectrum of its constituent nucleotides.

The ratio of the absorbancies of DNA at 260 and 280 mμ reaches a constant value near pH 3, characteristic of the molar proportions of the bases. This appears to form the basis of a rapid method for estimating base composition.

1. Introduction

Different attempts to correlate the spectrum of DNA with that of its constituent bases or nucleosides have been made in the past few years (Beaven, Holiday & Johnson, 1955). In native DNA, the absorbancy in the range of the maximum near 260 mμ is much lower than the theoretical sum derived from the nucleoside spectra. Calculated on the basis of one equivalent of phosphorus per litre, and designated E(P), it varies between 6,000 and 7,000, according to the author. When the pH, the DNA concentration or the ionic strength is decreased the absorbancy at 260 mμ increases and approaches the theoretical contribution of the nucleosides. It is admitted that DNA has undergone an important change in configuration; but, according to the method used to bring about these "denaturations", very discrepant results are obtained for the maximum absorbancy.

No systematic investigation of the spectra of the nucleotides has been published; partial data only have been given for deoxyribonucleotides (Beaven *et al.*, 1955). It seemed worthwhile to investigate this point and to look for conditions where reproducible and reliable values would be obtained for the spectrum of DNA. We were able to find a denaturation procedure which fulfils these conditions. Since we obtained very constant values for the ratio of absorbancies at 260 and 280 mμ corresponding to the chemical composition of thymus DNA, we investigated the possibilities of using these data as a rapid estimation of base ratios in DNA.

2. Experimental

5′-deoxyribonucleotides were purchased from the California Corporation for Biochemical Research. They have an analytical grade purity. For all of them, except deoxyadenylic acid, the absorbancies obtained at the maximum at pH 2 corresponded to the data of the California Corporation, on a dry weight basis; in the case of deoxyadenylic acid, phosphorus determinations were made by the method of Macheboeuf & Delsal (1943). The molar absorbancy calculated on the phosphorus basis coincided with the data of the California Corporation.

Calf thymus DNA was prepared according to Kay, Simmons & Dounce (1952). It was dissolved in 0·01 M-NaCl and had a molecular weight of $7{\cdot}5\times10^6$, as deduced from intrinsic viscosity at zero gradient. The molar absorbancy on the phosphorus basis, $E(P)$, was 6,500 in 0·2 M-NaCl at pH 6.

The DNAs from *E. coli* and *H. influenzae* were kindly supplied to us by Professor C. Sadron, together with their base compositions.

Ultraviolet spectra were determined at 20°C under specified conditions with a DU Beckman spectrophotometer at intervals of 5 mμ, except in the neighbourhood of the maximum and the minimum, where the intervals were reduced to 1 mμ. Standard conditions were used for determining the absorbancy ratio E_{260}/E_{280}. A solution of DNA at a concentration near 0·002% was made in 0·1 N-acetic acid with final pH very close to 3. The absorbancy was measured in a 1 cm cell.

3. Results

(a) *Nucleotides*

For all nucleotides the spectra were determined at pH 1 and 2 in HCl, at pH 3 in acetic acid, at pH 5 in 0·1 M, 0·01 M and 0·001 M-acetate buffer and at pH 7 in 0·1 M-phosphate buffer. The nucleotide concentrations were around 0·0001 M. Figures 1 to 4 give the molar absorbancies; only the spectra presenting significant differences are reported in the figures.

Deoxyguanylic acid. Identical spectra at pH 7 and 5, and at pH 1 and 2. Some changes occur with time at pH 1 (Fig. 1).

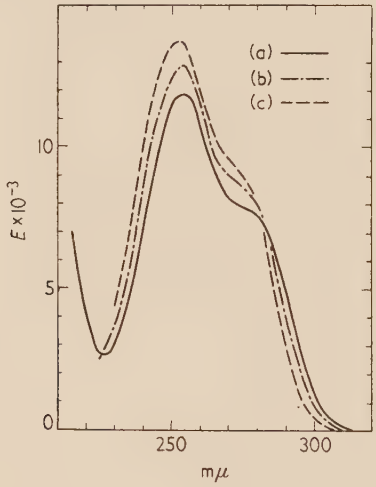

Fig. 1. Spectrum of deoxyguanylic acid: (a) pH 2, (b) pH 3, (c) pH 5.

Deoxyadenylic acid. Spectrum at pH 1 somewhat unstable with time and similar to spectrum at pH 2. Identical spectra at pH 2 and 3, and pH 5 and 7 (Fig. 2).

Thymidylic acid. Identical spectra at pH 1, 2, 3, 5 and 7 (Fig. 3).

Deoxycytidylic acid. Identical spectra at pH 1, 2 and 3 (Fig. 4). This is the only deoxyribonucleotide of which the spectrum has already been published (Beaven *et al.*, 1955); the published results are in very good agreement with our data.

None of the spectra were significantly affected by the ionic strength at pH 5. The instability of the purine derivatives at pH 1 is possibly related to some hydrolysis. It is well known that the glycosidic linkage is more susceptible to acid hydrolysis in the purine compounds (Chargaff, 1955).

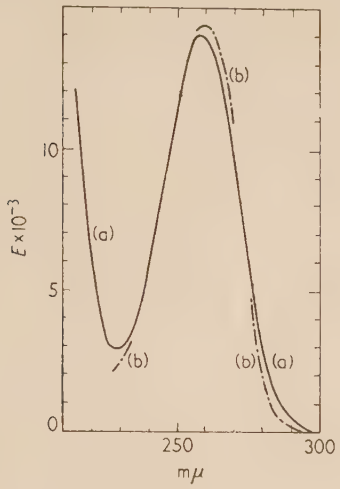

FIG. 2. Spectrum of deoxyadenylic acid: (a) pH 2, (b) pH 5.

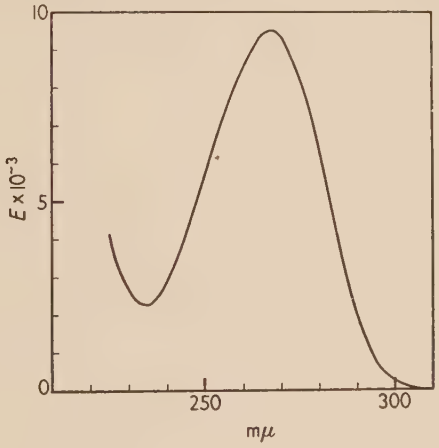

FIG. 3. Spectrum of thymidylic acid.

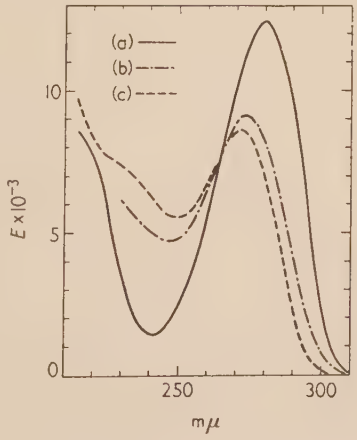

FIG. 4. Spectrum of deoxycytidylic acid: (a) pH 1, (b) pH 5, (c) pH 7.

A mixture of nucleotides based on the molar composition of thymus DNA was realized at pH 3 (molar percentages: adenine and thymine 28, guanine and cytosine 22). Its spectrum was compared to a curve calculated by the addition of the individual spectra. There was agreement within the limits of error in the range above 240 mμ. This shows that, at least at these concentrations, the additivity of the nucleotide spectra is respected.

(b) *Comparison with DNA at pH 3*

A comparison of the spectrum of DNA with that of its constituents was made at pH 3. This pH was chosen because previous work has shown that at this pH the hypochromic effects due to base interaction are becoming minimal and the molar absorbancy at 260 mμ approaches a maximum value, particularly at low ionic strength (Beaven *et al.*, 1955; Cavalieri, Rosoff & Rosenberg, 1956; Lawley, 1956; Duggan, Stevens & Grunbaum, 1957). On the other hand DNA becomes insoluble near pH 2·5 and there is some danger of aggregation when this pH is approached. At very low pH, DNA is soluble again but is then slowly hydrolysed.

The DNA was diluted in 0·1 N-acetic acid at a concentration of 0·0015%. The molar absorbancy (on the phosphorus basis) is plotted in Fig. 5 in comparison with the

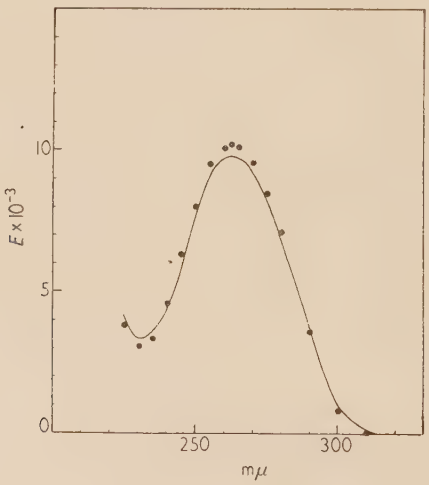

Fig. 5. Molar absorbancy (on the phosphorus basis) of DNA at pH 3. Filled circles: calculated values.

molar absorbancy calculated from the nucleotide contributions. It may be seen that DNA absorbancy is very close to the calculated value but remains a few percent lower in the range near 260 mμ. The position of the maximum is identically 262·5 mμ in both cases. In previous reports from the literature lower values for the absorbancies of denatured DNA are given. This is due to the fact that conditions of complete denaturation have not been generally realized. The maximum for E(P) of DNA at pH 3 is reported to be 9,400 (Duggan *et al.*, 1957). The values at very low pH would approach the theoretical value since hydrolysis is going on. In our experiments E(P) = 9,700 at 260 mμ. Since our value for native DNA is 6,500, the increase is almost 50%.

(c) *The analytical applications*

Although the absorbancy at 260 mμ is strongly dependent upon denaturation conditions, and never attains the theoretical value, it is remarkable to observe that the ratio of absorbancies at 260 and 280 mμ, E_{260}/E_{280}, is identical to the figure calculated for the nucleotide mixture. In Fig. 6 is plotted the value of this ratio for DNA as a

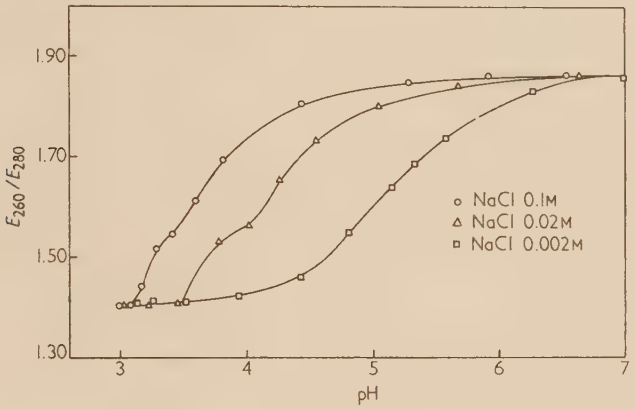

Fig. 6. Ratio of absorbancies of DNA at 260 and 280 mμ.

function of pH: it approaches the theoretical value of 1·41 when the pH is lowered; at low ionic strength this value is obtained at higher pH.

It appears, therefore, that the hypochromic effect at pH 3, due to DNA structure, affects the absorbancies at 260 and 280 mμ equally and that their ratio should be characteristic of the nucleotide composition of the nucleic acid. We calculated the value of the absorbancy ratio for varying proportions of the nucleotides. This absorbancy ratio is determined by the relative proportions of the sums: adenine + thymine/cytosine + guanine. From the data in Table 1 we calculated the value of the absorbancy

Table 1

Molar absorbancies of nucleotides at pH 3

	λ = 260 mμ	λ = 280 mμ
Deoxyadenylic acid	13,800	2,950
Deoxyguanylic acid	11,500	8,000
Deoxycytidylic acid	5,800	12,500
Thymidylic acid	8,600	6,350

ratio as a function of the base ratios. Since it is well established that DNA samples of different origins always contain the same molar proportions of adenine and thymine on the one hand, and of guanine and cytosine on the other (Chargaff, 1955), it is in principle sufficient to determine the ratio adenine + thymine/guanine + cytosine to know the complete composition of the molecule; in one instance only (Sinsheimer, 1959) the isolation of a phage DNA constituted by a single strand and having base

proportions differing from unity has been reported. Accepting the postulate of the bases pairing, we plotted in Fig. 7 the molar percentage of adenine (considered equal to that of thymine) as a function of the absorbancy ratio. The latter value can be measured to within $\pm$ 0·005 when the average of several readings is taken; in the absence of complicating factors, this would give an ideal accuracy of 0·25% in the molar percentage of bases.

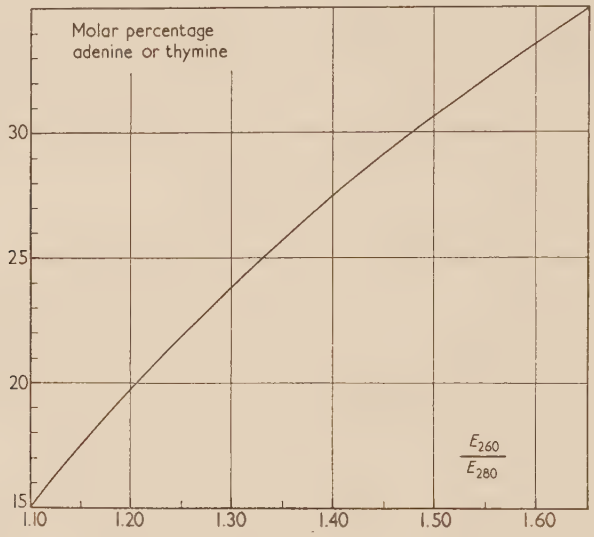

FIG. 7. Molar percentage of bases in DNA deduced from the absorbancy ratios.

Only impurities which absorb in the spectral range 260 to 280 mμ would interfere. RNA for instance should be absent; a small amount of proteins (less than 5%) would not significantly alter the results. It is true that it is sometimes difficult to know what kind of impurities are present in a new preparation of DNA. In such cases, of course,

TABLE 2

Base composition of different DNAs

Origin	E_{260}/E_{280}	Molar percentage of adenine or thymine from absorbancy	from chemical analysis
Calf thymus	1·405	27·7	28·0
Herring sperm †	1·39	27·2	27·6
E. coli	1·33	25·0	25·0
H. influenzae	1·505	30·9	31·0

† Methylcytosine is assimilated to cytosine.

the method would not be applicable. It would be very useful for instance, because of its simplicity and rapidity, for following the fractionation of a given DNA or for checking the purification of a known DNA.

A good number of determinations were made on calf thymus DNA. They consistently gave an absorbancy ratio of 1·405. Other determinations were made on three samples

of different DNAs. Results are given in Table 2. In all instances the spectroscopic determinations agreed with the chemical analysis within the limits of errors of the latter method.

4. Conclusions

The spectra of deoxyribonucleotides appear to be very similar to those already reported for deoxyribonucleosides (Beaven *et al.*, 1955). The influence of pH from 1 to 7 reflects the dissociation of the amino groups, the spectrum changing only in the range near the pK of the group. We may also notice the independence of the spectra from ionic strength at pH 5.

The occurrence at pH 3 of a denatured DNA with a spectrum very close to that of its constituent nucleotides indicates a strong lowering of interactions between the bases of the two chains. These interactions are generally assigned to hydrogen bonding. It is also very likely that in native DNA a residual hypochromism is due to other interactions that result from the polymeric structure (Spirin, Gavrilova & Belozersky, 1959). In our conditions of denaturation it appears that this residual hypochromism is very low and the number of hydrogen bonds possibly subsisting is very small. It should be pointed out that this stage of denaturation is reached when a number of conditions is realized. In many instances, in particular in the presence of small quantities of other electrolytes, the absorbancy at 260 mμ is lower and very different results may be obtained, as is evident from the variety of data for E(P) reported in the literature for denatured DNA (Cavalieri *et al.*, 1956; Lawley, 1956; Duggan *et al.*, 1957; Spirin *et al.*, 1959).

The constancy of the ratio E_{260}/E_{280} at pH 3 provides a very simple method for a rapid evaluation of the base ratios in DNA. It is limited, however, to cases where the absence of impurities absorbing in the same range could be guaranteed. Whether it is sufficient for the complete analysis of the four bases lies in the assumption of the classical correlation between the molar proportions of the bases.

This work was supported by grants from the "Centre anticancéreux de l'Université de Liège" and from the "Centre national de Biologie physico-chimique".

REFERENCES

Beaven, G. H., Holiday, E. R. & Johnson, E. A. (1955). In *The Nucleic Acids*, ed. by E. Chargaff & J. N. Davidson, Vol. I, p. 493. New York: Academic Press.
Cavalieri, L. F., Rosoff, M. & Rosenberg, B. H. (1956). *J. Amer. Chem. Soc.* **78**, 5239.
Chargaff, E. (1955). In *The Nucleic Acids*, ed. by E. Chargaff & J. M. Davidson, Vol. I, p. 307. New York: Academic Press.
Duggan, E. L., Stevens, V. L. & Grunbaum, B. W. (1957). *J. Amer. Chem. Soc.* **79**, 4859.
Kay, E., Simmons, N. S. & Dounce, A. L. (1952). *J. Amer. Chem. Soc.* **74**, 1724.
Lawley, P. D. (1956). *Biochim. biophys. Acta*, **21**, 481.
Macheboeuf, M. & Delsal, J. (1943). *Bull. Soc. Chim. Biol., Paris*, **25**, 116.
Sinsheimer, R. L. (1959). *J. Mol. Biol.* **1**, 43.
Spirin, A. S., Gavrilova, L. P. & Belozersky, A. N. (1959). *Biokhimiya*, **24**, 600.

J. Mol. Biol. (1961) **3**, 18–30

Structural Considerations in the Interaction of DNA and Acridines†

L. S. Lerman‡

Medical Research Council Unit for Molecular Biology, University of Cambridge, England and Department of Biophysics, University of Colorado Medical Center, Denver, Colorado, U.S.A.

(*Received 15 August 1960*)

The combination in solution of DNA with small amounts of acridine, proflavine, or acridine orange results in markedly enhanced viscosity and a diminution of the sedimentation coefficient of the DNA. These changes are contrary to those expected on the basis of aggregation or simple electrostatic effects. Characteristic changes, which suggest considerable modification of the usual helical structure of DNA, are found in the X-ray diffraction patterns of fibers of the complex with proflavine.

It is inferred that these compounds, which are potent mutagens, are intercalated between adjacent nucleotide-pair layers by extension and unwinding of the deoxyribose-phosphate backbone. The hydrodynamic changes are the consequence of the diminished bending between layers, the lengthening of the molecule, and the diminished length-specific mass. The effects are fully reversible at ordinary temperatures. The proposed structural change is compatible with the normal restrictions on bond lengths, angles, and non-bonded contacts, and maintenance of the hydrogen-bonded base pairs perpendicular to the axis of the molecule.

Another singly charged dye, pinacyanol, fails to elicit the effects of intercalation, yielding only lowered viscosity and increased sedimentation coefficient.

1. Introduction

The mode of combination of acridine derivatives with DNA is of interest because of the mutagenicity of these compounds and the carcinogenicity of the related benzacridines. While the possibility of strong electronic interactions would favor flat, face-to-face binding of the acridine to the bases of the nucleotides, this mode is not accessible in the Watson-Crick structure, where the bases are in close van der Waals contact. However, it can be supposed that untwisting of the double helix might provide spaces of suitable depth between layers, yet leave undisturbed the hydrogen-bonded pairing of the nucleotides constituting each layer. The partly extended molecule containing intercalated acridine layers would differ from native DNA in several properties measurable in solution: (a) The length of the molecule would be increased in proportion to the amount of acridine bound. (b) The further extensibility of the helix, which ordinarily permits considerable irregular coiling of the DNA molecule in solution, would be diminished. If the molecule with intercalated acridine is locally straighter

† Department of Biophysics contribution number 111. This work was supported by a research grant from the Institute of Arthritis and Metabolic Diseases, Public Health Service and received some assistance from a grant by the Damon Runyon Fund to the Department of Biophysics.

‡ Senior Research Fellow, Public Health Service.

and stiffer, the random coil will be less compact. (c) Since the additional length due to each acridine is about the same as that of a nucleotide pair, while the mass increment is less than one-half of a nucleotide pair, the average mass per unit length of the molecule would decrease. If the structure in solution is retained on drying, it may be expected to introduce substantial changes in the X-ray diffraction pattern of an oriented fiber.

The intrinsic viscosity of a coiled macromolecule depends on both the contour length along the molecule and the average breadth of the random coil. The sedimentation coefficient of a long slender molecule (which is not tightly coiled) depends only weakly on the length but is expected to be nearly proportional to the mass per unit length (Schachman, 1959). The changes found in the diffraction pattern and in these physical properties of DNA when combined with some acridine derivatives will be seen to be consistent with the expected effects of intercalated layers and incompatible with any simple alternative scheme of bonding.

2. Methods

The DNA used in viscometry and sedimentation was isolated from fresh calf thymus and chicken erythrocytes by a conventional extraction with strong NaCl and deproteinization with chloroform (but not dried or rendered salt-free) (Chargaff, 1955). Commercial dyes were used without further purification; the acridine orange contained an equimolar quantity of zinc chloride and some dextrin. Proflavine is 2,8-diaminoacridine; acridine orange is similar but each amino nitrogen carries two methyl groups. All solutions were buffered near pH 6·8 with 0·001 M-phosphate and contained, in addition, NaCl and 10^{-4} M-EDTA (ethylenediaminetetra-acetate). DNA-acridine complexes were prepared by mixing dilute solutions of both components. Mixing at high concentrations frequently produces fibrous precipitates. DNA analyses were carried out by the modified diphenylamine method (Burton, 1956).

For dissociation of the acridine orange complex the solution was equilibrated with blotted beads of Dowex 50, which strongly binds the dye, and decanted several times. The resin was first washed by repeated cycling with acid and base and equilibrated with the DNA solvent to prevent any pH disturbance.

Viscosities were measured in glass capillary shear viscometers at 25·1 °C. In solutions where the reduced specific viscosity was high a marked deviation of the measurements from linear dependence on the shear rate was noted. Since plots of the logarithm of the reduced specific viscosity against the square root of the shear were more persuasively linear and provided a more sharply defined extrapolation, this method was used in deriving the zero-shear values. The tabulation also includes, however, values obtained by extrapolation of a visually fitted straight line in Cartesian coordinates.

Sedimentation of the DNA and its complexes was observed during ultracentrifugation by means of ultraviolet absorption optics. Approximate median sedimentation coefficients were calculated from the position at which each densitometer profile reached half its plateau value. This procedure, while simple and rapid, introduces a slight, but probably significant, underestimate of the actual median value; but the error should be similar for the complexes and controls. A calculation, based on an assumed extreme case having a uniform distribution of sedimentation coefficients extending from 0·5 to 1·5 of the median, indicates that the true median of this distribution would be underestimated by 3%. In all cases the first derivative of the absorption profiles shows only a single peak, in some cases slightly sharper in the complex than in pure DNA.

Because of the complexity of a dissociating system, the sedimentation coefficients have not been extrapolated to zero concentration, nor are all of the viscosities extrapolated to the intrinsic viscosity. The difference between the measured sedimentation coefficient and its extrapolated limit is negligible for DNA at these concentrations in the presence of 0·1 M salt, but because of the lower salt concentration in the present experiments, the measured values will be smaller than the values at infinite dilution.

For the preparation of fibers, solutions containing about 4 mg/ml. lithium DNA (kindly provided by Dr. M. H. F. Wilkins) were dialysed to equilibrium against a suitable proflavine solution. Centrifugation of the resulting solution at 10^5 ***g*** yielded a stiff gel. Slices of the gel were allowed to dry while stretched by small attached weights (paper clips) to their maximum extension, and equilibrated over salt solutions of the appropriate relative humidity. Diffraction patterns were taken in a Philips microcamera (lent by Dr. D. Davies) with CuKα radiation from a rotating anode tube. Hydrogen bubbled through a saturated salt solution was circulated through the camera for an hour preceding and during each exposure. Distances between symmetrical spots were measured on microdensitometer tracings drawn at 5- to 20-fold magnification. The fibers contained roughly one proflavine per three nucleotide pairs. The dichroism of the fibers was easily observed under the polarizing microscope.

3. Results and Discussion

While an accurate general theoretical description of the hydrodynamic properties of DNA has not yet been achieved, the molecule appears to conform roughly to the properties of an open random coil of limited flexibility through which solvent can pass more or less freely. Although it is convenient to discuss the results in terms of this model, the main questions are answered by the direction in which the properties change, and the interpretation should not be sensitive to the details of the model.

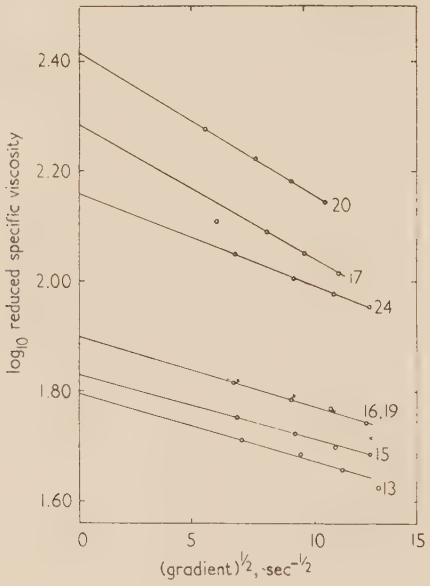

Fig. 1. The effect of salt, pinacyanol and some acridines on the reduced specific viscosity of calf thymus DNA solutions. For details of the conditions, see Table 1.

16—no dye
15—no dye, added salt
13—pinacyanol
20—proflavine
24—acridine
17—acridine orange
19—(X), solution 17 after ion exchange treatment to remove the dye

(a) *Viscosities*

A set of measurements carried out at uniform concentration of calf thymus DNA, showing reduced specific viscosity plotted against shear gradient, is presented in Fig. 1.

The extrapolated intercepts at zero shear for these and similar experiments under varying conditions are presented in Table 1. The viscosity contribution of the DNA is

TABLE 1

Reduced specific viscosities at zero shear for DNA-acridine complexes, DNA preparation S

Index number	Dye	Nominal dye concentration M × 10^5	DNA concentration μg/ml.	Sodium concentration M × 10^3	Zero shear reduced specific viscosity $(g/dl.)^{-1}$ (a)†	(b)†
16	—	—	68	3·7	68·5	78
7	—	—	60·8	3·7	68·7	82·5
13	Pinacyanol	2	66	3·7	55·5	61
9	Acridine orange	2	50	3·7	110	140
10	Acridine orange	3	52	3·7	115	153
14	Acridine orange	8	58·6	3·7	124	157
17	Acridine orange	8	65	3·7	141	196
19	(17 after ion exchange)	—	65	3·8	68·5	79
20	Proflavine	8	68	3·7	203	257
11	Acridine orange	3	30·4	2·7	94·5	115
24	Acridine	10	38	3·7	122	155
21	—	—	35	12·7	47	56·7
22	Proflavine	10	18·6	12·7	199	247
15	—	—	68·6	13·7	60·5	67
18	Acridine orange	8	76	13·7	86·1	100

† (a) linear extrapolation.
(b) log *vs.* $(\text{shear})^{1/2}$ extrapolation.

somewhat depressed, in the expected way (Cavalieri, Rosoff & Rosenberg, 1956) on increasing the sodium chloride concentration (comparing curve 16, the control under standard conditions, with curve 15, that obtained at a higher salt concentration).

For comparison with the supposed geometrical suitability of the acridine for intercalary binding, a supposedly unsuitable singly charged dye, pinacyanol, was studied;

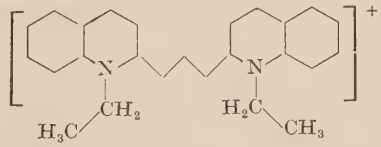

it could be expected neither to be fully accommodated in the internucleotide space nor to fill it completely if partially admitted. Curve 13 shows that pinacyanol, like other cations, diminishes the viscosity of the DNA solution.

The acridines, on the other hand, produce an astonishing enhancement of viscosity. The maximum effect here is given by proflavine, which yields a more than threefold higher value.

The complete reversibility of the effect is shown by the return of the viscosity of the acridine orange complex to the value for pure DNA after removal of the dye by

ion exchange. A more sensitive test of the reversibility of the effect was carried out by measurement of the transforming activity of genetically marked pneumococcal DNA which had been dissociated in the same way from a complex with acridine orange. No change in the transforming activity was detected (Lerman & Tolmach, in preparation).

(b) *The apparent intrinsic viscosity*

In the simple theory of the relation of the viscosity of a polymer solution to its molecular parameters, the contribution of intermolecular interactions to the viscosity of the solution is neglected. It is necessary, therefore, to infer from the experimental measurements the limiting value of the viscosity contribution per molecule as the concentration approaches zero. In dealing with a dissociating multicomponent system, as in the present experiments, direct measurement of the concentration dependence of a complex of fixed composition is impracticable. Instead, a mixture of proflavine and

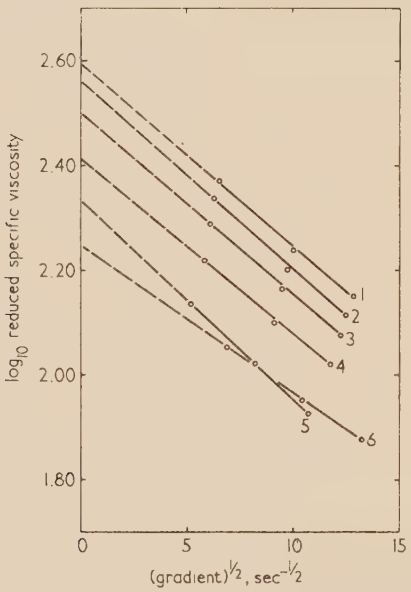

Fig. 2. The effect of proflavine on the reduced specific viscosity of chicken erythrocyte DNA solutions with 3×10^{-3} M-Na. Nearly superposed curves for some DNA concentrations have been omitted for clarity.

1, 2, 3, and 4—$2{\cdot}0 \times 10^{-5}$ M-proflavine; 41, 27·3, 20·5, and 14·7 μg/ml. DNA, respectively

5 and 6—no dye, 82 and 29·5 μg/ml. DNA, respectively

DNA was further diluted after each set of viscosity measurements with solvent containing the same total proflavine concentration. There are thus two major contributions to the slope of the curve which is to be extrapolated to infinite dilution, (a) the concentration dependence of the reduced specific viscosity of the complex, and (b) the changing composition of the complex as more proflavine is provided. In the equilibrium composition at the extrapolated limit, the concentration of *free* proflavine is the same as the total concentration. An extrapolation of this kind, labeled curve P, is shown in Fig. 3 together with a conventional dilution curve for pure DNA in the same solvent without proflavine, curve D. The points in Fig. 3 are taken from the extrapolation to zero shear at each dilution, shown in Fig. 2 (chicken erythrocyte

DNA). It will be seen that pure DNA shows the usual slight positive concentration dependence; while with proflavine η_{sp}/c rises strongly as infinite dilution is approached, apparently linear with concentration. The interesting feature of the measurements, the very high values in the presence of an acridine, is retained in the extrapolation. Similar results were obtained with calf thymus DNA (preparation Z).

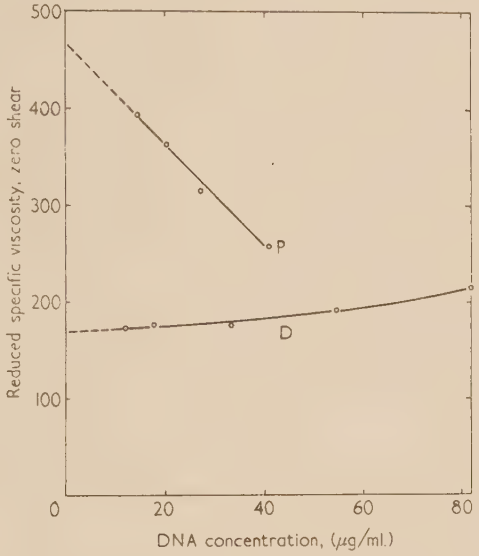

FIG. 3. The concentration dependence of the reduced specific viscosity of chicken erythrocyte DNA at zero shear, alone and in the presence of proflavine. The points are the extrapolated values given by Fig. 2.

D—no dye
P—$2{\cdot}0 \times 10^{-5}$ M-proflavine

(c) *Sedimentation*

Since aggregation would lead to an increased viscosity, it is useful to anticipate what changes it would introduce into the sedimentation properties of DNA. Although trimers or larger aggregates must be invoked to provide random coil dimensions corresponding to the observed viscosity changes, a discussion of the properties of dimers will be sufficient. The effect of the variable length of overlapping in the dimer can be ignored by considering only the limiting cases in which two molecules are joined either end-to-end or are in contact along their entire length. The sedimentation coefficient of a DNA molecule of twice the normal length is best estimated from the empirical relation derived from measurements on sonic fragments (Doty, McGill & Rice, 1958), for which S^0 varies as the 0·37 power of the molecular weight. The sedimentation coefficient of the other extreme hypothetical dimer, a cable of four polynucleotide strands, is estimated from the mass per unit length as roughly twice that of the monomer (Schachman, 1959). Thus, the dimer can be expected to have a sedimentation coefficient between 1·29 and 2 times that of the original DNA. Sedimentation coefficients for these DNA preparations and their complexes with proflavine, acridine, and pinacyanol are presented in Table 2. It will be seen that the positive increments in Table 2 fall below the lower limit for dimers, and the largest value is given by the pinacyanol complex.

The changes in the sedimentation coefficient seem to be accountable in terms of the changes in the mass per unit length of the DNA molecule according to the mode of binding of the attached dye. Binding to the outer surface increases the effective mass while intercalated binding decreases the effective mass of a given length of the molecule. Where a molecule of molecular weight 210 (proflavine, free base) replaces by intercalation a nucleotide pair of mean molecular weight 670, while maintaining constant length, density and frictional properties, the sedimentation coefficient will be expected to decline about 0·69% for each substituted segment in a hundred (neglecting possible changes in sodium binding). With an upper limit of 0·22 proflavine molecules strongly bound per nucleotide (Peacocke & Skerrett, 1956), the fractional replacement is 0·305 and hence the sedimentation coefficient would be 0·79 that of

Table 2

Sedimentation coefficients for DNA-acridine complexes

Index	Preparation	Dye	Total dye concentration M × 10^5	Sodium concentration M × 10^3	$S_{20,w}$ s	Ratio to control
869	Z	—	—	18	15·4	1·0
871	Z	Proflavine	2	18	13·5	0·88
870	Z	Proflavine	5	18	12·9	0·84
844	S	—	—	3·7	13·2	1·0
854	S	Proflavine	10	3·7	15·6	1·18
850	S	Acridine	3·3	3·7	14·3	1·08
851	S	Pinacyanol	2·0	3·7	16·4	1·24

Two separate DNA preparations are represented. All measurements were carried out with the DNA concentration near 33 μg/ml.

unmodified DNA. Since the length does not remain constant, but increases in direct proportion to the number of proflavine molecules bound, the effect of the diminished length-specific mass would be in some part compensated by the increased size. Although a simple estimate of the net effect is not possible, it appears unlikely that the sedimentation is more sensitive than the 0·37 power to the extra length due to intercalation; the net change in S at proflavine saturation would then be to 0·90 of pure DNA.

External binding, also assuming constant length, density, sodium binding and frictional properties, would effect an increase of 0·31% for each proflavine bound per hundred nucleotide pairs, or 0·51% for each pinacyanol (mol wt 353). At 44 dye molecules per hundred nucleotide pairs (an arbitrary figure), S would be increased by factors of 1·14 or 1·22 respectively.

Table 2 shows a depression in the sedimentation coefficient in the region of that predicted for intercalation when moderate amounts of proflavine are bound. At higher dye concentrations the net effect suggests a balance between the consequences of intercalation and some further external binding (see Section (h)) such that the sedimentation coefficient increases slightly. The gain is largest with pinacyanol where the external binding is not counterbalanced by intercalation.

PLATE I. X-ray diffraction pattern given by the complex of Li DNA with proflavine at 75% relative humidity.

[*To face page* 24

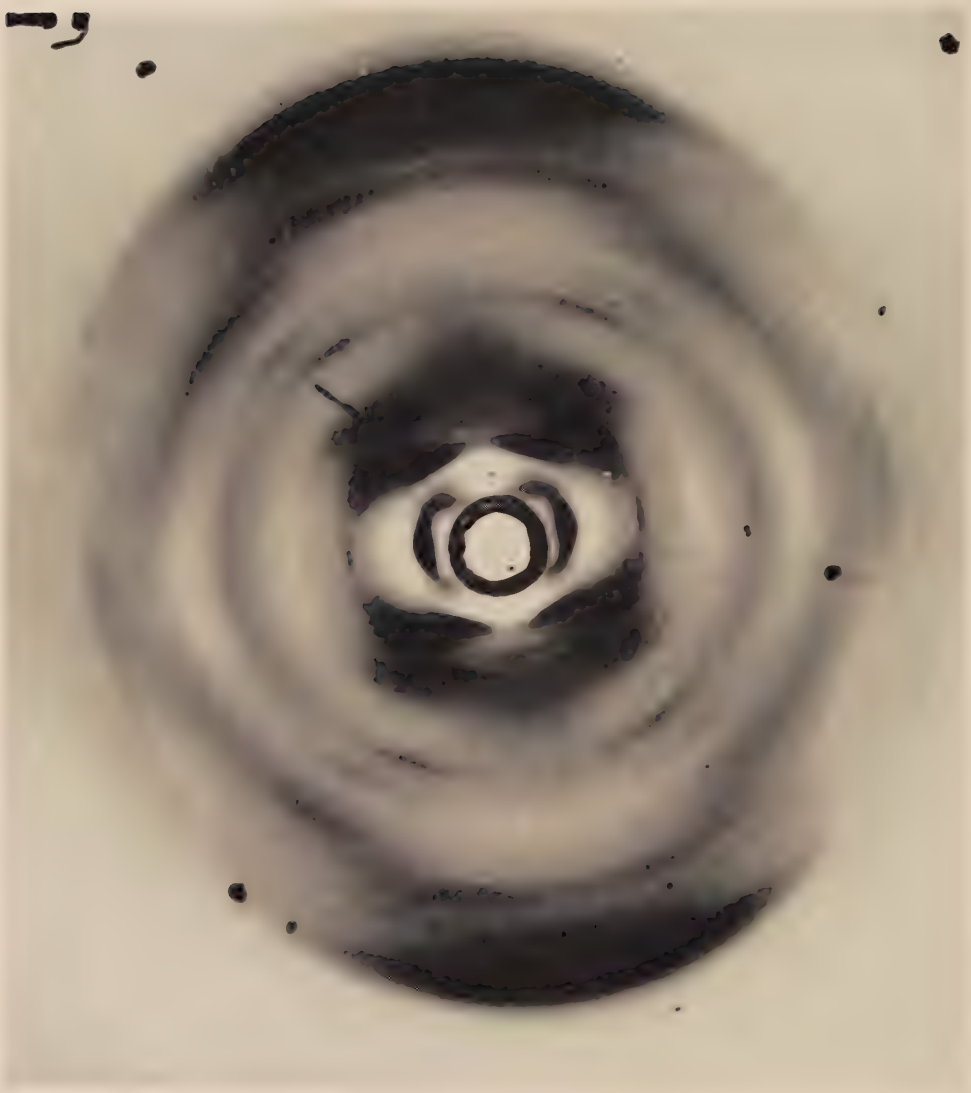

PLATE II. X-ray diffraction pattern given by Li DNA at 95% relative humidity.

It may be noted that two additional kinds of structural alterations which might be supposed to result from the binding of acridines would also have significant effects on the mass per unit length. If a space for the insertion of the acridine into the DNA molecule were provided by the rotation of each member of a base pair to the outside of the helix (see Fresco & Alberts, 1960), the same increment in mass per unit length as from simple external binding would be expected. If it is supposed that external attachment of acridines (but not other dyes) induces the structural modification which has been described for stretched DNA fibers (Wilkins, Gosling & Seeds, 1951), a decreased sedimentation coefficient can be expected. In this structure, where the bases are tilted about 45° from the fiber axis, the molecule is about 50% longer, with a corresponding diminution in the mass per unit length. Using the same mass increment for proflavine binding as above and the 0·37 power dependence on total length, the calculated net sedimentation coefficient at 0·44 proflavines per nucleotide pair is 0·89 of that for pure DNA. On the basis of sedimentation alone this model is indistinguishable from intercalation.

(d) *Fiber diffraction patterns*

Three main features may be discerned in the X-ray diffraction patterns of DNA-proflavine fibers: (a) the 3·4 Å meridional spots, which are prominent in the patterns of the *B* configuration of pure DNA, remain very strong in the complex and no new meridional reflexions appear. (b) The peak of the strong equatorial reflexion near the center, corresponding to the 110 reflexion of pure DNA, is found to lie slightly further from the center than the 110 reflexion of pure DNA *B* in its closest packing. (c) The characteristic layer-line pattern is abolished. Typical patterns of the proflavine complex and a comparably poorly oriented thick lithium DNA fiber are shown in Plates I and II.

The retention of the 3·4 Å spot as the sole meridional reflexion indicates that in the complex the purine and pyrimidine rings are perpendicular, or nearly so, to the helix axis. If the bases are replaced by intercalated acridines, the same 3·4 Å spacing obtains between the acridine and the bases above and below.

The spacing between DNA molecules, as indicated by the equatorial spots, appears to be incompatible with models based on binding of the acridines to the surface of the DNA helix. In fibers containing about one proflavine per three nucleotide pairs, the first equatorial spot indicates a spacing of 17·4 Å at relative humidity of 75% and 100%. For comparison, the closest spacing observed for pure DNA in the *B* configuration is 18·4 Å; the molecules are then in van der Waals contact through the penetration of the ridges of each helix in the grooves of four of its six neighbors (Langridge, Wilson, Hooper, Wilkins & Hamilton, 1960). The exterior attachment of one proflavine per two or three nucleotide pairs appears to just fill the large groove of the helix and would be expected, therefore, to prevent intermolecular separations closer than roughly 22 Å. Unlike pure DNA, which swells in both directions perpendicular to the *c* axis, the proflavine complex does not swell at higher humidities. This suggests that the 17·4 Å spacing is measured in the immediate vicinity of proflavine, rather than in regions from which it might be excluded.

In the *C* configuration of lithium DNA (see Langridge *et al.*, 1960*b*), which is found at 44% relative humidity, the closest intermolecular spacing is 17·0 Å. The slight tilt of the bases which is responsible for the smaller helix diameter would not be detectable in the meridional spots of the complexes within the precision of the present work.

However, the same considerations given for the *B* form apply, and the exterior attachment of proflavine would be expected to increase the spacing by 3 Å.

The requirements for additional intermolecular space are absent, of course, from the intercalated model, and it will be seen below (Section (f)) that because of the increased average pitch, further interpenetration of the helices is possible.

The disappearance of the layer lines, while both the meridional and equatorial spots are retained, suggests a disordering of the helical backbone, as would be expected if proflavine were intercalated aperiodically. It is reasonable to suppose that insertion of the acridines reflects the nucleotide sequence to some extent; the intercalation would then appear crudely random. Where there is an average of one proflavine per three nucleotide pairs the occurrence of large regions of well-ordered structure as statistical fluctuations in the proflavine distribution will be exceedingly rare.

(e) *Fiber dichroism*

The maximum light absorption by proflavine in fibers of the complex occurs when the electric vector of the incident light is perpendicular to the fiber axis. It may be inferred (see Seeds, 1953) that the normal to the plane of the proflavine molecules lies less than 55° from the fiber axis. While the ease of visual observation suggests that the angle is considerably smaller, no quantitative estimate has been made.

(f) *Extension of the DNA molecule*

The possibility of extending a double helix to accommodate an intercalated acridine has been tested with brass rod atomic models. The following conditions were imposed

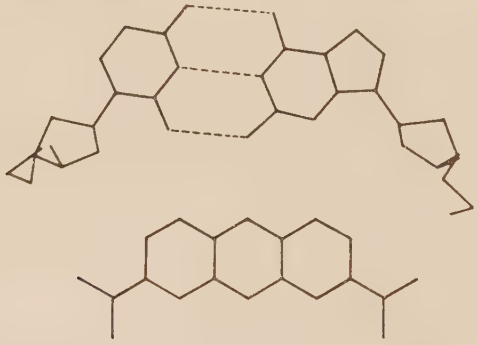

FIG. 4. A nucleotide pair at the site of intercalation, according to the model described in the text, projected on the plane perpendicular to the helix axis. A molecule of acridine orange is shown below to the same scale; hydrogen atoms are not indicated. The drawing shows the 5′ O—P—O attached to one base (the purine) and the 3′ O—P—O of the other as the extended sections of the backbone passing the intercalated acridine. The — 9° rotation of the next nucleotide pair would place it turned slightly clockwise above the pair shown, such that the ring oxygen of the left upper sugar is almost above the 1′ carbon of the lower. The most central obstructions to the placement of the intercalated molecule are the ring oxygens of the sugars of the right-hand nucleotide in the pair below and the left-hand nucleotide of the pair above.

arbitrarily: the purine-pyrimidine pairs should remain (1) at their normal, hydrogen-bonded configuration, (2) at their normal displacement from the helix axis, (3) perpendicular or nearly perpendicular to the helix axis, and (4) the backbone must continue demonstrably distortion-free to the next nucleotide above and below the separated pair at the normal internucleotide spacing.

Four bases of one chain were positioned with respect to the axis according to the coordinates of Langridge *et al.* (1960*a*) with vertical separations of 3·36, 6·72 and 3·36 Å, respectively, and a rotation of 36° between the normally spaced pairs. The deoxyribose-phosphate backbone, constructed with the bond angles selected for polyadenylic acid (Crick, personal communication, 1960) could be attached with very nearly equivalent sugar orientations and without unacceptably short contacts when the rotation between the extended pair was — 9° (left-handed, opposite to the normal direction of helix rotation). Little or no further extension of the backbone was possible without bond distortion. One intercalation per two nucleotide pairs would then extend the pitch of the helix from 33·6 Å to an average of 135 Å. While a limited search failed to disclose any other acceptable configurations, it is not impossible that others are equally appropriate.

The aperture between the backbone chains provides ample space for the acridines when suitably oriented, and can also comfortably accommodate the broader carcinogenic acridine, dibenz[a, j]acridine, found by Booth & Boyland (1953) to form soluble complexes with DNA.

A projection of a nucleotide pair with the backbones in the extended configuration is shown in Fig. 4, together with the skeleton of acridine orange to the same scale.

(g) *A model for the viscosity effects*

A polymer is described as a "worm-like chain" if bending between monomer segments is restricted to a small angle β, such that $\beta << \pi/2$ (see Tompa, 1956). Only for a fairly long string of segments can the direction of one end be considered to be randomly related to the direction of the other. The correlation between the directions of any two segments of the chain declines as the interval between them increases. The rate of decline is characterized by a length, a, known as the persistence length, given by the expression

$$a = t/(1 - \cos\beta) \tag{1}$$

if β and t are small. The mean-square end-to-end length $\langle l^2 \rangle$ is then

$$\langle l^2 \rangle = 2a(L - a + ae^{-L/a}) \tag{2}$$

where L is the total contour length of the polymer. For some purposes the properties of a complex chain model can be approximated by an "equivalent random chain" selected to have the same contour length and the same mean square end-to-end length. For the worm-like chain a fit of this kind is achieved when the length of the links of the equivalent random chain is made equal to twice the persistence length.

For a DNA molecule consisting of r nucleotide pairs, the persistence length is given approximately by equation (1), and can be inserted in equation (2) so that

$$\langle l^2 \rangle_0 = \frac{2rt^2}{1 - \cos\beta} \tag{3}$$

using only the first term, since L is much larger than a. Here t is the thickness of a nucleotide pair.

If n additional molecules with the same thickness, t, are intercalated into the chain, the new contour length is now

$$L_n = (r + n)t \tag{4}$$

If it is supposed that the insertion of the new molecule abolishes the flexibility of the backbone between the two nucleotide pairs that it separates, the number of flexible links will be diminished and there will be a larger effective mean link length, $\bar{t}$. This

will be the arithmetic mean of n units of length $3t$ where a molecule is intercalated, and the $(r - 2n)$ units of length t;

$$\bar{t} = (r + n)t/(r - n) \tag{5}$$

A new persistence length can be calculated from $\bar{t}$ by means of equation (1) and entered in the first term of equation (2), together with the new contour length, to determine the mean square end-to-end length of the polymer containing n intercalated layers. Thus

$$\langle l^2 \rangle_n = \frac{2t^2(r + n)^2}{(1 - \cos\beta)(r - n)} \tag{6}$$

Compared with the original polymer

$$\frac{\langle l^2 \rangle_n}{\langle l^2 \rangle_0} = \frac{(1 + n/r)^2}{1 - n/r} \tag{7}$$

Since the intrinsic viscosity of a free-draining random coil (the equivalent random chain) will be proportional to $\langle l^2 \rangle$, equation (7) represents also, approximately, the viscosity enhancement at infinite dilution due to the formation of the intercalated complex.

For the limit of strong binding in herring sperm DNA, where $n/r = 0{\cdot}44$ (Peacocke & Skerrett, 1956), the viscosity enhancement calculated from equation (7) is 3·7-fold; where 90% of the sites are occupied, the calculated enhancement factor is 3·2.

In the calf thymus DNA experiments, numbers 20 and 22, where the observed enhancement factors (not extrapolated) are 3·2 and 3·3, the fractional occupancy is estimated (from Peacocke & Skerrett's data on herring sperm DNA) to be near 0·95. The lower proflavine concentration in the experiments shown in Fig. 3, with chicken erythrocyte DNA, allows the estimated occupancy to vary from 0·60 at the highest DNA concentration to 0·95 at the extrapolated limit. Here, the observed limiting enhancement factor is 2·9.

The assumption of the stiffness of the link containing the intercalated layer is critical to the expectation of large viscosity changes. The assumption is supported by the impossibility of further extension of the backbone in the atomic model of the structure, and by consideration of the local electrostatic interactions. It may be noted that when $n/r = 0{\cdot}44$, the viscosity enhancement factor due only to the increment in contour length is 1·44, while the factor due to diminished curvature alone is 2·57. The latter would be reduced if flexibility is allowed around the intercalated layers.

(h) *The binding of dye aggregates*

It was shown by Peacocke & Skerrett (1956) that proflavine combines with DNA in at least two different ways. Regarding the DNA concentration as fixed, there is a strong, first order combination which saturates at one dye bound per four or five nucleotides, and a much weaker, higher order process with a limit of one dye per nucleotide. At the highest proflavine concentration of the present experiments, a small part would be expected to be bound by the second process.

The higher order process, which has been interpreted as the binding of dye aggregates, has been studied by Bradley & Wolf (1959) and Bradley & Felsenfeld (1959) with respect to other polyanions as well as DNA. Since aggregates cannot be accommodated by intercalation, and external binding is incompatible with the observed physical changes, intercalation is presumably to be identified with the mode of strong binding.

(i) *Structure of the complex*

The conclusions with respect to the mode of binding can be summarized by reference to the molecular hypotheses that have been considered and the inferences from the observed physical properties. The experimental results indicate that:

(i) The mass per unit length is diminished.
(ii) The molecules in fibers of the complex are more closely packed than DNA *B*.
(iii) The 3·4 Å spacing along the helix is retained.
(iv) The molecule is straighter in solution, in opposition to the electrostatic effect. Structurally dissimilar substances fail to elicit the straightening.
(v) The regular helical structure is lost.

It can be supposed that an acridine binds according to one of the following schemes:

(i) surface attachment to DNA in the *B* configuration.
(ii) surface attachment to a stretched form of DNA.
(iii) insertion into a DNA helix by separation and displacement of a base pair.
(iv) intercalation into the helix by extension of the backbone.

Of these, only the last is fully satisfactory.

(j) *Interactions* in vivo

Acridine, proflavine and acridine orange, as well as a variety of other amino-substituted acridines, have been shown to be strongly mutagenic in inducing reversion to wild type among a selected set of *r*II mutants of the bacteriophage T4 (Orgel & Brenner, in preparation), yielding reversion rates as much as 10^3 to 10^4 times greater than the spontaneous rates.

It is tempting to consider the well-known requirements of planarity for the carcinogenic activity of polycyclic aromatic hydrocarbons (see Greenstein, 1954) in terms of an intercalated complex with DNA. The formation of water-soluble complexes between certain polycyclic hydrocarbons and purines is second order in purine concentration (Weil-Malherbe, 1946) also suggesting a sandwich configuration.

I should like to thank Dr. F. H. C. Crick and Dr. J. R. Cann for their helpful discussions. I am indebted to Mrs. Catherine Fogg and Miss Christine Froud for assistance in viscometry, and to Mr. Stanley Fisher for operation of the ultracentrifuge.

REFERENCES

Booth, J. & Boyland, E. (1953). *Biochim. biophys. Acta*, **12**, 75
Bradley, D. F. & Felsenfeld, G. (1959). *Nature*, **184**, 1920.
Bradley, D. F. & Wolf, M. K. (1959). *Proc. Nat. Acad. Sci., Wash.* **45**, 944.
Burton, K. (1956). *Biochem. J.* **52**, 315.
Cavalieri, L. F., Rosoff, M. & Rosenberg, B. H. (1956). *J. Amer. Chem. Soc.* **78**, 5239.
Chargaff, E. (1955). In *The Nucleic Acids*, ed. by E. Chargaff & J. N. Davidson, Vol. I, p. 307. New York: Academic Press.
Doty, P., McGill, B. B. & Rice, S. A. (1958). *Proc. Nat. Acad. Sci., Wash.* **44**, 432.
Fresco, J. R. & Alberts, B. M. (1960). *Proc. Nat. Acad. Sci., Wash.* **46**, 311.
Greenstein, J. P. (1954). In *Biochemistry of Cancer*. New York: Academic Press.
Langridge, R., Marvin, D. A., Seeds, W. E., Wilson, H. R., Hooper, C. W., Wilkins, M. H. F. & Hamilton, L. D. (1960*a*). *J. Mol. Biol.* **2**, 38.
Langridge, R., Wilson, H. R., Hooper, C. W., Wilkins, M. H. F. & Hamilton, L. D. (1960*b*). *J. Mol. Biol.* **2**, 19.

Peacocke, A. R. & Skerrett, J. N. H. (1956). *Trans. Faraday Soc.* **52**, 261.
Schachman, H. K. (1959). In *Ultracentrifugation in Biochemistry*. New York: Academic Press.
Seeds, W. E. (1953). In *Progress in Biophysics and Biophysical Chemistry*, ed. by J. A. V. Butler & J. T. Randall, Vol. 3, p. 27. London: Pergamon Press.
Tompa, H. (1956). In *Polymer Solutions*. London: Butterworths.
Weil-Malherbe, H. (1946). *Biochem. J.* **40**, 351.
Wilkins, M. H. F., Gosling, R. G. & Seeds, W. E. (1951). *Nature*, **167**, 759.

J. Mol. Biol. (1961) **3**, 31–40

Variation and Heterogeneity of Base Composition of Deoxyribonucleic Acids: A Compilation of Old and New Data†

Noboru Sueoka‡

The Biological Laboratories, Harvard University, Cambridge, Massachusetts, U.S.A.

(*Received 24 August 1960*)

A compilation of the previously accumulated data as well as some new results on the base composition of DNA from various organisms reveals some general features of its variation and heterogeneity:

1. Among bacteria the mean guanine-cytosine (G-C) content of DNA varies approximately from 25 to 75%, and this extends over the range of the mean G-C content of DNA of higher organisms.

2. Phylogenetic relations may be reflected in the mean G-C content.

3. The distribution of G-C content of the DNA molecules of an organism is generally unimodal and the range is relatively narrow.

4. If the mean G-C contents of DNA of two species are different by 10% in bacteria, there are few DNA molecules of the same G-C content common to the two species.

5. The small heterogeneity of the base composition among the DNA molecules of an organism seems to be true for smaller regions within molecules.

Each point is discussed with respect to its genetic implication.

1. Introduction

The secondary structure of the DNA molecule has been well established and is known as the Watson-Crick double helix structure (Watson & Crick, 1953). In this structure four kinds of base pairs are possible: adenine-thymine, thymine-adenine, guanine-cytosine, cytosine-guanine. It is believed that the genetic information is stored in their sequence, and that the sequence eventually determines the primary structure of protein, that is, the amino acid sequence. If we follow this current concept of biochemical genetics it should eventually be possible to read the amino acid sequence of a protein in terms of the base sequence of its corresponding DNA molecule.

At present the main technical difficulty we encounter lies not in the analysis of amino acid sequence but in the analysis of the base sequence of nucleic acids. On the other hand a large amount of information is available on the composition of DNA, which is the main concern of this paper. It has two features: the *variation* of the mean DNA base composition in different organisms, and the heterogeneity of base composition of the DNA molecules within an individual or species. It has been shown in bacteria that there is a wide variation in the mean DNA base composition (Lee,

†Shortly before his paper was submitted to this journal, the author learned that F. Lanni (1960) had published a theoretical paper dealing with a similar subject. Owing to the independent considerations and to the somewhat different, and in some respects complementary, nature of the two treatments, the author has decided to publish his own without change from the original.

‡Present address: Department of Microbiology, University of Illinois, Urbana, Illinois, U.S.A.

TABLE 1

Base compositions of DNA of various organisms

G-C %	Bacteria	Fungi	Algae	Higher plants	Invertebrates	Vertebrates	G-C %
24							24
26	72						26
28							28
30	*18*, 32, 41, 49						30
32	17, *19*, 26, 51[a], 52						32
34	11, 29, 40, *64*, 65, 66, 68, 69				9		34
36	14, 38, 44, 70, 73[c]	2	2	10†	10‡, 11		36
38	12, 23[a], 28[a], 39				(5), 6, 7		38
40	*44*		1, 3	3, 5†, 6†, 7†, 8†, 11†	(2), 8‡	1, (1)	40
42	13, 53			2	(1), (4), 12‡	3§, 4, 5§, (6), 7§, 9, 10, 11§, 12, (14)	42
44	50[a], 71			4	(3)	2, 6, 8, 13	44
46							46
48	20			1, 9†			48
50	36, 37, 54, 55, 56, 57, 63						50
52	21, *25*						52
54	8[c], *24*, *43*, *57*, *58*, *62*	1	7				54
56	5, 10[c]						56
58	5, 6, 9[c], 15, 16, 22, 27, *35*, 61		6, 10				58
60			9				60
62			5				62
64	46, 60		4				64
66	7, 33, 45		(8)				66
68	*34*, (47[d]), 48, 59, *45*						68
70							70
72	30, 31, *42*, *60*						72
74	1[b], 2[b], 3[b], 4[b], *67*						74
76							76

† 3·8 to 6·4% 5-methylcytosine has been reported. ‡ 0·2 to 1·8% 5-methylcytosine has been reported. § 1·0 to 2·8% 5-methylcytosine has been reported.

Plain figures—Lee *et al.* (1956).
Italics—Belozersky & Spirin (1958).
a. See *N.A.*
c. Belozersky (1959).
d. Reported in this paper. By density gradient centrifugation. A stock culture of *Ps. saccharophila* was given by Professor H. P. Klein.

Figures with parentheses indicate that the DNA G-C content has been determined by the density gradient centrifugation technique (Table 2). For the available data of the base composition of coliphage DNA see Sinsheimer (1960).

BACTERIA

1. *Actinomyces globisporus flaveolus;* 2. *Actinomyces globisporus streptomycini;* 3. *Actinomyces griseus;* 4. *Actinomyces viridochromogenes;* 5. *Aerobacter aerogenes;* 6. *Agrobacteria tumefaciens;* 7. *Alcaligenes faecalis;* 8. *Azotobacter agile;* 9. *Azotobacter chroococcum;* 10. *Azotobacter vinelandii;* 11. *Bacillus cereus;* 12. *Bacillus megaterium;* 13. *Bacillus subtilis;* 14. *Bacillus thuringiensis;* 15. *Bifidibacterium bifidum;* 16. *Brucella abortus;* 17. *Clostridium bifermentans;* 18. *Clostridium perfringens;* 19. *Clostridium valerianicum;* 20. *Corynebacterium acnes;* 21. *Corynebacterium diphtheriae;* 22. *Corynebacterium parvum;* 23. *Diplococcus pneumoniae;* 24. *Erwinia carotovora;* 25. *Escherichia coli;* 26. *Fusiformis fusiformis;* 27. *Fusiformis polymorphus;* 28. *Hemophilus influenzae;* 29. *Micrococcus asaccharolyticus;* 30. *Micromonospora coerulea;* 31. *Micrococcus lysodeikticus;* 32. *Micrococcus pyogenes;* 33. *Mycobacterium phlei;* 34. *Mycobacterium tuberculosis;* 35. *Mycobacterium vadosum;* 36. *Neisseria gonorrhoeae;* 37. *Neisseria meningitidis;* 38. *Pasteurella aviseptica;* 39. *Pasteurella boviseptica;* 40. *Pasteurella tularensis;* 41. *Plectridium saprogenes;* 42. *Proactinomyces citreus;* 43. *Proteus morganii;* 44. *Proteus vulgaris;* 45. *Pseudomonas aeruginosa;* 46. *Pseudomonas fluorescens;* (47) *Pseudomonas saccharophila;* 48. *Pseudomonas tabaci;* 49. *Ramibacterium ramosum;* 50. *Rickettsia burneti;* 51. *Rickettsia prowazeki;* 52. *Ristella clostridiformis;* 53. *Ristella insolit;* 54. *Salmonella enteritidis;* 55. *Salmonella gallinarum;* 56. *Salmonella paratyphi;* 57. *Salmonella typhimurium;* 58. *Salmonella typhosa;* 59. *Sarcina flava;* 60. *Sarcina lutea;* 61. *Serratia marcescens;* 62. *Shigella dysenteriae;* 63. *Shigella paradysenteriae;* 64. *Staphylococcus pyogenes;* 65. *Streptococcus faecalis;* 66. *Streptococcus foetidus;* 67. *Streptococcus griseus;* 68. *Streptococcus pyogenes;* 69. *Streptococcus zymogenes;* 70. *Veillonella parvula;* 71. *Vibrio cholerae;* 72. *Welchia perfringens;* 73. *Micoplasma gallisepticum* (PPLO A5969).

FUNGI

1. *Neurospora crassa*, Minagawa, Wagner & Strauss (1959); 2. Yeast, *N.A.*

ALGAE—*Diatoms.*

1. *Chaetoceros decipiens;* 2. *Rhabdonema adriaticum;* 3. *Thalassiosira Nordenscheldii*, Serenkov (1957).

Green algae.

4. *Scenedesmus acuminatus;* 5. *Scenedesmus quadricauda;* 6. *Ankistrodesmus sp.;* 7. *Hydrodictyon reticulatum*, Serenkov (1957); (8) *Chlamydomonas reinhardi*, Sueoka (1960); 9. *Chlorella ellipsoidea*, Iwamura & Myers (1959).

Brown algae.

10. *Cystosira barbata*, Serenkov (1957).

HIGHER PLANTS

1. *Alnus barbata;* 2. *Salix acubifolia;* 3. *Salix caprea;* 4. *Crylus avelana;* 5. *Papaver somniferum;* 6. *Cucurbita pepo;* 7. *Phaseolus vulgaris;* 8. *Arachis hypogaea;* 9. *Triticum vulgare;* 10. *Allium cepa;* 11. *Finus sibirica*. Uryson & Serenkov, cited by Belozersky (1959).

INVERTEBRATES

(1) *Cancer borealis* (crab, the major DNA, see Table 2); (2) *Cancer irroratus* (crab, the major DNA, see Table 2); (3) *Carcinus maenas* (crab, see Table 2); (4) *Lumbricas terrestris* (earth worm, see Table 2); (5) *Venus mercenaria* (clam, see Table 2); reported in this paper (density gradient centrifugation); 6. *Arbacia lixula* (sea urchin) *N.A.;* 7. *Arbacia punctulata* (sea urchin), *N.A.;* 8. *Echinus esculentus* (sea urchin) *N.A.;* 9. *Echinocardium cordatum* (sea urchin) *N.A.* 10.; *Paracentrotus lividus* (sea urchin) *N.A.;* 11. *Psammechinus miliaris* (sea urchin) *N.A.;* 12. *Locusta migratoria* (locust) *N.A.*

VERTEBRATES

1. Man (thymus, liver, spleen, sperm) *N.A.;* (1) Man (kidney, tissue culture†) reported in this paper (density gradient centrifugation, Table 2); 2. Horse (spleen) *N.A.;* 3. Ox (thymus, spleen, liver, pancreas, kidney, testes, sperm) *N.A.;* 4. Sheep (thymus, liver, spleen, sperm) *N.A.;* 5. Pig (thymus, liver, spleen, thyroid) *N.A.;* 6. Mouse (sarcoma) *N.A.;* (6) Mouse (testes and spleen) reported in this paper (density gradient centrifugation, Table 2); 7. Rat (bone marrow) *N.A.;* 8. Hen (erythrocytes, egg) *N.A.;* 9. Salmon (sperm) *N.A.;* 10. Trout (sperm) *N.A.;* 11. Herring (testes) *N.A.;* 12. Shad (testes) *N.A.;* 13. Turtle (erythrocytes) *N.A.;* 14. Frog (*Rana pipiens*, testes) reported in this paper (density gradient centrifugation, Table 2).

† The culture cells were kindly supplied by Dr. I. Kato in Professor A. M. Pappenheimer Jr.'s laboratory.

Wahl & Barbu, 1956; Spirin, Belozersky, Kudlai, Skavronskaya & Mitereva, 1958). Furthermore, the heterogeneity in the base composition of DNA molecules of each bacterial species has a narrow range (Rolfe & Meselson, 1959; Sueoka, Marmur & Doty, 1959). In higher plants and animals the variation is considerably smaller (Chargaff, 1955).

In this paper pre-existent as well as some new information on the variation and heterogeneity of DNA base composition will be compiled for comparative purposes and some general features will be described.

2. Variation of the Mean DNA Base Composition Among Organisms

Through chromatographic analysis a large amount of data has been accumulated on the mean base composition of DNA from a wide variety of organisms. Recently

Table 2

Mean guanine-cytosine content of DNA estimated by density gradient centrifugation

Organism	Peak density	G-C content %	DNA preparation
Pseudomonas saccharophilia	1·732	68	cell lysate
Chlamydomonas reinhardi	1·728	64	purified
Cancer borealis (crab, testes, major fraction)	1·705	42	partially purified
Cancer irroratus (crab, testes, major fraction)	1·703	40	,,
Carcinus maenas (crab, testes)	1·707	44	,,
Lumbricas terrestris (earth worm, testes)	1·705	42	,,
Venus mercenaris (clam, testes)	1·700	37	,,
Rana pipiens (frog, testes)	1·705	42	,,
Mouse testes	1·704	41	,,
spleen	1·705	42	,,
Human (kidney cells, tissue culture)	1·703	40	cell lysate

All DNA samples were centrifuged separately in a CsCl solution (Meselson, Stahl & Vinograd, 1959), with ^{15}N-*Serratia marcescens* DNA as the reference. The density of the reference DNA (1·738) was previously determined with reference to *E. coli* K12 DNA, whose density was taken as 1·713 (see Appendix). Ultraviolet absorption photographs of almost equilibrated DNA bands (20 hr at 44,770 rev/min) were traced by Spinco Analytrol and the density at the peak was calculated as described in the Appendix. *Ps. saccharophila* and human kidney cells were lysed by 3% sodium lauryl sulfate and a portion of the lysate was used for the centrifugation. Animal tissues were washed with a saline EDTA solution (0·1 M-EDTA + 0·15 M-NaCl, pH 8·0), homogenized in the same solution, and lysed by adding sodium lauryl sulfate up to 3%. Sodium perchlorate was then added to one molar and shaken with 1 vol. chloroform and 0·1 vol. *iso*amyl alcohol for about 5 min by hand at room temperature. The aqueous portion was then isolated and treated in the same way 3 times. Subsequently, DNA was precipitated twice with 1·5 vol. 95% ethanol, dissolving the precipitate each time in a dilute saline citrate solution (0·015 M-NaCl + 0·0015 M-sodium citrate). The final precipitate was dissolved in saline citrate solution (0·15 M-NaCl + 0·015 M-sodium citrate) and kept in the refrigerator. The procedure is essentially the same as Marmur's method for the isolation of bacterial DNA (J. Marmur, personal communication).

it has become possible to determine the guanine-cytosine (G-C) content of DNA by density gradient centrifugation (Rolfe & Meselson, 1959; Sueoka *et al.*, 1959), by heat denaturation (Marmur & Doty, 1959), and by denaturation with increasing acidity (Bunville & Geiduschek, 1960). A compilation of the data available in the literature and reported in this paper is given in Tables 1 and 2.

The following features are apparent from the Tables:

(*i*) *Among bacteria the mean G-C content of DNA varies approximately from 25 to 75% and this extends over the range of the mean G-C content of DNA of higher organisms.*

The means of G-C contents of bacteria DNA are found in the range of 25 to 75%. The absence of natural DNA outside this range may suggest either that the genetic information cannot be stored by adenine and thymine or guanine and cytosine alone, or that the genetic information can be stored by adenine and thymine or guanine and cytosine alone but metabolically such DNA molecules cannot exist. In this connection it is noted that double helical DNA consisting only of deoxyadenylic and thymidylic acids can be synthesized enzymatically without any primer (Lehman *et al.*, 1958).

(*ii*) *Phylogenetic relations may be reflected in the mean G-C content.*

This point was first raised by Lee *et al.* (1956) from their analysis of the base composition of bacterial DNA. Among bacterial species there are several cases in which "taxonomically" related bacteria have similar values of G-C content. For example the genera of the Enterobacteriaceae *Escherichia*, *Salmonella* and *Shigella* have similar G-C contents of their DNA. A number of such examples have been discussed in their paper. Moreover, they have suggested that reclassification may be made for some species of bacteria according to the DNA base composition. In higher organisms the feature is even more evident. For example, all forms of vertebrates so far tested have a mean G-C content of 40 to 44%.

3. Heterogeneities of DNA Base Composition within an Organism

Further insight into the significance of the G-C content of DNA can be obtained when we know the compositional heterogeneity of DNA molecules from an organism. The presence of heterogeneity in DNA of several organisms was first demonstrated by chromatographic fractionation (Bendich, 1956; Brown & Watson, 1953; Chargaff, Crampton & Lipshitz, 1953; Lucy & Butler, 1954). Recently, quantitative assessment of the distribution has become possible by density gradient centrifugation (Rolfe & Meselson, 1959; Sueoka *et al.*, 1959), and by heat denaturation (Marmur & Doty, 1959).

Some salient points are as follows:

(*i*) *The distribution of G-C content of the DNA molecules of an organism is unimodal and the range is relatively narrow.*

Compared with the possible range of 25 to 75%, the G-C distribution of the DNA molecules of a given organism is rather narrow. Generally speaking, bacterial DNA has narrower distributions than that of higher organisms (Table 3). Except for a few cases, DNA preparations of all organisms that have been tested by density gradient centrifugation show unimodal distributions of G-C content. The unimodality of G-C distributions is a remarkable characteristic of DNA which will be considered further

in this paper. The only apparent exceptions are the cases of the testis DNA of two species of crab examined by the author. Each of the 5 individuals of *Cancer borealis* so far tested was found to have a secondary band of about 30% of the total DNA, and 2 individuals of *Cancer irroratus* a secondary band of about 10%. However, whether these cases are real exceptions is not clear, because the secondary band could be a fraction of crab DNA bound specifically to a less dense material (e.g. protein) or

TABLE 3

Heterogeneity of DNA base composition estimated by density gradient centrifugation†

	2σ (in G-C content, %)	Reference
VERTEBRATES		
Human kidney cells	$< 9{\cdot}6$	Reported in this paper
Mouse spleen	$< 7{\cdot}6$	
Frog testis	$< 6{\cdot}2$	
Calf thymus	$\sim 9{\cdot}6$	Sueoka (1959)
BACTERIA		
Diplococcus pneumoniae	$\sim 3{\cdot}9$	Sueoka (1959)
Bacillus megaterium *Bacillus subtilis* *Escherichia coli* *Micrococcus lysodeikticus* *Micrococcus pyogenes aureus* *Serratia marcescens* *Shigella dysenteriae* *Sarcina lutea* *Pseudomonas aeruginosa*	$< 6{\cdot}0$	Rolfe & Meselson (1959)

†The sign "$<$" indicates that the σ (standard deviation) has been calculated from the total variance (σ_T^2) of the DNA distribution in the density gradient field, which gives the maximum estimate of the heterogeneity.

DNA of a foreign organism symbiotic to the crabs. Another possibility is that the minor component is non-genetic DNA which happens to be produced by some metabolic anomaly. The absence of the secondary DNA band in another crab of a different genus (*Carcinus maenas*) supports these interpretations (Plate I).

It is pointed out here that some DNA preparations from calf thymus and mouse (both spleen and testes) have shown a minor, extra band in the density gradient field, consisting of approximately 2% of the total DNA. In calf thymus DNA the density of the minor band is higher than that of the main band, while the reverse is true in mouse DNA. The generality and significance of these minor bands remain to be seen.

(ii) If the mean G-C contents of DNA of two species are different by 10% in bacteria, there are few DNA molecules of the same G-C content common to the two species.

The range of compositional heterogeneity of the DNA molecules in terms of G-C content (mole percentage) has been observed in bacterial species to be less than 6% (expressed as twice the standard deviation) about the mean G-C content (Table 3). Higher organisms have wider ranges and extreme cases are found for vertebrate DNA.

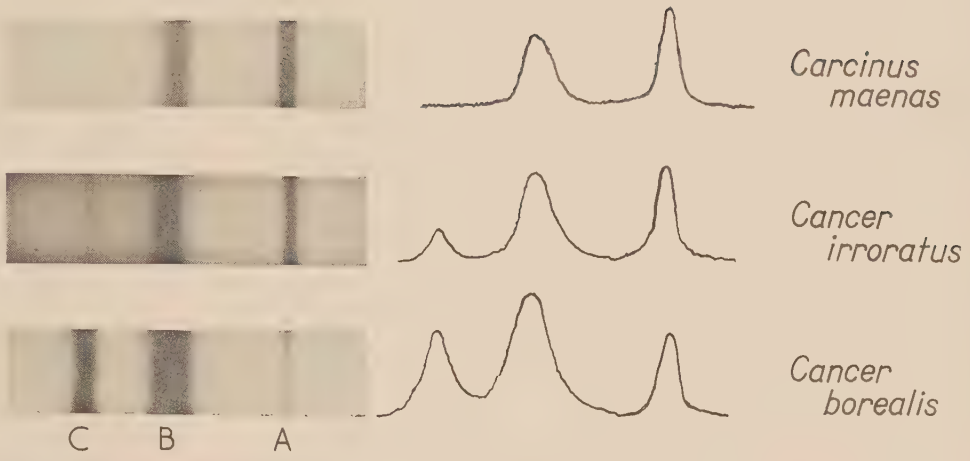

PLATE I. Ultraviolet absorption pictures of partially purified crab testis DNA banded in CsCl density gradient.

Band A is the ^{15}N-*Serratia marcescens* DNA added as a density reference. Bands B and C are crab DNA. Band B corresponds to 42 ± 2% G-C and Band C to 20 to 21%. The amounts of DNA in Band C are about 30% of the total DNA in *Cancer borealis*, and 11% in *Cancer irroratus*. Partial purification of DNA was made in the following manner. The testes of each species of crab were isolated individually and washed in a saline EDTA (ethylenediaminetetra-acetic acid) solution (0·1 M-EDTA + 0·15 M-NaCl, pH 8 0) once, resuspended in 5 ml. of the same solution, homogenized briefly and lysed with 3% sodium lauryl sulfate (final concentration). Subsequently, the DNA was isolated in the same way described in the legend of Table 2.

[*To face page* 36

Consequently, the statement that many organisms have entirely separate ranges of the G-C content of DNA imposes serious questions about the unitary view of the coding relation between DNA and protein. A number of theoretically possible explanations have been raised (Crick, 1959; Sueoka *et al.*, 1959).

(*iii*) *The small heterogeneity of the base composition among the DNA molecules of an organism seems to be true for smaller regions within molecules.*

Distribution of fragmented molecules of DNA in the cesium chloride density gradient field does not appreciably increase the density heterogeneity in calf thymus and pneumococcal DNA (Fig. 1; Sueoka, 1959). A similar result has been found in

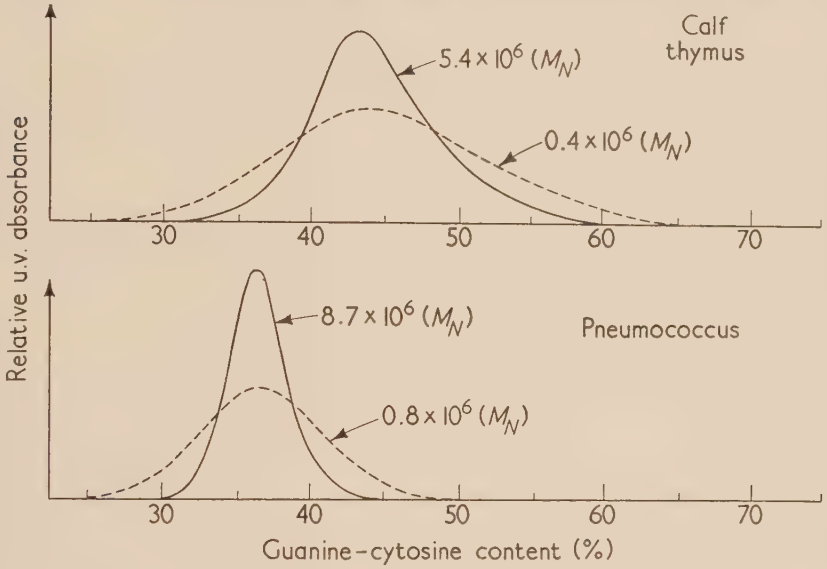

FIG. 1. Distribution of native and sonicated DNA of calf thymus and pneumococcus in density gradient centrifugation.

Solid curves are for native samples and dotted curves for sonicated samples. Ultraviolet absorption photographs of equilibrated DNA were traced by a Joyce-Loebl double beam microdensitometer. Number average molecular weights (M_N) indicated were calculated from sedimentation profiles in native samples, and approximated in sonicated samples by half of the weight average molecular weights estimated from sedimentation coefficient (Sueoka, 1959). As the scale of abscissa the G-C content in percentage is used to visualize the distribution range. It is noted that the curves in the figure represent the actual distributions including the spreading due to Brownian motion. The mean G-C contents for calf thymus and pneumococcus DNA adopted in this figure are 44 and 37%, respectively.

Micoplasma gallisepticum (Guild, Morowitz & Castro, 1960). The results indicate that the intramolecular distribution of G-C and A-T pairs is fairly uniform, although in short regions (for example, in triplets, quadruplets, etc.) non-randomness has been demonstrated (Sinsheimer, 1955; Shapiro & Chargaff, 1957; Josse & Kornberg, 1960).

4. Discussion

The purpose of this paper has been to compile the previously available and some new data on the base composition of DNA, in order to reveal the general features of its variation and heterogeneity.

Four points have been emphasized: in the first place, the variation of the mean

guanine-cytosine content of DNA lies between 25 and 75 mole %. Secondly, the mean base composition of DNA seems to be an extremely conservative (or evolutionally stable) characteristic. Thirdly, the guanine-cytosine content distribution of the DNA molecules of an organism is relatively narrow and generally *unimodal*. Finally the intra-molecular distribution of base-pairs seems to be fairly uniform.

The significance of the absence of organisms with DNA outside this range of G-C content is not clear. The absence may be the necessary consequence of the coding mechanism, and/or due to other metabolic reasons, for example, to the availability of the four deoxyribonucleotides. In this connection it may be interesting to note that in four-symbol codes (A, T, G, and C) the twenty kinds of amino acids we find in protein cannot be coded with A and T or G and C alone, while in the two-symbol code proposed by Sinsheimer (1959) the amino acids can in principle be coded with A and T or G and C alone. Therefore, from the study of the DNA base composition the two alternative coding principles cannot be conclusively distinguished, unless an organism exists whose DNA contains only A and T or only G and C, and whose proteins contain the usual twenty kinds of amino acids.

The minor band in crab DNA (Plate I) has a density of 1·683, which corresponds to 20 mole % G-C content according to an empirical relation between the density and the G-C content (see Appendix). However, it is recalled that the deoxypoly-AT which has been enzymatically synthesized in Kornberg's laboratory has a density of 1·68 (Sueoka *et al.*, 1959). Therefore it is quite possible that the minor band is a natural deoxypoly-AT. This possibility is now under experimental test.

Concerning the correlation of DNA base composition with phylogenetic relations of organisms, it should be pointed out that such correlation is very probable but has not yet been fully established. More data must be accumulated before we get a clearer picture. The DNA base composition of invertebrates, vertebrates and higher plants does not seem to supply much instructive information on this point since there is little variation in mean G-C content among these organisms. Bacteria have the greatest variation, but unfortunately the taxonomic relationships based on other criteria are somewhat arbitrary. The algae, fungi and possibly the protozoa may provide more information, for their range of DNA base composition seems to be wide, and their natural classification is certainly better established than that of bacteria.

The unimodality and the narrow distribution of the DNA molecules of an organism with respect to their G-C content are apparently the result of an interplay of various factors, systematic and non-systematic. A simple consideration of population genetics may lead to the following interpretation: the ultimate cause of changes in DNA base composition must lie in the conversions of AT $\rightleftharpoons$ GC. If the rates of both conversions (AT $\rightarrow$ GC and GC $\rightarrow$ AT) are equal, and there are no systematic selection pressures, the resulting distribution of the DNA molecules of an organism will, at equilibrium, be unimodal (a binomial distribution) with a mean GC content of 0·50 (in mole fraction) and a variance of $0{\cdot}25/b$. Here, b is the average number of base-pairs per molecule. However, if in an organism either type of conversion has a larger average "selective advantage", due to systematic selection pressures, the distribution at equilibrium will take the form of binomial distributions of various means and variances. At present this kind of treatment is, however, seriously limited by our ignorance of the factors influencing the conversion rates and selection pressures. Among these factors, the systematic selections caused by the mechanisms of coding and of mutation may be the most important.

I wish to thank Mrs. C. A. Young for her help in preparation of the manuscript. I am grateful to Professors P. Doty and R. P. Levine for their interest and helpful discussions. Professor J. H. Welsh's help in identifying the animals and their tissues used in the present work is gratefully acknowledged.

REFERENCES

Belozersky, A. N. (1959). *Les Nucléoprotéines*, p. 199. Institut International de Chimie Solvoy. Onzième Conseil de Chimie. Interscience Pub. Inc.
Belozersky, A. N., Shugayeva, N. Y. & Spirin, A. S. (1958). *Dokl. Akad. Nauk, S.S.S.R.* **119**, 330.
Belozersky, A. N. & Spirin, A. S. (1958). *Nature*, **182**, 111.
Bendich, A. (1956). *Essays in Biochemistry*, ed. by S. Graff, p. 14. New York: John Wiley.
Brown, G. L. & Watson, M. (1953). *Nature*, **172**, 339.
Bunville, L. G. & Geiduschek, E. P. (1960). *Biochem. Biophys. Res. Comm.* **2**, 287.
Chargaff, E. (1955). *The Nucleic Acids*, ed. by E. Chargaff & J. N. Davidson, Vol. I, 307. New York: Academic Press.
Chargaff, E., Crampton, C. R. & Lipshitz, R. (1953). *Nature*, **172**, 289.
Crick, F. H. C. (1959). *Brookhaven Symp. Biol.* no. 12, 35.
Guild, W. R., Morowitz, H. J. & Castro, E. (1960). *Abstracts*, Fourth Annual Meeting of the Biophysical Society, Feb., 24.
Iwamura, T. & Myers, J. (1959). *Arch. Biochem. Biophys.* **84**, 267.
Josse, J. & Kornberg, A. (1960). *Federation Proc., Abstr.* **19**, 305.
Lanni, F. (1960). *Perspectives in Biology and Medicine*, **3**, 418.
Lee, K. Y., Wahl, R. & Barbu, E. (1956). *Ann. Inst. Pasteur*, **91**, 212.
Lehman, I. R., Zimmerman, S. B., Adler, J., Bessman, M. J., Simms, E. S. & Kornberg, A. (1958). *Proc. Nat. Acad. Sci., Wash.* **44**, 1191.
Lucy, J. A. & Butler, J. A. V. (1954). *Nature*, **174**, 32.
Marmur, J. & Doty, P. (1959). *Nature*, **183**, 1427.
Meselson, M. (1957). Ph.D. thesis, California Institute of Technology.
Meselson, M., Stahl, F. & Vinograd, J. (1959). *Proc. Nat. Acad. Sci., Wash.* **43**, 581.
Minagawa, T., Wagner, B. & Strauss, B. (1959). *Arch. Biochem. Biophys.* **80**, 442.
Rolfe, R. & Meselson, M. (1959). *Proc. Nat. Acad. Sci., Wash.* **45**, 1039.
Serenkov, G. P. (1957). *Vestnik M.G.U.* no. 3.
Shapiro, H. S. & Chargaff, E. (1957). *Biochim. biophys. Acta*, **26**, 608.
Sinsheimer, R. L. (1955). *J. Biol. Chem.* **215**, 579.
Sinsheimer, R. L. (1959). *J. Mol. Biol.* **1**, 218.
Sinsheimer, R. L. (1960). *The Nucleic Acids*, ed. by E. Chargaff & J. N. Davidson, Vol. III (in the press). New York: Academic Press.
Spirin, A. S., Belozersky, A. N., Kudlai, D. G., Skavronskaya, A. G. & Mitereva, V. G. (1958). *Biokhimiya*, **23**, 154.
Sueoka, N. (1959). *Proc. Nat. Acad. Sci., Wash.* **45**, 1480.
Sueoka, N. (1960). *Proc. Nat. Acad. Sci., Wash*, **46**, 83.
Sueoka, N., Marmur, J. & Doty, P. (1959). *Nature*, **183**, 1429.
Watson, J. D. & Crick, F. H. C. (1953). *Cold Spr. Harb. Symp. Quant. Biol.* **18**, 123.

Appendix

The density and molar guanine-cytosine content of DNA in the CsCl density field presented in this paper were calculated in the manner described below:

According to equation (38) of Meselson (1957), the following relation has been approximated in the region of density 1·65 to 1·75.

$$\left(\frac{d\rho}{dr}\right)_r = 8{\cdot}3\omega^2 r \times 10^{-10} \qquad (1)$$

Here r is the distance of the peak of the DNA distribution from the center of rotation, ρ is the corresponding peak density and ω is the angular velocity per second. The solution of equation (1) is:

$$\rho = \rho_0 + 4{\cdot}2\omega^2(r^2 - r_0^2)\times 10^{-10} \quad (2)$$

ρ_0 and r_0 denote the peak density and peak position of the reference DNA band, respectively. For the speed of 44,770 rev/min, equation (2) becomes:

$$\rho = \rho_0 + 0{\cdot}0092\ (r^2 - r_0^2) \quad (3)$$

In the present paper the peak density of *E. coli* K12 DNA has been taken as 1·713, and the molar fractional content of guanine and cytosine (p) has been calculated using the following equation (Sueoka *et al.*, 1959):

$$\rho = 0{\cdot}103p + 1{\cdot}662 \quad (4)$$

It is noted that the absolute effective density of *E. coli* DNA is somewhat controversial, e.g. 1·708 according to Rolfe & Meselson (1959); 1·710 according to C. Schildkraut (personal communication). Rolfe & Meselson (1959) have obtained an equation

$$\rho = 0{\cdot}100p + 1{\cdot}658.$$

However, the guanine-cytosine contents calculated by either method are almost identical.

J. Mol. Biol. (1961) **3**, 41–46

Low-Angle X-Ray Reflections from Living Molluscan Muscles

G. F. Elliott and J. Lowy

Wheatstone Physics Laboratory and Medical Research Council Biophysics Research Unit, King's College, Strand, London W.C.2, England

(*Received 24 August 1960*)

A method is described for obtaining low-angle X-ray reflections from living muscles, checking the state of the muscle throughout the exposure. In the present work certain molluscan muscles were used in a relaxed condition.

X-ray diffraction patterns of the muscles when alive showed vestiges of an equatorial streak, together with a single clear equatorial reflection at $\sim$ 120 Å. When the muscle died the clear reflection disappeared, and the specimens then gave only the equatorial streak. Several meridional reflections were observed from all the muscles used, regardless of whether they were alive and relaxed or dead.

In the interpretation of the results it is suggested that both the equatorial and the meridional reflections come from diffracting systems situated in the paramyosin filaments, and that the equatorial reflection comes from the planes of ribbon-shaped sub-filaments stacked face-to-face within the paramyosin filaments and separated by 120 Å.

The finding that the meridional reflections are present in relaxed muscles is discussed in relation to the problem of the prolonged maintenance of tension in the molluscan muscles studied.

1. Introduction

The striated muscles of vertebrates and the paramyosin-containing muscles of lamellibranch molluscs have two kinds of myofilaments, and in both types of muscle one kind of filament is thin (diameter about 50 Å), and the other is thicker (Huxley, 1957; Elliott, 1958; Hanson & Lowy, 1959*a*,*b*; Philpott, Kahlbrock & Szent-Györgyi, 1960). But whereas in the striated muscles of vertebrates the thicker filaments have a diameter of about 100 Å and show no internal fine structure in the electron microscope (Huxley, 1957), in the molluscan muscles they are much thicker (diameters from 200 Å to 1500 Å) and longitudinal sections show a complex and variable banded structure with periods ranging between 130 Å and 380 Å and the bands often lying at an acute angle to the filament axis (Elliott, 1958, 1960). It is also known that the molluscan muscles give the most detailed low-angle X-ray diffraction pattern of any living system hitherto examined: the reflections extend to the 50th order, showing great regularity of the underlying macromolecular structure (Bear & Selby, 1956; Elliott, 1958). The first problem which arises in connection with the fine structure of the molluscan muscles is how to reconcile the regularity evident from the X-ray pattern with the varieties of pattern seen in the electron microscope.

By homogenizing the muscle it is possible to isolate ribbon-shaped filaments with a characteristic fine structure to which the name "paramyosin" has been given (Hall, Jakus & Schmitt, 1946). This structure is very likely due to the presence of the protein

tropomyosin A (Hanson *et al.*, 1957; Elliott, Hanson & Lowy, 1957). The second problem is to explain how these "paramyosin" ribbons fit into the thick filaments from which they are undoubtedly derived (Elliott *et al.*, 1957).

Both problems are soluble on the assumption that the thick filaments are made up of "paramyosin" ribbons stacked with their surfaces apposed (Elliott *et al.*, 1957; Elliott, 1958, 1960). Here we report evidence from X-ray diffraction studies which supports this hypothesis.

2. Methods and Materials

Low-angle X-ray reflections from living molluscan muscles were first obtained by Huxley (1952) using slit collimation. We have studied such muscles with an optically focusing low-angle X-ray camera (Franks, 1956, 1958) which gives meridional and equatorial reflections on a single negative.

Our apparatus was so arranged that the state of the muscle could be checked throughout the exposure. One end of the muscle was tied to a platinum hook fixed in a shallow Perspex bath in front of the camera guard-aperture. The other end of the muscle was connected to an isometric lever writing on a smoked drum. The platinum hook served as one stimulating electrode; the second electrode was another platinum wire in contact with the other end of the muscle.

The camera used has different horizontal and vertical resolutions, the horizontal resolution being about twice the vertical. The muscle was usually mounted vertically (or nearly so) to obtain maximum resolution on the equator.

The condition of the muscle was tested by measuring the tension developed in response to stimulation with square wave pulses, of 2 msec duration and 20 to 40 v, which corresponds to about 5 times threshold voltage. Failure to contract on stimulation with pulses of 20 msec duration and about 10 times threshold voltage was taken as the criterion of "death". The bathing solution was run over the muscle from a small pipette, supplied from a reservoir, inside a refrigerator. The temperature of the bathing solution at the muscle, measured with a thermocouple, was 5°C. The bathing solution was returned from the bath to the refrigerated reservoir with a motorized force pump made from methacrylate polymer.

Three molluscan muscles were used: the anterior byssus retractor of *Mytilus edulis* (ABRM), the translucent part of the adductor of *Crassostrea angulata* (the Portuguese oyster), and the opaque part of the same adductor. *Mytilus* was obtained from the Plymouth Marine Biological Station, the oyster from the Billingsgate fish market in London.

Hoyle & Lowy (1956) have described the dissection of the ABRM. Strips of the translucent and opaque parts of the oyster adductor muscle were prepared by the method of Abbott & Lowy (1956). The muscles used were 1 to 3 mm thick, and unless otherwise stated all experiments were done at a muscle length where maximum isometric tension was obtained on repetitive stimulation (Abbott & Lowy, 1958).

The bathing solution was natural sea water to which were added glucose (10 mg/ml.) and crystalline penicillin G (250 units/ml.). The muscles kept alive for 2 to 3 days, and at the end of this period they gave at least 1/3 and often well over 1/2 of the initial tension.

In the case of the ABRM, tests were also made to check whether it remains in a relaxed non-tonic condition, because in such muscles there is spontaneous electrical activity even after the (external) nervous systen has been destroyed (Lowy, 1955). Conceivably this could in time give rise to a tonic state, characterized by a great increase in the rigidity of the muscle. Rigidity was measured as the resistance to a constant-speed stretch (Lowy & Millman, 1959), and it was found that this parameter does not change appreciably in the resting ABRM under the conditions described above (Lowy & Millman, unpublished results). As a further measure to ensure that during the experimental period of about 3 days the muscle remains in a non-tonic state, the substance 5-hydroxytryptamine (5HT) was used. Twarog (1954) and Hoyle & Lowy (1956) have shown that in the presence of 5HT the ability of the ABRM to develop and/or sustain a tonic state is specifically abolished,

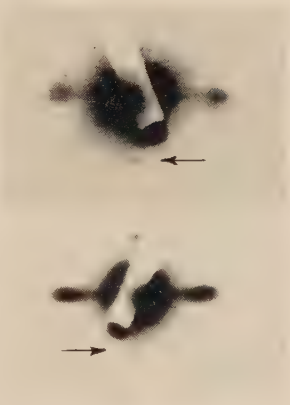

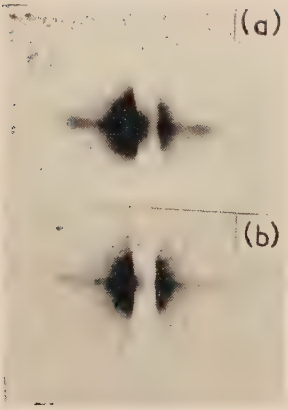

PLATE I

PLATE II

PLATE I. Two examples of the pattern from living ABRM. Fibre axis vertical. The 144 Å meridional reflections are marked with arrows.

PLATE II (a) Pattern from living opaque oyster adductor. Fibre axis vertical.
(b) The same specimen, having been allowed to die. Exposure somewhat shorter than (a).

[*To face page* 42

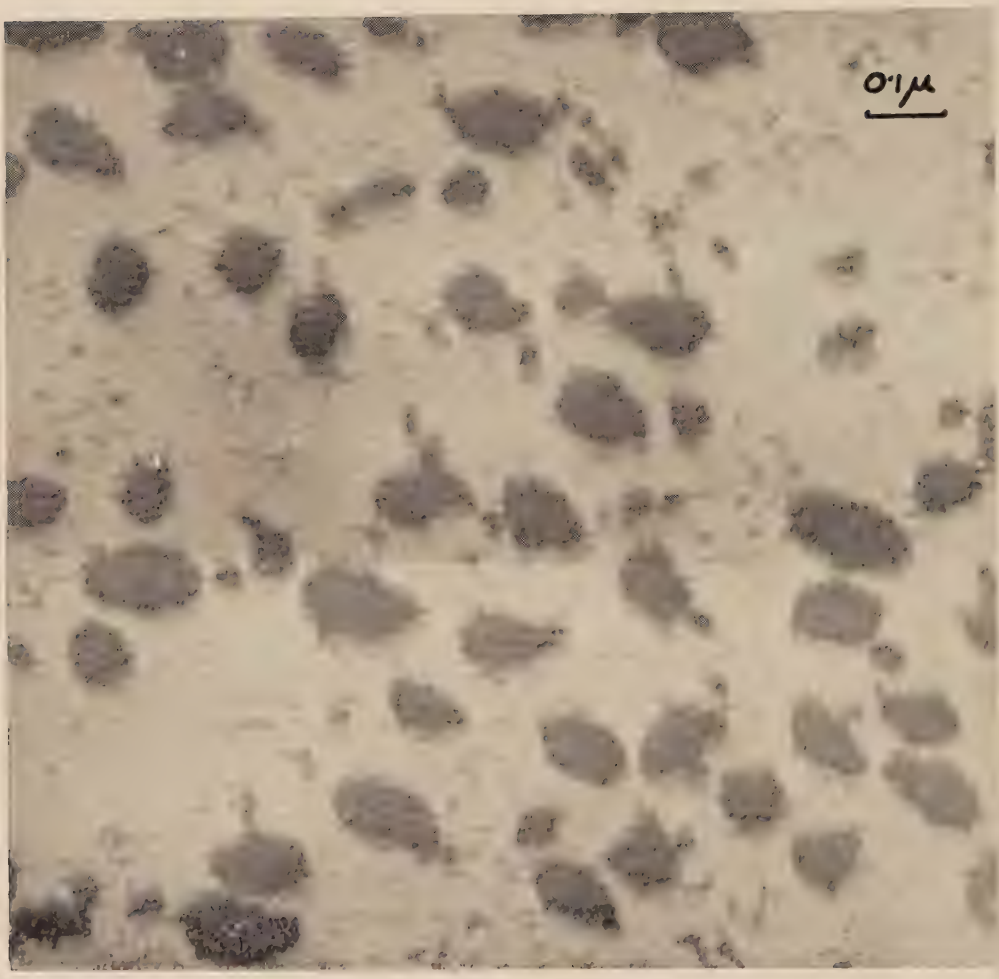

PLATE III. Electron micrograph of a cross-section of opaque oyster adductor muscle, showing the layered structure.

[*To face page* 43

though on appropriate stimulation it continues to give responses which resemble those shown by tetanized frog sartorius muscle (Hoyle & Lowy, 1956; Lowy & Millman, 1959). Accordingly, in some experiments with the ABRM, 5HT (to give 10^{-6} g/ml.) was added to the bathing solution once every 24 hr. As in the untreated muscle, it was found that during the experimental period of about 3 days, the muscle's rigidity did not change appreciably (Lowy & Millman, unpublished results). It is concluded that in the case of the ABRM, the experiments were done with muscles that were in a relaxed, non-tonic, condition.

3. Results

X-ray diffraction patterns of the muscles when alive showed vestiges of an equatorial streak, together with a single clear equatorial reflection at 122 $\pm$ 5 Å for the ABRM (Plate I) and translucent adductor, and at 125 $\pm$ 5 Å for the opaque adductor (Plate II(a)). When the muscle died the clear reflections disappeared, and the specimens then gave only the equatorial streak (Plate II(b)) which has been reported by Bear & Selby (1956) for dried and re-wetted adductor muscle from *Venus mercenaria*, and by Elliott (1958) for the formaldehyde-fixed opaque adductor from the Portuguese oyster.

Microdensitometer traces show that the equatorial spot is a clearly resolved Bragg reflection with a shape that is approximately Gaussian (Fig. 1). The standard deviation

Fig. 1. Microdensitometer trace of the equator of a pattern from living ABRM.

of this Gaussian line shape in the ABRM, corrected for the shape of the main beam, is about $1{\cdot}3 \times 10^{-3}$ Å^{-1} in the direction at right angles to the fibre axis.

When the ABRM was stretched about 20% and 40% above the length for maximum isometric tension (l_0) or shortened 20% below that length the equatorial spacing was unchanged within the limits of experimental error. The values obtained were:

$0{\cdot}8\, l_0$ — 125 $\pm$ 6 Å (Mean of 2 experiments)
$1{\cdot}0\, l_0$ — 122 $\pm$ 5 Å (Mean of 7 experiments)
$1{\cdot}2\, l_0$ — 124 $\pm$ 6 Å (Mean of 2 experiments)
$1{\cdot}4\, l_0$ — 122 $\pm$ 5 Å (Mean of 4 experiments)

All the errors quoted in this paper are estimated, and correspond roughly to the ranges of observed values. The standard error of the ABRM experiment at l_0 is $\pm$ 1 Å for seven determinations, but the reflections are somewhat difficult to measure, and it is considered that this standard error gives an over-optimistic view of the precision of the mean.

If the system giving the equatorial reflection had been stretched or shortened when working at constant volume, spacing changes of about 10% (for the 20% length change) and 19% (for the 40% length change) would have been expected. Such changes have been observed by Huxley (1952) and Elliott, Lowy & Worthington (unpublished results) in vertebrate striated muscle.

The meridional and near-meridional "paramyosin" reflections (Bear, 1944; Bear & Selby, 1956) were observed at 360 $\pm$ 5 Å, 240 $\pm$ 4 Å, and 144 $\pm$ 1 Å from all the muscles we have used *regardless of whether they were alive and relaxed or dead*. The line shapes of these reflections, at right angles to the fibre axis, were again found to be approximately Gaussian, and measurements of densitometer traces taken of the 144 Å reflection in the ABRM (from the same exposure as the equatorial reflections) showed a corrected standard deviation of about $1{\cdot}3 \times 10^{-3}$ Å^{-1}. The 144 Å meridional reflection is clearly seen in Plate I.

Exposure times were about 24 to 36 hr for the equatorial reflections, and at least 48 hr for the meridional and near-meridional reflections.

4. Discussion

Huxley (1952, p. 119) reported from living molluscan "paramyosin" muscles "the type of (transverse) pattern given by long scattering elements which are not arranged in a regular array. Measurements of the first minima and first subsidiary maxima indicate that the diffracting units are $\sim$ 150 Å in diameter in the adductor muscle, and $\sim$ 180 Å in the retractor" (both muscles were from *Mytilus edulis*). Dr. Huxley has kindly allowed us to inspect his negatives, and we consider that these "subsidiary maxima" could equally well be rather diffuse Bragg spacings, the positions of which agree approximately with our equatorial reflections.

Equatorial reflections in fibre diagrams are given by regularities at right angles to the fibre axis. What regularities in these muscles could give the equatorial reflections? We suggest that the reflections come from the planes of the "paramyosin" ribbons stacked face-to-face within the thick myofilaments and separated by 120 Å. The lamellar structure of the thick filaments in the opaque oyster adductor muscle was actually seen in accurate transverse sections in the electron microscope (Plate III) before the present work was started. The lamellar spacing was found to be 150 to 200 Å in the opaque part of the oyster adductor fixed in formaldehyde (Elliott, 1958, 1960), and about 100 Å in the translucent part fixed in osmium tetroxide (Hanson & Lowy, unpublished results). We suggest that the spacing *in vivo* is 120 Å, as shown by the equatorial X-ray reflections obtained from living muscles. It has been shown that "paramyosin" ribbons isolated by homogenizing these muscles can be very thin: seen on the electron microscope grid, ribbons over 1,000 Å wide have been found to measure as little as 100 to 120 Å in thickness (Elliott, 1960). Probably these ribbons have decreased in thickness whilst drying on the electron microscope grid. On the other hand the preparations are not monodisperse and perhaps a single lamella has not yet been measured. Some shadowed preparations show distinct layering.

The close agreement between line shapes (in the transverse direction with respect to the fibre axis) of the meridional and equatorial reflections in the ABRM suggests

that these reflections come from diffracting systems of the same size, in this case from two aspects of the thick "paramyosin" filaments. Calculations made by Elliott (1960) show that these shapes correspond to diffracting systems of about 500 Å in size, and this agrees well with the diameters (observed in the electron microscope) of the thick filaments, whose mean size is approximately 500 Å in the ABRM.

When "paramyosin" molluscan muscles are dried, diffuse equatorial reflections occasionally appear superimposed on the equatorial streak. These are variable in spacing and intensity, but the ones most often seen lie at 79 $\pm$ 4 Å, 60 $\pm$ 5 Å, and 49 $\pm$ 2 Å. The latter two spacings were observed first, and Elliott (1958) suggested tentatively that they might be orders of a spacing of about 200 Å, coming from the lamellae in the filament. However, very similar reflections have since been observed in a wide variety of dried muscles, including striated muscles (Elliott & C. R. Worthington, unpublished results) and it seems more likely that at least some of these reflections come not from the contractile apparatus but perhaps from lipoprotein aggregates produced when the muscle dries.

Some comment is called for about the meridional reflections in view of their relevance to the problem of a "catch" mechanism in these molluscan muscles. The adductor of the oyster, for instance, is well known for its highly developed tonic properties, i.e. it can maintain a steady high level of tension for long periods of time without any signs of fatigue. Thus the adductor can resist the pull of the springy hinge ligament which connects the valves of the shell and it can keep the shell closed for many hours and even days. Johnson, Kahn & Szent-Györgyi (1959) have put forward the idea that the tonic response of such muscles is due to a molecular "catch" mechanism mediated by "crystallization" of "paramyosin" *in vivo*. This was supported by the observation (Johnson & Philpott, 1959) that the 145 Å axial periodicity observed in "paramyosin" elements in the electron microscope was usually absent in specimens of the ABRM fixed while in a relaxed state. (Dr. Johnson informs us that the specimens were treated with 5HT to prevent a tonic response.) However, Hanson & Lowy (1959*a*) report that this fine structure is equally visible in electron micrographs of the ABRM fixed while relaxed or during a tonic response. The present finding of "paramyosin" reflections in the living 5HT-treated ABRM, i.e. in a muscle incapable of giving a tonic response, clearly demonstrates that the organized "paramyosin" network of scattering centres is in existence under these conditions. This again is not in agreement with the version of the "catch" mechanism hypothesis proposed by Johnson *et al.* (1959), Ruegg (1959) and Philpott *et al.* (1960). In fact other structural evidence argues in favour of a sliding filament contractile mechanism in "paramyosin" molluscan muscles (*cf* Hanson & Lowy, 1959*a*,*b*). In muscles that contract by such a mechanism the thick filaments do not extend from one end of the fibre to the other, and it is therefore difficult to see how tension in a tonic response could be maintained by crystallization of the protein in the "paramyosin" filaments. The present results help to eliminate this possibility.

We wish to thank Professor J. T. Randall for his constant encouragement, Dr. Jean Hanson and Dr. H. E. Huxley for stimulating discussions, and Dr. M. H. F. Wilkins for several helpful suggestions.

REFERENCES

Abbott, B. C. & Lowy, J. (1956). *J. Mar. Biol. Ass. U.K.* **35**, 521.
Abbott, B. C. & Lowy, J. (1958). *J. Physiol.* **141**, 398.
Bear, R. S. (1944). *J. Amer. Chem. Soc.* **66**, 2043.
Bear, R. S. & Selby, C. C. (1956). *J. Biophys. Biochem. Cytol.* **2**, 55.
Elliott, G. F. (1958). Proc. IVth Int. Conf. Electron Microscopy Berlin (Springer) 328.

Elliott, G. F. (1960). Ph.D. Thesis, University of London.
Elliott, G. F., Hanson, J. & Lowy, J. (1957). *Nature*, **180**, 1291.
Franks, A. (1956). *Proc. Phys. Soc. Lond.* B, **68**, 1054.
Franks, A. (1958). *Brit. J. Appl. Phys.* **9**, 349.
Hall, C. E., Jakus, M. A. & Schmitt, F. O. (1946). *Biol. Bull.* **90**, 32.
Hanson, J. & Lowy, J. (1959*a*). *J. Physiol.* **149**, 31P.
Hanson, J. & Lowy, J. (1959*b*). *Nature*, **184**, 286.
Hanson, J., Lowy, J., Huxley, H. E., Bailey, K., Kay, C. M. & Ruegg, J. C. (1957). *Nature*, **180**, 1134.
Hoyle, G. & Lowy, J. (1956). *J. Exp. Biol.* **33**, 295.
Huxley, H. E. (1952). Ph.D. Thesis, University of Cambridge.
Huxley, H. E. (1957). *J. Biochem. Biophys. Cytol.* **3**, 631.
Johnson, H. W., Kahn, J. S. & Szent-Györgyi, A. G. (1959). *Science*, **130**, 161.
Johnson, H. W. & Philpott, D. E. (1959). *Abstr. Amer. Biophys. Soc.* Pittsburgh, 1959.
Lowy, J. (1955). *Nature*, **176**, 345.
Lowy, J. & Millman, B. M. (1959). *Nature*, **183**, 1730.
Philpott, D. E., Kahlbrock, M. & Szent-Györgyi, A. G. (1960). *J. Ultrastructure Res.* **3**, 254.
Ruegg, J. C. (1959). *Biochim. biophys. Acta*, **35**, 278.
Twarog, B. M. (1954). *J. Cell. Comp. Physiol.* **44**, 141.

J. Mol. Biol. (1961) **3**, 47–60

The Reaction of Formaldehyde with Nucleotides and T2 Bacteriophage DNA

Lawrence Grossman, Stephen S. Levine and William S. Allison

The Graduate Department of Biochemistry, Brandeis University, Waltham, Massachusetts, U.S.A.

(*Received 30 August 1960*)

The mechanism of ribo- and deoxyribonucleotide reaction with formaldehyde has been examined with respect to kinetics, pH optima and structural specificity. Formaldehyde reacts only with those nucleotides bearing amino groups. The equilibrium constants for the reaction as well as the rate of the forward and reverse directions have been described. The difference between the reactivity of the ribo- and deoxyribo-nucleotides toward formaldehyde is negligible with the exception of the guanine ribo- and deoxyribo-nucleotides. That 5′-dGMP reacts at a faster rate than 5′-GMP has been attributed to a steric interference of the amino group hydroxymethylation and protonation by the 2′-hydroxyl group. Moreover nucleotide hydroxymethylation appears to be pH-dependent since the reaction is base-catalysed. The effect of formaldehyde on DNA thermal transitions was studied using spectrophotometric, viscometric and immunological methods. Hydroxymethylation is preceded by denaturation and lowers the temperature requirements for thermal transition. The depression of the temperature requirement for denaturation of bacteriophage DNA is attributed to the interference by formaldehyde of the equilibrium between native and denatured DNA by hydroxymethylation of the amino nitrogens associated with the purine and pyrimidine rings.

1. Introduction

The hypothetical structure of DNA proposed by Watson & Crick (1953) and Crick & Watson (1954) depicts DNA as consisting of two complementary strands attached through hydrogen bonds directed by single base pairing. Such a structure is imposed by the nature of the single-stranded polymers and is sensitive to heat and pH denaturation (Rice & Doty, 1957; Gulland, Jordan & Taylor, 1947; Creeth, Gulland & Jordan, 1947; Ehrlich & Doty, 1958). The concept that complementary strands of DNA separate during thermal transitions has been offered by Doty, Marmur, Eigner & Schildkraut (1960) and Marmur & Lane (1960). They further suggest that after thermal denaturation the rate at which the temperature is reduced apparently controls the point of equilibrium governing the union of the complementary strands. Thus, according to this hypothesis, slow cooling rates provide for renaturation whereas rapid cooling, temporarily at least, prevents reformation of the hydrogen-bonded structure. If, therefore, masking of the responsible hydrogen bonds by specific chemical reagents could be achieved, then reformation should be effectively blocked permitting the "single-stranded" species to be preserved.

Formaldehyde has long been used as an amino-group reagent for amino acids and proteins. Fraenkel-Conrat (1954) first extended the use of formaldehyde to show that

the amino groups of purines and pyrimidines are susceptible to formaldehyde addition, and that such a reaction is accompanied by spectral alterations. The contents of this communication describe the usefulness of this reagent in interfering with the equilibrium between denatured and native DNA.

2. Materials and Experimental Methods

(a) *Materials*

5′-AMP, 5′-GMP, 5′-CMP and 5′-IMP were obtained from The California Foundation for Biochemical Research. 5′-dAMP, 5′-dGMP, 5′-dCMP and 5′-TMP were purchased from the Sigma Chemical Company. T2 bacteriophage was generously provided by Dr. Helen Van Vunakis.

(b) *Isolation of DNA by phenol extraction*

(Alexander, Koch, Mountain & Van Damme, 1958)

DNA was isolated from the bacteriophage by shaking 1×10^{12} phage particles/ml. for 15 min at 37°C with an equal volume of freshly distilled phenol which had been saturated with 0·01 M-potassium phosphate buffer pH 7·0. The mixture was centrifuged at 20,000 ***g*** for 15 min and the aqueous layer poured into a separatory funnel. The residual phenol layer was discarded. The aqueous DNA layer was further re-extracted twice with equal volumes of the phosphate buffer-saturated phenol mixture. The final aqueous DNA layer was extracted 3 times with 4 vol ether. The ether was removed from the viscous DNA solution by bubbling nitrogen through the mixture with constant stirring. When the presence of ether could no longer be detected in the preparation 2 vol 100% ethanol were added. The precipitated DNA was adsorbed to a glass stirring rod and washed several times with ethanol until the washings were clear. The DNA was suspended in 0·85% NaCl and solution effected by slowly rotating the preparation in a graduated cylinder.

(c) *Isolation of DNA by detergent extraction*

(Kay, Simmons & Dounce, 1952)

Five grams of sodium lauryl sulfate recrystallized from hot ethanol were dissolved in 100 ml. 45% ethanol. A final concentration of 0·5% detergent solution was added with stirring to the DNA solution obtained from phenol extraction. Stirring was continued for 3 hr after which 28 g solid NaCl were added. Stirring, continued for 10 min, was followed by centrifugation at 15,000 ***g*** for 30 min. The sedimented protein was discarded. The DNA was precipitated from the supernatant fluid with 2 vol ethanol and the washed, precipitated DNA dissolved in 0·85% NaCl. The concentration of DNA was determined by the diphenylamine reaction of Burton (1956) and protein contamination estimated by the method of Lowry, Rosebrough, Farr & Randall (1951). The DNA preparations used in these studies contained no protein estimated by the latter colorimetric method. However, amino acid analysis on the Moore & Stein amino acid analyzer revealed a 0·5% amino acid contamination of this DNA preparation.

(d) *The purification of formaldehyde*

The formaldehyde solutions were prepared initially by distilling an acidified paraformaldehyde solution. The freshly distilled formaldehyde was stored in dark bottles and refrigerated. Stock solutions of formaldehyde consisted of a final concentration of 10% in ionic strength 0·10 buffer at the desired pH. It was subsequently found that commercial preparations of formaldehyde solutions were adequate for hydroxymethylation reactions with both nucleotides and DNA.

(e) *Spectrophotometric determinations*

Spectral determinations were obtained on the Carey recording spectrophotometer using quartz cells with a 1 cm light path.

Kinetic analyses of nucleotide hydroxymethylations were carried out in the Zeiss spectrophotometer at room temperature. Kinetic experiments at elevated temperatures were performed by heating samples for varying time periods followed by chilling. The absorbance of the cooled samples was determined in the Beckman DU spectrophotometer.

The concentration of nucleotides for all kinetic experiments was maintained at 5×10^{-4} M in buffer of ionic strength 0·10. The DNA solutions used for absorbance studies were kept at 0·05% final concentration in 0·10 ionic strength potassium phosphate buffer.

(f) *Intrinsic viscosity determinations*

The intrinsic viscosity was obtained by plotting values of η_{sp}/c values at concentrations from 10 to 75 μg/ml. at a number of different gradients. The DNA solutions were dissolved in 0·1 M-potassium phosphate buffer pH 8·0. An Ostwald micro-viscometer of low shear was employed for all viscometric determinations.

(g) *Immunochemical analysis*

Antigenic activity was determined by the use of quantitative complement (C′) fixation technique (Levine, Barlow & Van Vunakis, 1958) with antisera obtained against bacteriophage DNA (Levine, Murakami, Van Vunakis & Grossman, 1960*b*).

3. Experimental Results

(a) *Kinetic experiments*

The reaction of formaldehyde with amino groups associated with purines and pyrimidines is accompanied by shifts in the ultraviolet absorption spectra to higher wavelengths as well as by alterations in hyperchromic absorbance. An examination of the spectral differences between the hydroxymethylated and non-hydroxymethylated nucleotides revealed wavelengths at which there were differences of absorption between the two species. These difference spectra (see Fig. 1) show that a common wavelength region of absorption difference for the formaldehyde reaction occurs between 275 and 280 mμ.

The kinetics of the formaldehyde reaction with the mononucleotides were examined, and the rate constants and equilibrium constants were defined. All kinetic experiments were conducted under apparent pseudo first-order conditions in which the formaldehyde concentration was in excess. The rate experiments were followed at 275 mμ. It was assumed that the increase in absorbance at this wavelength was directly proportional to the concentration of the hydroxymethylated nucleotide. In addition, at this wavelength the absorbance of the unreacted nucleotide did not vary significantly with concentration. With these assumptions the rate expression for the spectrophotometric determination of rate approach to equilibrium can be written:

$$-k't = \ln \frac{A_e - A_t}{A_e - A_o}$$

where A_e = the absorbance difference at 275 mμ measured at equilibrium
A_o = the absorbance of the free nucleotide at 275 mμ
A_t = the absorbance difference at 275 mμ measured at time t
k' = the forward rate constant

By measuring the increase in absorbance at 275 mμ and then plotting

$$\ln (A_e - A_t / A_e - A_o)$$

against time a straight line is obtained, the slope of which is k'. Such a plot at pH 7·05 is shown in Fig. 2.

The equilibrium constant was determined by the following method. A constant concentration of each nucleotide was incubated with increasing concentrations of formaldehyde to saturation levels until equilibrium was reached. The

$$(A_e - A_o)_{obs}/(A_e - A_o)_{max}$$

was calculated and termed α, where α is proportional to the concentration of the

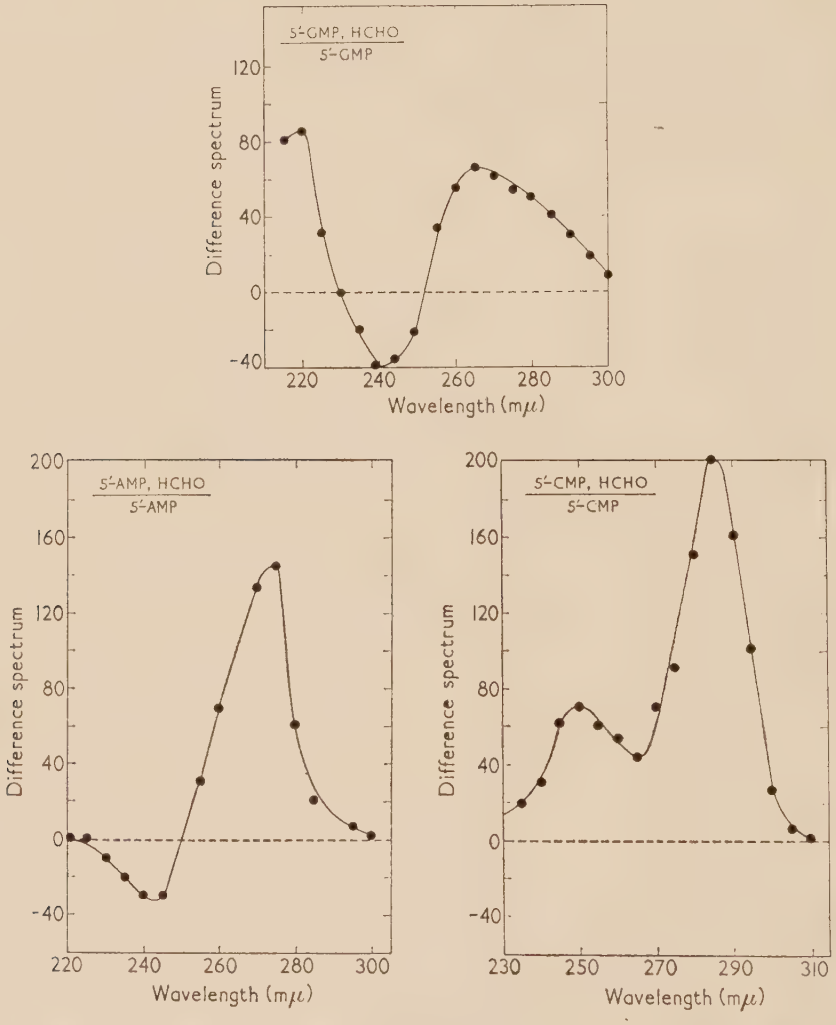

FIG. 1. Difference spectrum of 5′-GMP, 5′-AMP, 5′-CMP and their hydroxymethylated derivatives. Spectra were obtained on the Cary recording spectrophotometer of 5×10^{-4} M solutions of the nucleotides in 0·10 M-potassium phosphate buffer pH 8·5. The hydroxymethylated nucleotides contained 1% formaldehyde in the above buffer. The difference spectra were obtained by determining the absorbance of each nucleotide over the entire spectrum and subtracting the non-hydroxymethylated spectrum.

modified nucleotide at equilibrium. The equilibrium constant was then calculated using the following expression:

$$K = \frac{\alpha}{(1 - \alpha)\,[\mathrm{HCHO}]}$$

By calling k' the apparent rate constant for approach to equilibrium, k'', the reverse rate constant, was calculated. The equilibrium constants at pH 7·05 and reverse rate constants at this pH are shown in Table 1.

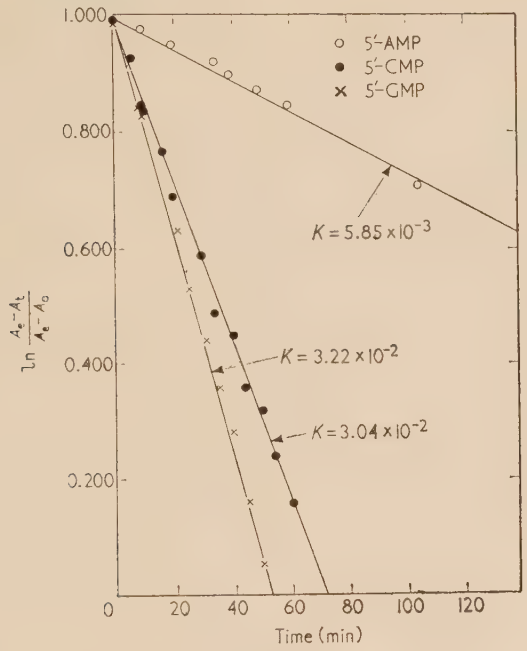

FIG. 2. Pseudo first-order kinetics of nucleotide reaction with formaldehyde. Solution of 5×10^{-4} M nucleotides in 0·10 M-potassium phosphate buffer, pH 7·05 and 1% formaldehyde were incubated in the Zeiss spectrophotometer at 275 mμ. The reactions were permitted to come to equilibrium and the absorbance defined as A_e.

TABLE 1

The equilibrium and rate constants for hydroxymethylation of nucleotides at pH 7·05

Nucleotide	$k' \times 10^2$, min^{-1}	$k'' \times 10^3$, min^{-1}	K
5′-AMP	0·585	0·51	11·4
5′-dAMP	1·20	1·06	11·3
5′-CMP	3·04	1·83	16·6
5′-dCMP	4·20	2·71	15·5
5′-GMP	3·50	6·60	5·3
5′-dGMP	1·30	0·29	45·0

The rate constants were little effected by buffers where concentration varied over a wide range of ionic strengths.

(b) *Effect of pH on the hydroxymethylation reaction*

The reaction of formaldehyde with the amino groups of amino acids is inhibited at pH values within the pK range of the primary amino group. The pK values for

purine and pyrimidine amino groups are 2·40 for guanine, 3·70 for adenine and 4·50 for cytosine nucleotides. The formaldehyde reaction, therefore, should occur in pH ranges approaching neutrality. However, hydroxymethylation of the purine and pyrimidine nucleotides is influenced by pH values above neutrality (Fig. 3). The rate

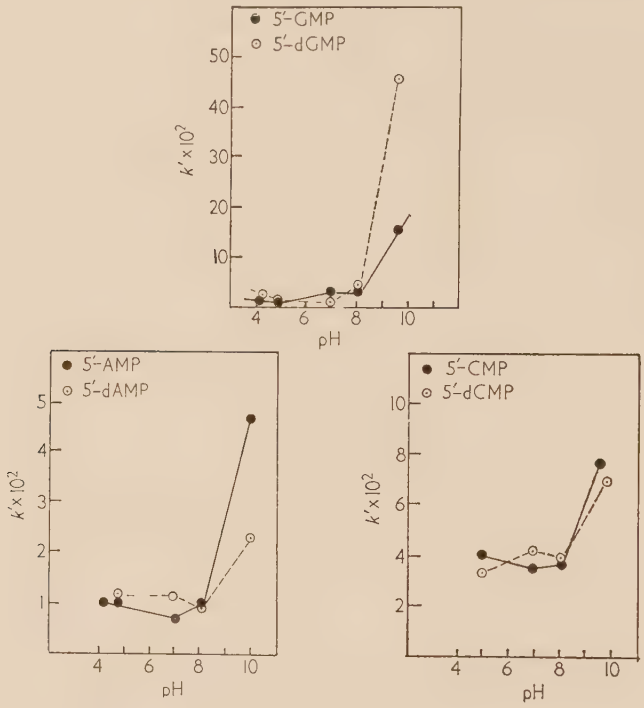

Fig. 3. The pH profile for nucleotide reaction with formaldehyde. Solutions of 5×10^{-4} M-nucleotide were incubated in the Zeiss spectrophotometer. The buffers employed were as follows: below pH 6, 0·10 M-acetate buffer; from pH 6 to pH 8, 0·10 M-phosphate buffer; and above pH 8, 0·10 M-carbonate buffer. The reactions were permitted to come to equilibrium and the absorbance at 275 mμ defined as A_e. The forward rate constants were obtained from the method described in the text.

constants of formaldehyde reaction with the nucleotides are increased in the presence of increasing hydroxyl ion concentrations and as such appears to be base-catalysed under alkaline conditions and not catalysed at neutral pH or below.

Of further interest is the difference in reaction between 5′-GMP and 5′-dGMP and formaldehyde under alkaline conditions. From stereochemical molecular models of guanosine and deoxyguanosine it is apparent that the 2′-hydroxyl group is sufficiently close to the purine amino group to form a hydrogen bond. Steric influence can also account for the differences in the pK values of the purine amino group. The pKs for the ionization of the amino group of guanosine and deoxyguanosine were measured spectrophotometrically in 0·1 M-HCl–KCl buffers ranging in pH from 1·6 to 3·40 and at constant ionic strength. The pK obtained for the amino group of deoxyguanosine was 2·80, whereas the pK for the same group on guanosine was determined to be 2·15. Values for the ionization of the 5′-GMP amino group have been reported by Cohn (1955) to be 2·3 when obtained spectrophotometrically, whereas Hurst, Marko & Butler (1953) obtained a value of 2·90 from electrometric titrations of 5′-dGMP. It

would appear then that the 2′-hydroxyl group can influence the approach of a proton to the amino group on the purine ring. By analogy it appears feasible for the 2′-hydroxyl group to influence the addition of a formaldehyde molecule to the same amino group. The pK data in addition to the rate differences for the reaction with formaldehyde appears to be parallel.

(c) *The reaction of formaldehyde with denatured bacteriophage T2 DNA*

Solutions of bacteriophage DNA (0·05% in 0·1 M-potassium phosphate buffer pH 8·5) were heated at varying temperatures for 15 min either in the presence or absence of formaldehyde (final concentration of 1%). The stock solutions of formaldehyde were made up to 10% in potassium phosphate buffer at the same concentration and pH as that employed for the DNA solution. Following the period of heating, the DNA solutions were cooled quickly. The absorbance of the chilled samples was determined in the Beckman DU spectrophotometer at 260 and 275 mμ at room temperature. These data (Fig. 4) indicate that the temperature profile of denaturation is shifted to

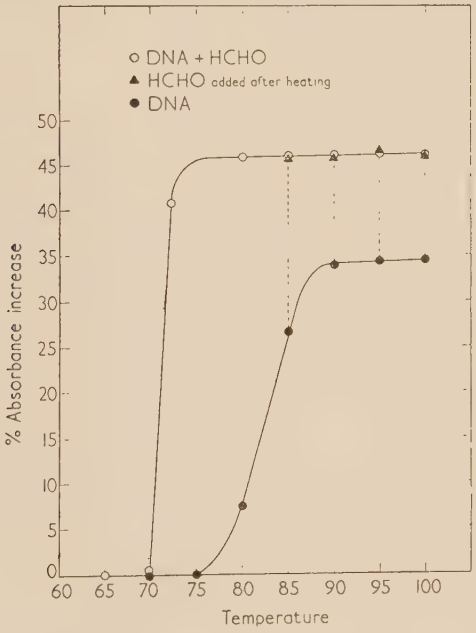

Fig. 4. The effect of formaldehyde on the temperature profile of DNA heat denaturation. Solutions of bacteriophage DNA (0·05% in 0·10 M-potassium phosphate buffer pH 8·5) were heated for 15 min and cooled rapidly. The final concentration of formaldehyde employed was 1%, taken from a stock solution of 10% formaldehyde in 0·10 M-potassium phosphate buffer pH 8·5.

lower temperatures in the presence of formaldehyde. That formaldehyde itself was not causing any additional denaturation was shown by adding formaldehyde to the DNA following heat denaturation. The absorbance of this DNA solution was essentially the same as that of the DNA which had been heated in the presence of formaldehyde. From this information it can be inferred that the amino groups associated with the DNA do not become available for reaction with formaldehyde until the molecule has been denatured. These data are consistent with the hypothesis that hydrogen bonds,

linked through the amino groups, provide for the stability of native DNA. Heating sufficient to break such bonds must cause a marked change in the helical structure, making available new groups originally refractive to formaldehyde. The fact that denatured DNA can react with formaldehyde does not imply that heating necessarily causes complete strand separation. Were it possible to determine the exact number of nucleotides hydroxymethylated within the polymer, then some estimate might be made as to the extent of strand separation.

(d) *The effect of formaldehyde on the viscosity of DNA*

Intrinsic viscosity was determined at varying temperatures to verify the influence of formaldehyde in lowering the temperature profile. These data (Fig. 5) are in accord

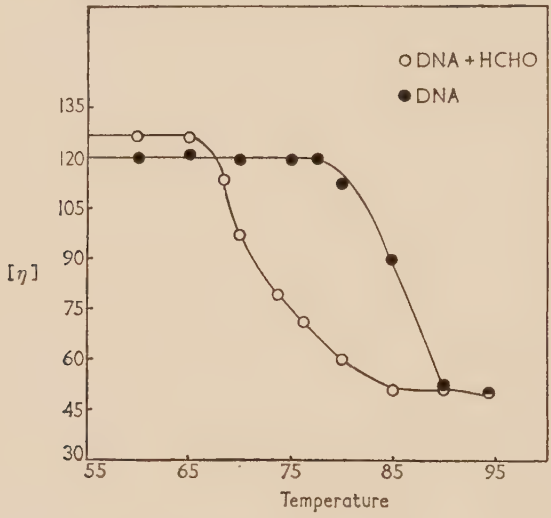

Fig. 5. The effect of formaldehyde on the intrinsic viscosity as a measure of DNA heat denaturation.

with those obtained spectrophotometrically (Fig. 4). The final intrinsic viscosities of the two samples are identical, indicating that formaldehyde causes no further denaturation.

(e) *Immunochemical analysis of heat denaturation*

It has been shown that heat denatured bacteriophage DNA is antigenic (Levine *et al.*, 1960*b*). The antigenic sites are presumably masked in native DNA and require heat denaturation for full activity to be demonstrated (Murakami, Van Vunakis, Grossman & Levine, 1960). Complement fixation was employed to determine the influence of formaldehyde on heat denaturation of bacteriophage DNA. From the results, shown in Fig. 6, it can be seen that the profile obtained is identical to that of the spectrophotometric and viscometric measurements of the same process.

(f) *Kinetics of DNA hydroxymethylation and denaturation*

Staehelin (1958) indicated that hydroxymethylation of TMV-RNA is apparently a biphasic reaction in which formaldehyde initially denatures RNA and then proceeds to react with the newly exposed groupings. These experiments, however, were carried

out in the presence of formaldehyde for periods ranging from 18 to 48 hr. For time periods of this length it is possible that formaldehyde could exert a non-specific effect

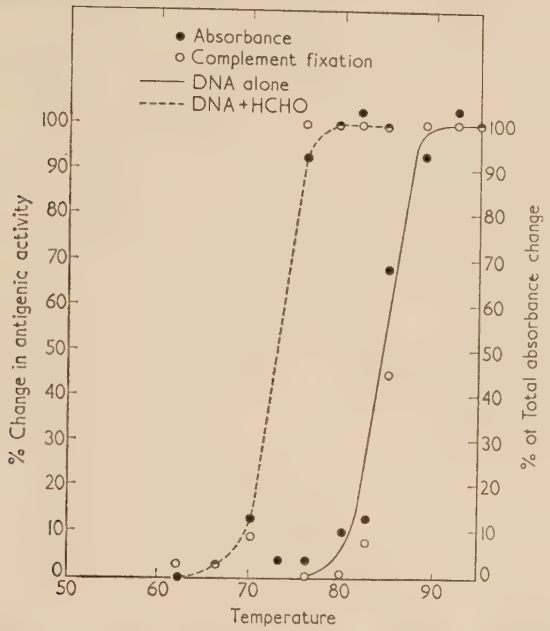

FIG. 6. Immunochemical analysis of heat denaturation. Solutions of bacteriophage DNA (0·05% in 0·10 M-potassium phosphate buffer pH 8·2) were heated at varying temperatures for 15 min and diluted immediately into ice-cold isotonic saline for complement fixing activity. Spectrophotometric determinations were applied directly to the undiluted cold DNA samples. The final concentration of formaldehyde employed was 1%. The values are expressed in terms of percentage of the maximum complement fixing activity or absorbance at 260 mμ.

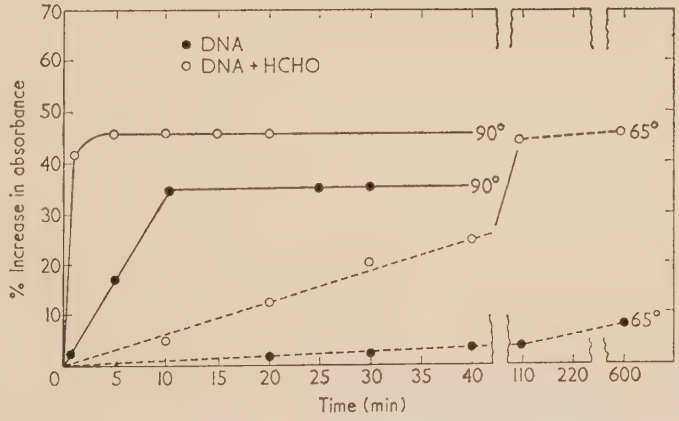

FIG. 7. The kinetics of bacteriophage DNA hydroxymethylation and heat denaturation. Solutions of bacteriophage DNA (0·05% in 0·10 M-potassium phosphate buffer pH 8·50) were heated at 90°C and 65°C for the times indicated. At the end of the heating period the samples were removed and chilled immediately. The absorbance of the hydroxymethylated samples was determined at 275 mμ whereas the absorbance of non-hydroxymethylated samples was measured at 260 mμ.

on the structure of nucleic acids independent of its reaction with the amino groups. From the previous experiments (Fig. 4) it is apparent that formaldehyde addition for

short periods (up to 15 min) to denatured bacteriophage DNA caused no further spectral changes. In addition, sedimentation analysis of denatured and hydroxymethylated DNA revealed no significant differences in molecular weight. Thus, exposure of DNA to formaldehyde for short periods under optimum conditions for hydroxymethylation did not result in further denaturation. In Fig. 7 the kinetics of the heat denaturation reaction are depicted. It can be seen that the reaction is essentially monophasic with no contribution by formaldehyde to denaturation. At temperatures of 65°C or below, where essentially no hyperchromic effect is observed, the influence of formaldehyde is quite marked. The point of equilibrium is unchanged by the formaldehyde since the increase in hyperchromicity over that of the control samples is due to the normal absorbance of the formaldehyde addition product.

(g) *The influence of formaldehyde on the renaturation of heat denatured DNA*

Marmur & Lane (1960) and Doty *et al.* (1960) postulated that denatured DNA if cooled at a slow rate following denaturation will essentially renature or recombine

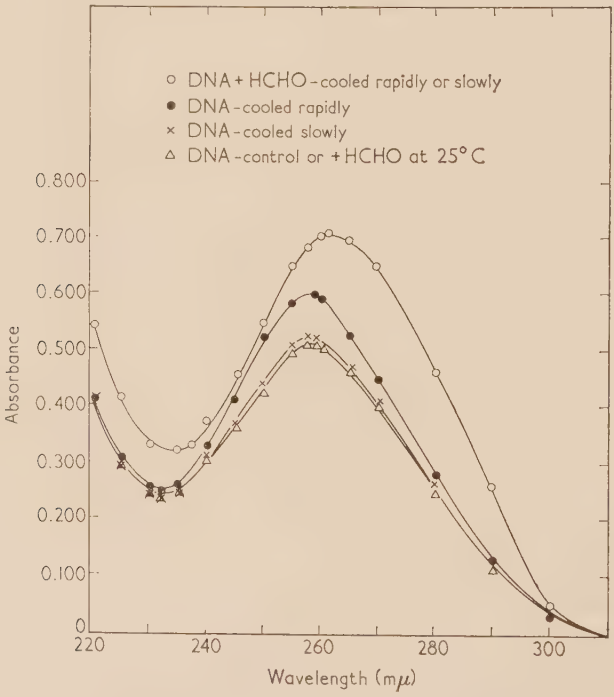

Fig. 8. The influences of formaldehyde on the spectra of native and heat denatured bacteriophage DNA. Solutions of bacteriophage DNA (0·05% in 0·10 M-potassium phosphate buffer pH 8·5) were heated to 100°C for 10 min either in the absence or presence of 1% formaldehyde. The heated samples were cooled slowly by maintaining the heated DNA samples at 55°C for 30 min. Rapidly cooled samples of DNA were chilled immediately after the period of heating by immersing in an ice water bath. The spectra of these samples were determined at room temperature.

strands. The mechanism of renaturation and the structure of the renatured products are, however, unknown. From the physical as well as the biological data it would appear that the product bears a reasonable likeness to the native DNA.

DNA solutions were heated at 100°C for 10 min followed by cooling at varying rates

and the spectra were compared with similar solutions in which formaldehyde was present. These experiments (Fig. 8) indicated that DNA which had been cooled slowly possessed an absorption spectrum which was not too different from that of the native DNA. Rapidly cooled DNA possessed an absorption spectrum which was different from that of the control; presumably this represented the denatured species of the DNA. However, formaldehyde tended to "fix" the spectrum associated with the denatured species independent of the rate of cooling.

Dialysis of the hydroxymethylated DNA overnight against 0·1 M-phosphate buffer pH 8·5 restored the spectrum to that of the control (Fig. 9). Therefore, removal of the

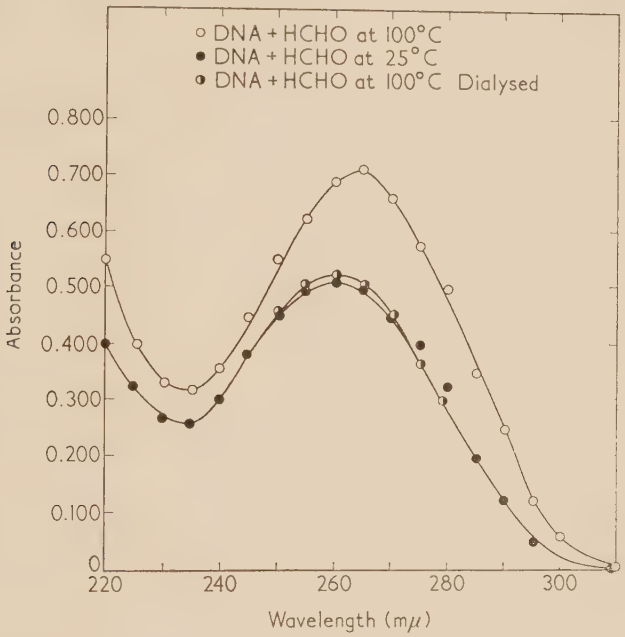

FIG. 9. The effect of dialysis on the spectrum of hydroxymethylated bacteriophage DNA. The experimental conditions employed were essentially those described in the legend for Fig. 8 with the exception that the hydroxymethylated DNA was dialysed overnight against 0·10 M-potassium phosphate buffer pH 8·5. The dialysed samples were heated to 100°C and incubated at 55°C for 30 min.

formaldehyde groups then permitted reformation of the spectrum associated with the native DNA.

The effect of renaturation was also demonstrable immunochemically. Solutions of DNA were heated to 100°C for 10 min and then incubated at 55°C for a period up to 120 min. Samples were withdrawn at various times and assayed by complement fixation for antigenic activity. It can be seen from Fig. 10 that DNA that had been heated and then maintained at 55°C for an extended period gradually lost 70% of its antigenic activity. The loss of immunological activity was not observed with the DNA heated with formaldehyde. The immunological requirement for denaturated DNA indicates that the responsive sites on the antigen reside within the internal regions of the native species prior to heating. Slow cooling of the heated DNA resulted in loss of antigenicity. It may be inferred from these results that those antigenic sites

previously exposed by heat are masked on renaturation and are no longer available to antibody molecules.

The 30% activity remaining after renaturation may represent a non-identical matching of the DNA strands, or it may represent the equilibrium concentration of denatured DNA molecules. This difference, not observable spectrophotometrically, is quite significant when measured immunochemically. From previous data (Murakami *et al.*, 1960) the antigenic sites on T4 DNA appeared to be located at one end of

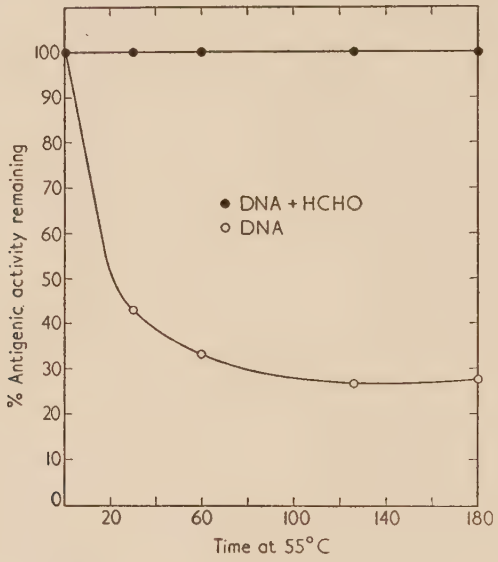

FIG. 10. The effect of formaldehyde on the complement fixing ability of "renatured" bacteriophage DNA. Solutions of bacteriophage DNA (24 μg/ml. in 0·01 M-potassium phosphate buffer pH 8·2) were heated to 100°C for 10 min and incubated at 55°C for 30 min. The samples were diluted to 1 μg/ml. with cold isotonic saline and complement-fixing activity determined.

TABLE 2

The intrinsic viscosity of renatured DNA solutions

Experimental conditions	Intrinsic viscosity	
	− HCHO	+HCHO
1. Incubation at 29°C	130·0	132·0
2. Incubation at 90°C	37·2	37·2
3. (2) followed by slow cooling	93·6	47·7
4. (2) followed by fast cooling	48·2	47·3

the nucleic acid chain. The electron micrographs of renatured DNA reported by Doty *et al.* (1960) showed incomplete end-portions of the molecule. Perhaps there are sufficient end-groups exposed for approach and attachment of antibody molecules.

The effect of formaldehyde in stabilizing denatured DNA has also been measured viscometrically, employing the conditions of measurement described in a previous section of this communication. DNA was heated to 90°C for 15 min and cooled either

slowly or rapidly. The effect of formaldehyde on this process is seen in Table 2. The loss of viscosity associated with denaturation was partially reversible depending on the conditions of cooling following the period of thermal transition. The addition of formaldehyde again blocked this equilibrium when observed by an additional experimental parameter.

4. Discussion

The reaction of formaldehyde with nucleotides appears to be reasonably specific in that hydroxymethylation was evident only with those nucleotides bearing amino groups. Thymidylic acid, thymidine, uridylic acid, uridine, inosinic acid and inosine were refractive toward the addition of formaldehyde. The reaction with the receptive nucleotides is reasonably rapid, with the equilibrium tending in the direction of hydroxymethylation. The spectral alterations associated with hydroxymethylation provide an easy tool for measuring the extent of reaction of a given nucleotide. In addition these spectral alterations are significantly different from those associated with the heat denaturation of DNA. This provides a measure for discriminating between denaturation, which can be followed at 260 mμ, and hydroxymethylation, which can be determined between 270 and 280 mμ. The reaction of formaldehyde with the nucleotides is base-catalysed, and increases markedly with temperature. The hydroxymethylation of the mononucleotides obeys first-order kinetics when formaldehyde is present in excess, and as such it differs from the same reaction with amino acids (French & Edsall, 1945).

Whether the amino group on the purine and pyrimidine ring is the site of hydroxymethylation, or whether reaction occurs on the ring nitrogen, cannot be determined from these data. The fact that only purine and pyrimidines bearing amino groups are receptive to formaldehyde does not necessarily preclude that hydroxymethylation is directed to a ring nitrogen by nucleophilic groups such as an amino group, whereas electrophilic groups such as carbonyls may retard reaction with formaldehyde.

Since the site of hydroxymethylation on the purine or pyrimidine ring cannot be assigned with any degree of certainty, it is not possible to make any assumption as to the number of nucleotide molecules reacting with saturating levels of formaldehyde. Therefore, the use of an extinction coefficient for the nucleotide hydroxymethylation as a means of determining the total number of reacting mononucleotides within a polymer appears not to be feasible.

The fact that DNA which has been denatured by heat can renature implies that the heat denaturation process is a reversible one. At a constant ionic strength and nucleic acid concentration the direction of the reaction depends to a great extent upon the temperature as well as the rate of cooling following thermal transition. At temperatures where essentially no change in the DNA absorption spectrum occurs, the reaction of DNA with formaldehyde is easily demonstrable either spectrophotometrically, viscometrically or immunochemically. Under these conditions it is possible that formaldehyde is reacting with a small proportion of the total DNA molecules existing in a non-hydrogen bonded form. Formaldehyde-treated nucleic acid would then be trapped in the non-hydrogen bonded form thereby inhibiting renaturation. Similarly hydroxymethylation could interfere with the reverse reaction either by sterically hindering the formation of hydrogen bonds or by causing a derangement in the necessary configurational requirements for renaturation.

Doty and Marmur (Doty, *et al.*, 1960; Marmur & Lane, 1960) have interpreted heat denaturation as strand separation, and renaturation as strand recombination. The data presented in this communication are consistent with their interpretation to the extent that heat denaturation causes some separation of the strands. Whether separation is complete, occurs in the middle of the chain, or affects only a proportion of the molecule, can only be answered by more quantitative measures. The reaction with formaldehyde only requires that the groupings involved in hydrogen bond linkages be broken for hydroxymethylation.

This work was supported by grants from the National Institutes of Health (C 3572) and from the National Science Foundation (G 4551). Portions of this work were presented at the 44th Annual Meeting of The Federation of American Societies for Experimental Biology, April, 1960 (Levine, Grossman & Simon). We would also like to express our appreciation to Dr. Helen Van Vunakis for her help with the amino acid analysis experiments and to Dr. Lawrence Levine for his help with the immunological experiments. Contribution No. 80 in the series "Publications of the Graduate Department of Biochemistry, Brandeis University."

REFERENCES

Alexander, H. E., Koch, G., Mountain, I. M. & Van Damme, O. (1958). *J. Exp. Med.* **108**, 493.

Burton, K. (1956). *Biochem. J.* **62**, 315.

Cohn, W. E. (1955). In *The Nucleic Acids*, ed. by E. Chargaff & J. N. Davidson, Vol. I, p. 217. New York: Academic Press.

Creeth, J. M., Gulland, J. M. & Jordan, D. O. (1947). *J. Chem. Soc.* 1141.

Crick, F. H. C. & Watson, J. D. (1954). *Proc. Roy. Soc.*, A. **223**, 80.

Doty, P., Marmur, J., Eigner, J. & Schildkraut, C. (1960). *Proc. Nat. Acad. Sci., Wash.* **46**, 461.

Ehrlich, P. & Doty, P. (1958). *J. Amer. Chem. Soc.* **80**, 4251.

Fraenkel-Conrat, H. (1954). *Biochim. biophys. Acta*, **15**, 307.

French, D. & Edsall, J. T. (1945). *Advanc. Protein Chem.* **2**, 277.

Gulland, J. M., Jordan, D. O. & Taylor, H. F. W. (1947). *J. Chem. Soc.* 1131.

Hurst, R. O., Marko, A. M. & Butler, G. C. (1953). *J. Biol. Chem.* **204**, 847.

Kay, E. R. M., Simmons, N. S. & Dounce, A. L. (1952). *J. Amer. Chem. Soc.* **74**, 1724.

Levine, L., Barlow, J. L. & Van Vunakis, H. (1958). *Virology*, **6**, 702.

Levine, S. S., Grossman, L. & Simon, M. (1960*a*). *Fed. Proc.* **19**, 307.

Levine, L., Murakami, W. T., Van Vunakis, H. & Grossman, L. (1960*b*). *Proc. Nat. Acad. Sci., Wash.* **46**, 1038.

Lowry, O. H., Rosebrough, N. J., Farr, A. L. & Randall, R. J. (1951). *J. Biol. Chem.* **193**, 265.

Marmur, J. & Lane, D. (1960). *Proc. Nat. Acad. Sci., Wash.* **46**, 453.

Murakami, W. T., Van Vunakis H., Grossman, L. & Levine, L. (1960). *Virology*, in the press.

Rice, S. A. & Doty, P. (1957). *J. Amer. Chem. Soc.* **79**, 3937.

Staehelin, M. (1958). *Biochim. biophys. Acta*, **29**, 410.

Watson, J. D. & Crick, F. H. C. (1953). *Nature*, **171**, 964.

J. Mol. Biol. (1961) **3**, 61–70

Multiplicity Reactivation after the Decay of Incorporated Radioactive Phosphorus in Phage T4

N. Symonds and D. A. Ritchie

Medical Research Council Microbial Genetics Research Unit, Hammersmith Hospital, London W.12, England

(*Received 31 August 1960*)

Multiplicity reactivation (MR) has been investigated in phage T4 after inactivation caused by the decay of ^{32}P incorporated into phage DNA. Radioactive phage particles were adsorbed onto either radioactive or non-radioactive host bacteria, and ^{32}P decay allowed to take place intracellularly in the resulting multicomplexes while they were stored in liquid nitrogen. When the multicomplexes were formed from radioactive host bacteria it was possible to demonstrate the existence of extensive MR. When the multicomplexes were formed from non-radioactive host bacteria some MR could be demonstrated but to a lesser extent than in the former case. The shape of the survival curves indicated that in both cases the population of multicomplexes was composed of two fractions, only one of which exhibited MR. This fraction comprised over 80% of the population in the multicomplexes formed from radioactive host bacteria, but only about 20% in the multicomplexes formed from non-radioactive host bacteria. It appears that MR after intracellular ^{32}P decay in phage T4 is potentially a very efficient process, but that its expression is largely determined by the physiological condition of the host bacteria. For some unknown reason, host bacteria that have suffered radiation damage are better able to support the reactivation process than are undamaged bacteria.

The bearing of these results is discussed on the following two proposals, which have been put forward previously to explain the radiation stability of monocomplexes observed in Luria-Latarjet experiments:

1. the stability is due to the occurrence of efficient MR between damaged replicas of the parental DNA, or

2. it is due to the transfer of genetic information from DNA to some non-DNA substance which is more resistant than DNA to inactivation.

1. Introduction

Recent experiments of the Luria-Latarjet type (in which the radiation resistance of infected bacteria is compared at different times during intracellular phage growth) have shown that by half-way through the latent period monocomplexes of the phages T2 and T4 are remarkably stable to inactivation caused either by ultraviolet light (Luria & Latarjet, 1947; Benzer, 1952; Symonds & McCloy, 1958), by soft X-rays (Latarjet, 1948; Stent, 1958; Symonds & McCloy, 1958), or by the decay of radiophosphorus ^{32}P incorporated both into phage and bacterial DNA (Stent, 1955). As intracellular synthesis of new phage DNA has taken place by this stage in the latent period (Hershey, Dixon & Chase, 1953; Vidaver & Kozloff, 1957), a possible explanation of this radiation stability is the occurrence of efficient multiplicity reactivation (MR) between the damaged phage genomes present in the monocomplexes after

irradiation (Stent, 1955). (MR can be defined as the phenomenon whereby two or more phage genomes, each inactive *in solo*, may co-operate to yield phage progeny when in the same bacterial cell.) However, although MR has been demonstrated experimentally with the phages T2 and T4 after inactivation by ultraviolet light (Luria, 1947; Luria & Dulbecco, 1949), and by soft X-rays (Weigle & Bertani, 1956; Harm, 1958), no MR has previously been observed after inactivation caused by the decay of ^{32}P atoms incorporated into phage DNA (Stent & Fuerst, 1955). This inability to demonstrate any MR after ^{32}P decay has therefore cast some doubt on the generality of the MR explanation of the Luria-Latarjet experiments, and has stimulated the proposal of a different type of explanation, which postulates that a necessary stage in DNA replication is the transfer of genetic information from DNA to a protein or other non-DNA substance, which is more resistant than DNA to inactivation (Stent, 1955). It was because of its bearing on this proposal, with its implications in respect to the mechanism of DNA replication (Stent, 1958), that the question of the existence of MR after ^{32}P decay was reinvestigated.

The experimental conditions employed in the present work were a modification of those used previously by Stent & Fuerst (1955), and were suggested by the experiments of Weigle & Bertani (1956) on the existence of MR in phage T2 after inactivation by soft X-rays. In their first experiments Weigle & Bertani found that phage particles irradiated with soft X-rays showed no MR when adsorbed onto non-irradiated bacteria. As this failure to demonstrate MR could have been due to radiation damage which affected the ability of the irradiated phage particles to inject their DNA into the cells, a second type of experiment was performed in which the phage particles were first adsorbed onto non-irradiated bacteria (under conditions which allowed injection of the phage DNA while preventing any phage development in the complexes) and the resulting multicomplexes were irradiated with soft X-rays. Under these experimental conditions, in which the phage DNA was irradiated intracellularly, extensive MR was observed. However, in yet a third type of experiment Weigle & Bertani showed that MR also occurred (although to a lesser extent) when extracellularly irradiated phage particles were adsorbed onto *irradiated* host bacteria. This last finding strongly suggested that after inactivation with soft X-rays there was a much greater chance of MR occurring in host bacteria that were themselves damaged by irradiation, than in undamaged bacteria. It also implied that the success of the second experiment in demonstrating MR was not solely because injection damage (the existence of which has been confirmed by Harm (1958)) was by-passed, but was also due to the fact that in irradiating the multicomplexes both the phage DNA and the host bacteria received radiation damage.

In the light of these results, MR was investigated in the present experiments under conditions in which the ^{32}P decay in the phage DNA occurred intracellularly both in non-radioactive host bacteria (as in the experiments of Stent & Fuerst (1955)), and also in host bacteria that were themselves heavily labelled with radio-phosphorus and so were continually being damaged by ^{32}P decay. These experiments have demonstrated the existence of extensive MR when the ^{32}P decay in the phage DNA takes place intracellularly in radioactive host bacteria. To a lesser extent MR has also been observed when the ^{32}P decay occurs intracellularly in non-radioactive host bacteria. These results with ^{32}P decay are thus in accord with the conclusions reached from the X-ray experiments in that there is a much greater chance of MR occurring in host bacteria that are damaged by radiation, than in undamaged host bacteria.

2. Materials and Methods

Phages. The phages used were two *r*II-type mutants of T4 B, *r*147 and *r*271, isolated by Dr. Seymour Benzer. These mutants are both situated in the A cistron of the *r*II region, and yield approximately 2% wild-type recombinants in standard crosses. Following the notation of Stent (1955) the presence of radiophosphorus will be indicated throughout this paper by an asterisk: T4* represents phage containing a high level of ^{32}P.

Bacteria. All bacteria were strains of *Escherichia coli*. B/r, a radiation-resistant mutant of B(Berkeley) (Benzer, 1957), growing at 37°C, was used as host bacterium. Assays of *r* and r^+ phage were carried out on a streptomycin-resistant strain of *E. coli* B. Strain K12(λ), also resistant to streptomycin, was used for the selective assay of r^+ phage (Benzer, 1957). Because of contamination in the laboratory, all strains were made T1-resistant. As with the phage, the notation B/r* refers to host bacteria containing a high level of ^{32}P.

Liquid media. The basic (phosphorus-free) medium employed was a modification of the tris-glucose medium described by Hershey (1955). It had the following composition (g/litre of solution): glucose 4·0, NaCl 5·4, KCl 3·0, NH_4Cl 1·1, $CaCl_2$ 0·0011, $MgSO_4$ 0·012, 2-amino-2-hydroxymethylpropane-1:3-diol (tris) 12·1, L-tryptophan 0·01, $FeCl_3$ 0·0016, gelatin 0·004, amino acids (in the proportion in which they occur in casein) 1·0 and sufficient HCl to adjust to pH 7·4 at 21°C.

At different stages of the experiments the following supplements were added to this medium: (i) preparation of radioactive phage and bacteria: 4 μg/ml. phosphorus (as orthophosphate); carrier-free ^{32}P isotope to give a specific ^{32}P content of 160 mc/mg P, (ii) freezing of phage and complexes in liquid nitrogen: 4 μg/ml. phosphorus; 5% glycerol, (iii) study of phage development in complexes after thawing: 100 μg/ml. phosphorus.

Solid media. Assays were made both on tris-glucose and on broth plates. Bottom-layer agar for tris-glucose plates contained the basic medium (except that the amino acid mixture was replaced by Difco casamino acids) supplemented with 100 μg/ml. of phosphorus and 10 g/litre of Difco agar. Bottom-layer agar for broth plates contained (g/litre): Bacto-tryptone 10·0, Difco agar 10·0, NaCl 8·0, glucose 1·0. Top-layer agar was of the same composition as the bottom-layer except that the agar concentration was reduced to 6 g/litre.

Anti-serum. Antiphage horse serum (prepared by Dr. N. Jerne) was rendered free of phosphorus by dialysis against 0·1 M-saline.

Freezing and thawing. Samples of 0·1 ml. volume were frozen and stored in small tubes suspended in liquid nitrogen at a temperature of − 196°C. Samples were thawed by transferring the tubes to a waterbath at 37°C. After 1 min (by which time the samples had melted) fresh medium was added to the tubes and the samples were immediately assayed to determine the number of infective centres they contained.

Intracellular development of phage. The average number both of total phage particles and of wild-type recombinants present in complexes at any time in the latent period was determined by adding streptomycin at a concentration of 2000 μg/ml. to samples of the complexes (which, like the host bacteria, are sensitive to streptomycin), and assaying the phage particles released after lysis on broth plates seeded with streptomycin-resistant indicator strains of *E. coli* B or K12 (λ) (Symonds, 1957).

Tests for MR after intracellular ^{32}P decay. Multicomplexes were prepared from radioactive phage adsorbed to both radioactive and non-radioactive host bacteria. In order to test for MR the survival of these multicomplexes was compared, in the same experiment, with that of monocomplexes prepared under the same conditions. Separate lysates of the phages *r*147 and *r*271 containing ^{32}P at a specific activity of 160 mc/mg phosphorus were prepared by the techniques described by Stent & Fuerst (1955) and these lysates were immediately assayed. After 4 hr (i.e. as soon as the assay plates showed plaques that could be counted) a phage suspension was prepared containing approximately 7×10^8 particles/ml. of each mutant. This concentrated suspension was subsequently used in the preparation of multicomplexes. In addition 400- and 600-fold dilutions of this suspension were made. The former was used in preparing monocomplexes, while samples from the latter were frozen and stored in liquid nitrogen in order to follow the ^{32}P-inactivation rate of the free phage particles.

Cultures of both B/r and B/r* host bacteria had in the meantime been grown at 37°C, and their concentration was adjusted to approximately 2×10^8 cells/ml. with the aid of a Petroff-Hauser counting chamber. Chloramphenicol at a concentration of 20 μg/ml. was then added to the concentrated and dilute phage suspensions, and also to the cultures of B/r and B/r*. Adsorption mixtures of all four combinations of the two phage suspensions and two bacterial cultures were then prepared. In each case equal volumes of phage and bacteria were mixed, and adsorption was allowed to proceed for 10 min. Antiphage serum was then added at a concentration sufficient to inactivate 99% of the unadsorbed phage particles in 2·5 min. After a further 5 min the adsorption mixtures were diluted 20-fold into iced medium containing glycerol, and samples were then frozen and stored in liquid nitrogen. As a control on the stability of the complexes during storage in liquid nitrogen, multicomplexes from non-radioactive phage and non-radioactive host bacteria were prepared and frozen in the same way.

From day to day, samples were thawed and assayed for the number of infective centres they contained. The intracellular development of both total phage particles and wild-type recombinants was followed in all surviving complexes.

In order to test whether the number of complexes that could produce plaques depended on the growth conditions after thawing, assays were made both on tris-glucose and on broth plates (originally at room temperature), and the plates incubated at 20°, 30° and 37°C. In addition, assays were made on plates that were pre-warmed to 37°C and immediately returned to that temperature after plating.

Tests for MR after extracellular ^{32}P decay. Only one experiment of this type was performed. A portion of the radioactive lysate of the mutant *r*271, which originally contained $6{\cdot}5 \times 10^9$ viable particles per ml., was diluted with an equal volume of broth (to diminish any indirect radiation effects originating from ^{32}P disintegrations occurring in the medium) and stored at 4°C until ^{32}P decay had reduced the number of viable phages in the suspension to 4×10^3 particles/ml. Cultures of both B/r and B/r* were then prepared, concentrated to 10^9 cells/ml., and one volume of each bacterial culture was added separately to 10 volumes of the inactivated phage suspension. After allowing 30 min for adsorption in the presence of 20 μg/ml. of chloramphenicol, each of the phage-bacterium mixtures was assayed to determine the number of infective centres it contained.

3. Results

(a) *Effect of plating conditions on survival*

Assays carried out under different plating conditions of either free phage particles or of non-radioactive complexes gave identical results. However, assays of survivors from all radioactive complexes gave results which depended both on the composition of the assay plates and on the temperature at which the plates were incubated. For some undetermined reason, assays of these complexes on broth plates gave very erratic results, duplicate plates often giving counts which differed from each other by as much as a factor of four. Assays on tris-glucose plates gave reproducible results which were consistently higher (by about 30%) than parallel assays on broth plates. Plates incubated at higher temperatures gave more plaques than similar plates incubated at lower temperatures. The highest assays were obtained on plates that were prewarmed to 37°C before plating, and immediately returned to that temperature for incubation. The approximate efficiencies of plating (compared with that obtained on prewarmed plates) at the different temperatures of incubation were: 37°C—0·8; 30°C—0·6; 20°C—0·3. (One effect of the higher temperatures of incubation in increasing the plating efficiency of radioactive complexes was possibly in reducing the viscosity of the top agar, thus allowing plaques arising from complexes with extended latent periods to grow large enough to be counted.) The extent to which the assays varied with different plating conditions did not change appreciably through the course of the experiments.

As the greatest efficiency of plating for complexes was obtained on prewarmed tris-glucose plates, the survival curves discussed in the next section all refer to assays made under these conditions.

(*b*) *MR after intracellular* ^{32}P *decay*

The results of the experiment designed to investigate MR under conditions where the ^{32}P disintegrations in the phage DNA take place intracellularly are presented in Fig. 1. In this figure, the logarithm of the fraction of surviving infective centres (of

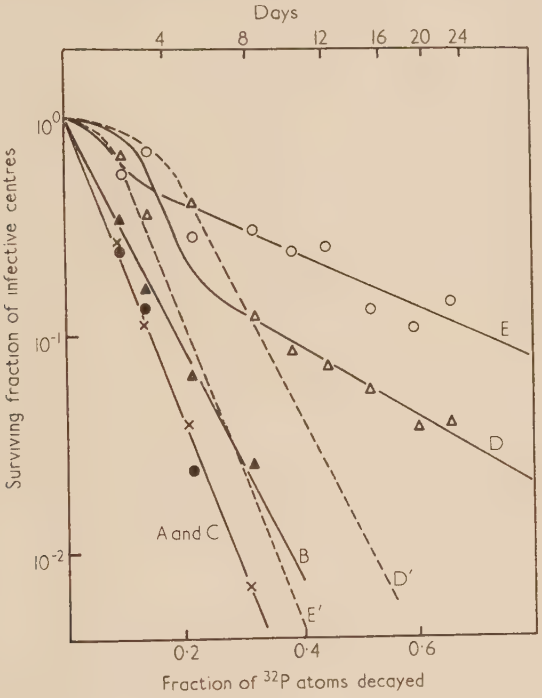

Fig. 1. The survival of different types of infective centres as a function of the fraction of initial ^{32}P atoms which have decayed by the day of the assay.

Curve A (×): parental T4* phage; curve B(▲): T4*-B/r monocomplexes; curve C (●): T4*-B/r* monocomplexes; curve D (△): T4*-B/r multicomplexes; curve E (○): T4*-B/r* multicomplexes; curve D′: expected survival of T4*-B/r multicomplexes in the absence of MR; curve E′: expected survival of T4*-B/r* multicomplexes in the absence of MR.

The survival curve for the control (T4-B/r) multicomplexes is not shown in the figure. These multicomplexes exhibited no inactivation during the course of the experiment.

complexes or free phage) has been plotted against the fraction of the original ^{32}P atoms which have decayed by the day of assay. (The surviving fraction is taken as the ratio of the titre of infective centres obtained after thawing on the day of assay to that of survivors of freezing and thawing on the first day.) It can be seen from curve A that the stock of parental T4* loses titre exponentially, as was to be expected from previous work (Hershey, Kamen, Kennedy & Gest, 1951; Stent & Fuerst, 1955). The two preparations of monocomplexes also lose their ability to produce viable phage progeny in an exponential manner. T4*-B/r monocomplexes (curve B) are slightly more resistant to ^{32}P decay than the parental phage (a result in agreement with previous work (Stent, 1955; Symonds & McCloy, 1958)), while the resistance

to ^{32}P decay of the T4*-B/r* monocomplexes (curve C) is approximately the same as that of the parental phage.

The survival curves for the multicomplexes formed from T4* and B/r, and from T4* and B/r*, are the curves D and E. The multiplicity of infection in the two cases (as calculated from the fraction of bacterial survivors) was respectively 5·7 and 3·0. If no MR occurred, the survival curves for each of these multicomplexes would have a shoulder at the origin and a final slope identical with that of the related monocomplexes. These theoretical survival curves are the dotted curves D′ and E′ in Fig. 1. It can be seen that the experimental curves D and E differ significantly from the theoretical curves D′ and E′. The experimental curves are composed of two parts. First they have a shoulder at the origin which roughly follows the initial part of the relevant theoretical curves. Later the experimental curves become approximately linear, with a final slope which in both cases is 3 to 4 times less than that of the curves D′ and E′. The presence of the two components in the experimental curves D and E indicates that in both populations of multicomplexes there are two fractions. In the first fraction no measurable MR occurs, while the second fraction exhibits efficient MR. In the case of multicomplexes formed from radioactive bacteria about 80% of the population exhibits MR; with multicomplexes formed from non-radioactive bacteria only 30% exhibit MR, even though the multiplicity of infection is nearly twice as large as in the former case.

The experiment therefore demonstrates that efficient MR after ^{32}P decay can occur in bacteria which are multiply infected with labelled bacteriophage. However, the fraction of these multicomplexes that exhibit MR appears to depend on the physiological state of the host bacteria. When these host bacteria are also labelled with ^{32}P, this fraction comprises most of the population. (In other experiments using ^{32}P-labelled host bacteria this fraction was over 95%.) When the host bacteria are non-radioactive, the fraction of multicomplexes that exhibit MR is considerably smaller.

These results suggest an explanation for the previous finding of Stent & Fuerst (1955), that no MR occurred after intracellular ^{32}P decay in multicomplexes of phage T2. In their experiment, the multicomplexes consisted of non-radioactive bacteria that had been infected with an average multiplicity of 2·2 labelled phage per cell. At this multiplicity it is possible that the fraction of multicomplexes which exhibit MR is appreciably less than the 30% obtained in the analogous experiment described above where the multiplicity of infection was 5·7. If this were the case, then the presence of the fraction that exhibited MR may well not have been noticed in their experiment in which the inactivation of the multicomplexes was followed down to a survival of 1%.

In drawing the conclusion that efficient MR can occur after ^{32}P decay, it has been assumed that the concentration of chloramphenicol added to the adsorption tubes (20 μg/ml.) was sufficient to prevent any appreciable phage development in the complexes. Otherwise the survival of the multicomplexes would not necessarily reflect the occurrence of MR, but could be interpreted in terms of some steps associated with normal phage development. Previous experiments with chloramphenicol indicate that a concentration of 20 μg/ml. is sufficient to arrest any intracellular phage development (Tomizawa & Sunakawa, 1956; Hershey & Melechen, 1957; Murakami, Van Vunakis & Levine, 1959). Also the following evidence from the present experiments suggests that the assumption is justified: (i) both cultures of

radioactive monocomplexes were inactivated at roughly the same rate as free phage particles (Fig. 1). No appreciable phage development therefore occurred in these monocomplexes during adsorption, as otherwise their resistance to ^{32}P decay would have been much greater than that of the extracellular phage (Stent, 1955); (ii) intracellular phage development in thawed samples from the control culture of non-radioactive multicomplexes commenced at the same time and proceeded at the same rate as in similar multicomplexes in which adsorption had taken place either in buffer or in cyanide; (iii) other experiments, in which the existence of MR after ^{32}P decay was studied in multicomplexes where adsorption occurred in the presence of 0·002 M-cyanide, gave similar results to those reported above after adsorption in chloramphenicol.

(c) *Intracellular phage growth in surviving complexes*

It was found that the time elapsing between thawing and the appearance of the first intracellular phage particles (i.e. the eclipse period) varied both with the type of multicomplexes being investigated and also with the length of storage of the samples in liquid nitrogen. This is illustrated in Table 1, where the approximate

TABLE 1

Length of the eclipse period of phage growth in surviving multicomplexes

Average eclipse period (in min) during the:	Type of multicomplexes T4*-B/r	T4*-B/r*	T4-B/r
first week of the experiment	18	28	15
final week of the experiment	25	36	15

periods of incubation necessary for multicomplexes to contain an average of one phage per cell is shown for samples thawed both in the initial and final stages of the experiment. It can be seen that in the case of the non-radioactive complexes the time of appearance of the first phages is the same both at the beginning and end of the experiment, showing that the course of phage maturation is unaffected by the length of storage of the samples in liquid nitrogen. In contrast to this result, the appearance of the first phages in both cultures of radioactive multicomplexes occurs at a later time in the final stages of the experiment than in the initial stages. One effect of ^{32}P decay on the surviving multicomplexes is therefore to extend that part of the latent period which precedes phage maturation.

The percentage of wild-type recombinants in the phage progeny released from multicomplexes after 60 and 90 min of incubation is shown in Table 2, along with the average burst sizes at these times. Throughout the experiment there is no significant variation in the recombination frequency obtained from the control non-radioactive multicomplexes. However, there is a significant increase during the

course of the experiment in the percentage of recombinants obtained from both types of radioactive multicomplexes. This increase is by a factor of approximately 1·5 in the case of the T4*-B/r multicomplexes, and about 2·0 in the T4*-B/r* multicomplexes (if one neglects the first recombination result, which is abnormally low and resulted perhaps from some experimental error).

TABLE 2

Percentage of wild-type recombinants in surviving multicomplexes

Days	Type of multicomplexes					
	T4*-B/r		T4*-B/r*		T4-B/r	
	% wild-type	phage/cell	% wild-type	phage/cell	% wild-type	phage/cell
2	2·1	100	1·3	18	2·7	90
5	1·8	90	2·4	26	2·3	70
8	2·1	180	2·3	26	2·3	70
10	1·7	60	2·2	28	2·4	55
	2·1	*100*	*2·7*	*33*	*2·4*	*92*
12	2·2	33	2·5	11	2·3	40
	2·9	*41*	*3·2*	*17*	*2·1*	*70*
15	3·0	44	2·1	14	2·0	50
	2·5	*63*	*2·8*	*20*	*2·3*	*60*
17	3·0	50	4·0	43	2·1	61
	3·0	*85*	*4·4*	*75*	*2·1*	*79*
19	2·5	20	5·3	11	2·3	40
	3·2	*37*	*5·3*	*27*	*2·9*	*40*
22	3·4	43	4·9	32	2·3	60
	3·3	*68*	*5·5*	*46*	*2·6*	*74*

The numbers in ordinary type are measurements made after 60 min of phage growth, while those in italic type were made after 90 min of growth. On the 2nd, 5th and 8th days of the experiment measurements were made only after 60 min of growth.

(d) *MR after extracellular* ^{32}P *decay*

The one experiment of this type which was performed showed no evidence for MR, a result in agreement with the experiments of Stent & Fuerst (1955). The failure to demonstrate MR under these experimental conditions can be explained by the finding of Tomizawa (personal communication) that phage particles in which ^{32}P decay is occurring progressively lose their ability to inject their DNA upon adsorption. However, as in the analogous experiments using soft X-rays, it might still be expected that some MR could be demonstrated if the inactive phage particles were adsorbed onto radioactive host bacteria in which ^{32}P decay had proceeded for some days. More extensive experiments than that described here are necessary to test this possibility.

4. Discussion

The present results have shown that, in a population of T4 multicomplexes in which ^{32}P decay in the phage DNA has taken place intracellularly, there are two fractions

which can be distinguished experimentally. In one efficient MR occurs, while in the other no MR can be demonstrated. Apparently the process of MR after ^{32}P decay is potentially a very efficient one, but experimentally its expression is largely determined by the physiological condition of the host bacteria used to form the multicomplexes. When these host bacteria are non-radioactive cells from a logarithmically growing culture, only a small fraction of the cells are in the proper physiological condition to support the reactivation process, so that in this case only a small proportion of the multicomplexes exhibit any MR. However, when the host bacteria are themselves heavily labelled with ^{32}P isotope, the greater proportion of the cells can successfully support the reactivation process, so that extensive MR can be demonstrated.

It is of interest to compare the present results with those previously found with the phages T2 and T4 using soft X-rays (Weigle & Bertani, 1956; Harm, 1958) and ultraviolet light (Luria & Dulbecco, 1949; Streisinger & Franklin, 1956; Epstein, 1958) as inactivating agents. In one respect the three sets of results are similar in that intracellular phage growth in those multicomplexes in which MR occurs is always associated both with a lengthening of the eclipse period, and with a stimulation of the frequency of genetic recombination. This similarity indicates that one part of the process of MR is identical in all three cases, and consists in the sorting out, by genetic recombination, of an undamaged phage genome from the damaged genomes originally present in the multicomplexes. This explanation of MR has been tested with great ingenuity by Epstein (1958) after phage inactivation with ultraviolet light, and in principle is similar to that originally proposed by Luria (1947). In another respect there is a difference between the results obtained with ^{32}P decay and soft X-rays as opposed to those obtained with ultraviolet light. With the former radiations MR occurs to a much greater extent in host bacteria that are damaged by radiation than in undamaged bacteria, while after inactivation by ultraviolet light MR occurs equally well in damaged or undamaged bacteria. The present experiments do not give any clue as to whether this difference in behaviour is related to some difference in the actual mechanism of genetic recombination that must occur between the damaged genomes if MR is to take place, or whether it is related to some other part of the reactivation process (for example, the physiological co-operation between undamaged cistrons which has been shown to be a necessary prerequisite for MR (Barricelli, 1956, 1960; Epstein, 1958)).

It is now possible to reconsider the question of the interpretation of the radiation stability of T2 and T4 monocomplexes observed in the Luria-Latarjet experiments. This radiation stability has been observed when monocomplexes, which have developed to a stage in the latent period where they contain a number of replicas of the parental DNA, are inactivated either by ultraviolet light, by soft X-rays, or by ^{32}P decay. In the first two cases it is clear that the irradiation automatically damages both the phage and the bacterial part of the monocomplexes. In the latter case the conditions can be varied (Stent, 1955), but the most critical experiment is that in which monocomplexes formed from radioactive phage and radioactive bacteria are incubated in radioactive medium before being frozen and stored in liquid nitrogen; so again the experimental conditions are such as to damage both parts of the monocomplexes. In all three cases the irradiated monocomplexes therefore consist of a number of damaged phage genomes present inside damaged host cells, and so are in a state similar to that existing immediately after infection in multicomplexes which

have been subjected to the same inactivating agents. As it has now been demonstrated that it is just under these conditions that the three types of damaged multicomplexes exhibit efficient MR, it is to be expected that the same process of efficient MR would occur in the damaged monocomplexes, and so confer on them the high degree of radiation stability observed in the Luria-Latarjet experiments. (There is even reason to believe that more efficient MR would occur in complexes in which the pre-DNA steps in phage development had taken place, than occurs immediately after infection (Stahl, 1959).) In the three cases where inactivation is caused either by ultraviolet light, soft X-rays, or ^{32}P decay, it is therefore now possible to give a satisfactory explanation of radiation stability in terms of MR. From this it does not necessarily follow that the other explanation of radiation stability, in terms of the transfer of genetic information from DNA to a protein or other non-DNA substance, is incorrect; only that the evidence of the Luria-Latarjet experiments cannot be considered as evidence in its favour. It seems unlikely that a critical test of this second explanation, with its implications with regard to DNA replication, will come from radiation studies, but from experiments of a more biochemical nature.

REFERENCES

Barricelli, N. A. (1956). *Acta Biotheor.* (*Leiden*), **11**, 107.
Barricelli, N. A. (1960). *Virology*, **11**, 99.
Benzer, S. (1952). *J. Bact.* **63**, 59.
Benzer, S. (1957). In *The Chemical Basis of Heredity*, ed. by W. D. McElroy & B. Glass. Baltimore: Johns Hopkins Press.
Epstein, R. H. (1958). *Virology*, **6**, 382.
Harm, W. (1958). *Virology*, **5**, 337.
Hershey, A. D. (1955). *Virology*, **1**, 108.
Hershey, A. D. & Melechen, N. E. (1957). *Virology*, **3**, 207.
Hershey, A. D., Dixon, J. & Chase, M. (1953). *J. Gen. Physiol.* **36**, 777.
Hershey, A. D., Kamen, M. D., Kennedy, J. M. & Gest, H. (1951). *J. Gen. Physiol.* **34**, 305.
Latarjet, R. (1948). *J. Gen. Physiol.* **31**, 529.
Luria, S. E. (1947). *Proc. Nat. Acad. Sci., Wash.* **33**, 253.
Luria, S. E. & Dulbecco, R. (1949). *Genetics*, **34**, 93.
Luria, S. E. & Latarjet, R. (1947). *J. Bact.* **53**, 149.
Murakami, W. T., Van Vunakis, H. & Levine, L. (1959). *Virology*, **9**, 624.
Stahl, F. W. (1959). In *The Viruses*, ed. by F. M. Burnet & W. M. Stanley, Vol. 2, p. 353. New York: Academic Press.
Stent, G. S. (1955). *J. Gen. Physiol.* **38**, 853.
Stent, G. S. (1958). *Adv. Virus Res.* **5**, 95.
Stent, G. S. & Fuerst, C. R. (1955). *J. Gen. Physiol.* **38**, 441.
Streisinger, G. & Franklin, N. C. (1956). *Cold Spr. Harb. Symp. Quant. Biol.* **21**, 103.
Symonds, N. (1957). *Virology*, **3**, 485.
Symonds, N. & McCloy, E. W. (1958). *Virology*, **6**, 649.
Tomizawa, J. & Sunakawa, S. (1956). *J. Gen. Physiol.* **39**, 553.
Vidaver, G. A. & Kozloff, L. M. (1957). *J. Biol. Chem.* **225**, 335.
Weigle, J. J. & Bertani, G. (1956). *Virology*, **2**, 344.

J. Mol. Biol. (1961) **3**, 71–86

The Molecular Structure of Polyadenylic Acid

Alexander Rich
Department of Biology, Massachusetts Institute of Technology, Cambridge, Mass., U.S.A.

David R. Davies
National Institute of Mental Health, Bethesda, Maryland, U.S.A.

F. H. C. Crick
Medical Research Council Unit for Molecular Biology, Cavendish Laboratory, Cambridge, England

J. D. Watson
Department of Biology, Harvard University, Cambridge, Mass., U.S.A.

(*Received 28 September 1960*)

The structure of fibers of polyadenylic acid at acid pH has been studied by X-ray diffraction. A model is proposed consisting of two parallel intertwined helical chains, each having a screw of 3·8 Å and 45° and related to each other by a dyad axis parallel to the fiber axis. Coordinates, bond distances and angles and the calculated Fourier transform are given for this model.

Reasons are given why the quite different model of Morgan & Bear is thought to be wrong.

1. Introduction

The isolation of polynucleotide phosphorylase by Grunberg-Manago, Ortiz & Ochoa (1955) has made possible the synthesis of a variety of ribonucleotide polymers all having the same covalent backbone as natural RNA. Physical and chemical studies on these polymers have been widespread and have led to a better understanding of the general principles underlying nucleic acid structures. Among the first of these polymers to be investigated by the technique of X-ray diffraction was polyadenylic acid. In this paper we describe our studies of this material and give the precise coordinates for a molecular model which is in excellent agreement with all the experimental facts.

Preliminary accounts of this work have appeared previously (Watson, 1957; Rich, 1957*a*; Crick, 1957). Since that time additional information has been obtained from the physical chemical investigations of Beers & Steiner (1957), Fresco & Doty (1957) and Fresco (1959), and the results of these investigations will be incorporated into the present discussion.

2. Materials and Methods

The polyadenylic acid originally used in this investigation was kindly supplied by S. Ochoa. Later preparations were synthesized by methods already described. A large number of preparations was investigated and the results were very similar in all cases except that some specimens of low molecular weight could not be oriented.

Fibers were pulled from concentrated solutions of polyadenylic acid and X-ray diffraction photographs of these fibers were obtained with fiber micro-cameras. The humidity of

the helium atmosphere surrounding the fibers was controlled by bubbling the helium through appropriate saturated salt solutions before it entered the camera. Both the microfocus X-ray tube (Hilger, London) and the rotating anode tube which has been developed at the Cavendish Laboratory, Cambridge, were used as high intensity X-ray sources. The intensities of the diffraction maxima on the photographs were measured with a Joyce-Loebl recording microdensitometer.

The structural investigation was carried out with the aid of molecular models built from 1/8 in brass rod to a scale of 5 cm = 1 Å. Models were built of plausible helical structures and from these models a set of coordinates could be obtained for the repeat unit of the helix. In the early stages the diffraction pattern was obtained using an optical transform machine. Later, IBM computers were used to calculate from the coordinates the cylindrically averaged Fourier transform of the model. This calculation has been described previously (Davies & Rich, 1959). Comparison between observed and calculated diffraction patterns was then made, and from this a decision could be reached as to the acceptability of the model. The coordinates of the final model were then refined so that all distances and angles were stereochemically acceptable.

3. Results

Well oriented fibers of polyadenylic acid are negatively birefringent with values up to $\Delta n = -0{\cdot}10$. Some less well oriented fibers produced smaller values of the birefringence but always of negative sign. Some preparations produced well oriented samples while others yielded poor orientation. The degree of orientation was best correlated to the molecular length of the polymer, and the pH of the material. If the sample had been prepared near neutral pH, it was very difficult to get a well oriented sample; however, lowering the pH usually resulted in a sample with more orientation.

An X-ray diffraction photograph of polyadenylic acid is shown in Plate I. This is a typical fiber diffraction photograph characterized by a series of off-equatorial streaks rather than a number of discrete spots such as one would expect for a crystalline material. The diffraction photograph is dominated by a sharp, very intense meridional reflexion at 3·80 Å on the fourth layer line. The first layer line in the photograph has a spacing of 15·2 Å, and has a medium to weak reflexion near the meridian; further out there is a moderately strong reflexion at a Bragg spacing of 5·2 Å. The latter reflexion shows some arcing and is not confined entirely to the first layer line, but merges with a reflexion on the equator. It is of interest to note that a similar reflexion also occurs in the diffraction pattern of natural ribonucleic acid fibers (Rich & Watson, 1954). The second layer line has nothing while the third layer line has a reflexion which is moderately weak and is located just off the meridian. Sometimes this layer line can be broken up into two reflexions, one of which is closer to the meridian than the other. The fourth layer line has, in addition to the very intense meridional reflexion, a suggestion of much weaker components which are further away from the meridian and blurred. The fifth layer line has a reflexion of moderate intensity which is off meridional but arcs across it.

In addition to the above reflexions which can be seen with untilted fibers, there are two layer line reflexions which can only be seen by tipping the specimens. An example of a tipped diffraction pattern is shown in Plate II. As can be seen, there are two near-meridional reflexions which occur at a Bragg spacing of 1·90 Å and 1·68 Å. It should be noted that the 1·90 Å reflexion is most intense on the meridian while the outer 1·68 Å reflexion covers a somewhat wider arc.

Diffraction photographs were taken of polyadenylic acid at a variety of relative humidities in order to determine the influence of water on the structure. One of the

PLATE I. An X-ray diffraction photograph of polyadenylic acid. The fiber axis is vertical and the relative humidity is 78%. The weak reflexion on the meridian just inside the intense 3·8 Å arc is due to Kβ radiation.

[*To face page* 72

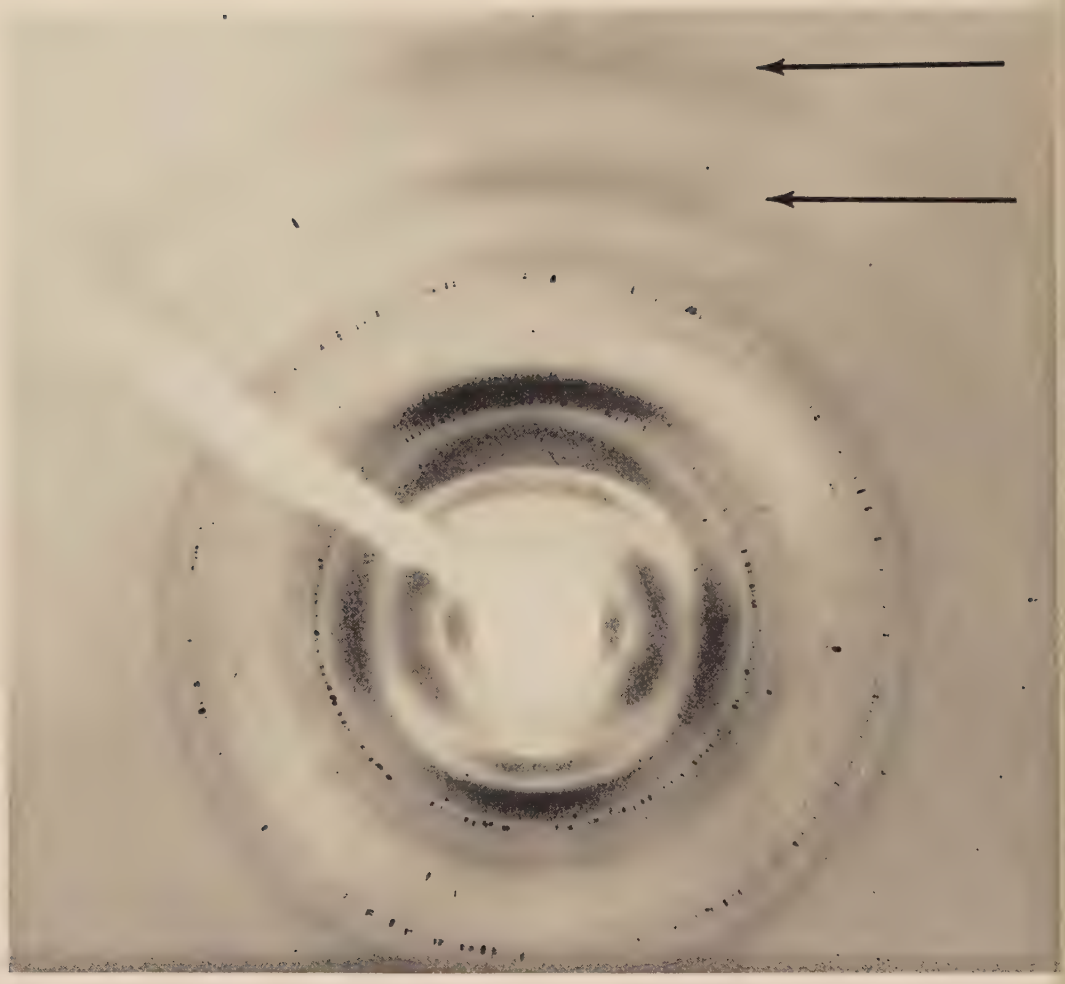

PLATE II. An X-ray diffraction photograph of polyadenylic acid obtained with the fiber axis vertical, but tipped about 20° into the beam. Two additional strong reflexions are seen as shown by the arrows.

most unusual features of polyadenylic acid is the fact that the diffraction pattern remains intact even if the photograph is taken with the specimen in an evacuated camera at zero relative humidity, so that almost all the labile water molecules are removed. This stability is in marked contrast to deoxyribonucleic acid and most of the other synthetic polyribonucleotides, in which the diffraction pattern becomes amorphous or blurred when the fiber is put in a vacuum. The variations in relative humidity have only a small effect on the equatorial diffraction pattern of polyadenylic acid. The first reflexion on the equator, 100, is very strong and occurs at a spacing between 16 and 18 Å. The 100 spacing is shown for polyadenylic acid as a function of relative humidity in Fig. 1, and it can be seen that there is only a small change of less

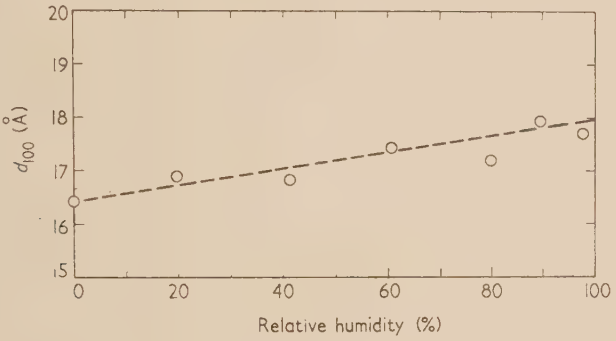

Fig. 1. The change in the 100 reflexion with changes in relative humidity. Zero relative humidity was produced by taking the diffraction photograph under vacuum.

than 2 Å in this spacing over the whole range of relative humidity. In the two-stranded molecule of polyadenylic acid *plus* polyuridylic acid, the 100 spacing increases by over 8 Å when the relative humidity is changed from near zero to 98% (Rich, 1957*b*).

The reflexions on the equator are not particularly well defined and a degree of uncertainty must be attached to their spacings. They were measured with the Joyce-Loebl recording microdensitometer from twelve films which were the product of 10 separate photographs at different relative humidities. In general, only two reflexions could be seen easily, having a spacing of about 17 Å and about 7·6 Å. On several films a reflexion of spacing near 8·6 Å could be seen, and on two films a fourth faint reflexion could be observed, but not measured.

The first two reflexions may be tentatively indexed as the 100 and 210 reflexions from a square net of spacing 17 Å. The third would then correspond to 200 and the fourth to 110. It seems to us most unlikely that these could be the result of diffraction from a hexagonal net, but in view of the paucity of the equatorial reflexions, and the rather diffuse nature of those which are observed, their assignment to a tetragonal cell is not entirely certain.

4. Interpretation of the Diffraction Pattern

The strong negative birefringence of the fibers of polyadenylic acid suggested that the purine bases are oriented more or less at right angles to the fiber axis. This interpretation was reinforced by the extremely strong meridional reflexion at 3·8 Å.

However, since the thickness of the purine bases is 3·4 Å, it is clear that they must be tilted a little in order to explain the observed 3·8 Å axial spacing.

The distribution of meridional and off-meridional reflexions clearly suggests that the molecule is helical in character. The simplest helix that is compatible with this distribution would be one in which there are four residues per turn with a pitch of 15·2 Å. Accordingly, we spent some time investigating configurations of a variety of single-stranded polyadenylic acid models, since we were at that time uncertain of the diameter of the molecule. We tried to find a natural explanation for the 3·8 Å reflexion, and in addition to normal stereochemistry, we looked for a reasonable system of hydrogen bonding to hold the structure together. After considerable effort in this direction, we concluded that it was impossible with a single-stranded molecule.

Shortly after this we obtained somewhat more reliable data on the equatorial reflexions of polyadenylic acid which indicated that there was a larger unit cell having an edge about 16 to 17 Å long. It was clear that a single strand of polyadenylic acid could not easily fill a volume of this sort and accordingly we then began to investigate multi-stranded helical models.

In general, there are two different classes of multi-stranded structures: those in which the purine residues are located in the center of the molecule, and those in which they are located on the outside of the molecule. Investigations of the configurations possible in the latter class led us to the conclusion that there were none that were plausible. This point will be discussed in greater detail when we consider the model advanced by Morgan & Bear (1958).

Investigation of multi-stranded models with the bases on the inside showed that the ribose-phosphate backbone is not long enough to cover the distance required for a translation of 3·8 Å and a rotation of 90° which was indicated by the strong meridional reflexion on the 4th layer line. However, two-stranded models can be built with a twofold rotation axis running down the helix axis. The effect of this symmetry axis is to reduce the unit rotation to 45°, and within this framework there are two structures in which the adenines of opposite chains are joined together in pairs by hydrogen bonds.

In the first of these structures the 6-amino group is hydrogen bonded to N_1 of the opposite purine ring. Models of this type were rejected by us because they require a large radial separation between phosphates of opposite chains. This would lead to strong reflexions near the meridian on the first layer line, contrary to what is observed. They were examined in more detail by Morgan & Bear (1958), and rejected for similar reasons.

The second of these structures has the adenines paired in the same way as in the crystal structure of adenine hydrochloride (Broomhead, 1948; Cochran, 1951), namely, with hydrogen bonds between the 6-amino nitrogen and N_7 of the opposite ring. A first primitive model of this sort had the bases stacked perpendicular to the helix axis with a separation of 3·8 Å, and no attempt was made to pull in the ribose phosphate backbones closer to the axis. The calculated diffraction pattern showed reasonable agreement with the observed pattern, although the intensities of the first layer line reflexions were reversed, the first being strong and the second weak.

However, at the same time a second model of this kind was constructed in which an additional hydrogen bond was made between the 6-amino nitrogen and a phosphate oxygen of the opposite chain. This additional hydrogen bond meant that the two strands were now held together by two purine-purine hydrogen bonds and two

purine-phosphate hydrogen bonds. Formation of this additional hydrogen bond results in pulling in the phosphates closer to the helix axis with consequent improvement of the agreement between the diffraction patterns. Furthermore, in order to make this bond, it is necessary to tip the bases so that they are no longer perpendicular to the helix axis, but inclined by 10° to 11° from the perpendicular. This tilting provides a natural explanation for the 3·8 Å spacing rather than the expected 3·4 Å spacing.

TABLE 1

Coordinates of polyadenylic acid

(The atoms listed are those illustrated in Fig. 5)

	x	y	z	r	ϕ
Adenine residue					
N_1	1·77	3·68	0·35	4·08	64·3°
C_2	3·14	3·73	0·46	4·88	49·9°
N_3	3·92	2·70	0·35	4·76	34·5°
C_4	3·24	1·54	0·11	3·59	25·5°
C_5	1·89	1·39	− 0·02	2·35	36·3°
C_6	1·08	2·52	0·10	2·74	66·7°
N_7	1·59	0·08	− 0·27	1·59	2·7°
C_8	2·80	− 0·50	− 0·27	2·84	− 10·1°
N_9	3·81	0·33	− 0·05	3·82	4·9°
N_{10}	− 0·21	2·55	0·01	2·56	94·7°
Ribose-phosphate chain					
C'_1	5·24	0·00	0·00	5·24	0·0°
C'_2	5·69	0·29	1·44	5·70	2·9°
C'_3	5·58	− 1·09	2·09	5·69	− 11·0°
C'_4	6·04	− 2·02	0·98	6·37	− 18·5°
C'_5	5·51	− 3·45	1·19	6·51	− 32·1°
O'_1	5·48	− 1·42	−0·21	5·66	− 14·5°
O'_2	7·03	0·78	1·48	7·08	6·3°
O'_3	6·46	− 1·22	3·26	6·58	− 10·7°
P	3·34	− 4·92	0·89	5·95	− 55·8°
O_5	4·07	− 3·53	1·00	5·39	− 40·9°
O_6	1·86	− 4·65	0·90	5·01	− 68·2°
O_7	3·89	− 5·91	1·89	7·07	− 56·6°
lower O'_3	3·71	− 5·45	− 0·54	6·58	− 55·7°

A right-handed coordinate system is used for both Cartesian and cylindrical polar coordinates.

Furthermore, tilting the bases alters the distribution of scattering intensity on the upper layer lines. If the bases were not tilted we would only expect higher orders of 3·8 Å, e.g. the 1·9 Å reflexion which is observed as moderately strong (Plate II). However, tilting also throws some diffracted intensity somewhat off the meridian so that we might expect additional reflexions to occur in that region. We have pointed out the occurrence of a second strong reflexion at 1·68 Å which, as we will see below, is predicted by this model.

By hydrogen-bonding the phosphate group to the adenine residue of the opposite chain, the molecule tended to become more rounded in cross section, and the helical

grooves, which are so marked in DNA, are considerably reduced in polyadenylic acid. This has the effect of reducing the predicted intensity of the second layer line near the meridian so that it is in closer agreement with the observed diffraction pattern.

5. Description of the Molecule

Once we were convinced that this model was along the right general lines for predicting the overall diffraction pattern, we carried out a series of successive adjustments whereby a careful set of atomic coordinates was obtained which showed that it is stereochemically feasible to have a model of this sort. Thus, we have a set of atomic

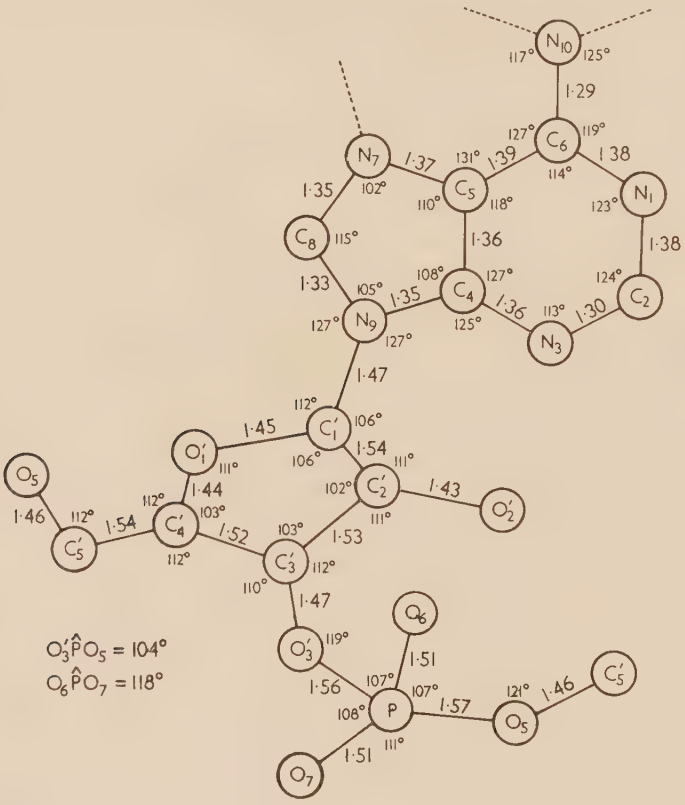

Fig. 2. A sketch to show the bond angles and distances of polyadenylic acid. Not to scale.

coordinates which yield an accepted range of values for bond angles, distances, and van der Waals contacts between the atoms. The coordinates for polyadenylic acid are listed in Table 1, the bond distances and angles are shown in Fig. 2 (not to scale), and the shorter van der Waals contacts are marked on the projection of part of the structure shown in Fig. 3.

The coordinates were finalized before the publication of the papers of Fuller (1959) and Spencer (1959). They could be revised slightly with advantage but all the distances and angles are acceptable, although the angle $N_9\hat{C}_1C_2'$ (106°) is strained a little owing to the formation of the hydrogen bond between N_{10} and O_6. The adenine has been based on Cochran's parameters for adenine hydrochloride (Cochran, 1951).

The hydrogen bond from N_{10} to N_7 is 6° away from the straight direction and that from N_{10} to O_6 is 14° away; that is, the angle $O_6\hat{N}_{10}H$ is 14°. This is on the large side, but acceptable.

It should be mentioned here that it is necessary in the determination of molecular structure from fiber patterns to show that a given molecular model is stereochemically

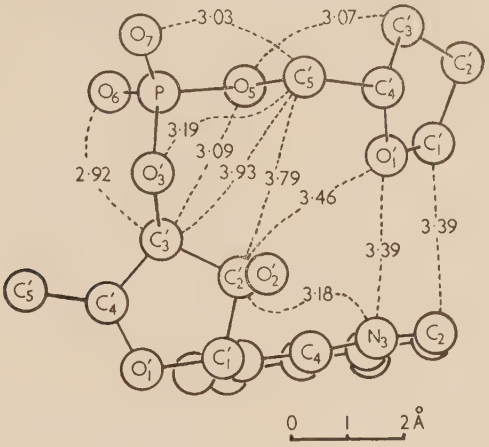

FIG. 3. Part of the structure projected in the direction of the x axis. The shorter van der Waals contacts are shown by dotted lines.

FIG. 4. Schematic view of polyadenylic acid as seen from the side. The flat ribbons represent the ribose-phosphate backbones which are parallel to each other. The disks represent the adenine rings which are hydrogen bonded together.

feasible, and to present reasonably exact atomic coordinates. This is not because it is necessary to compare in great detail the diffraction pattern of this refined model with what is observed experimentally, for very often the experimental data on an X-ray

fiber diffraction pattern are not of high quality. The importance of presenting exact coordinates rests on the fact that this is a means for ruling out certain structures. It may be very easy to obtain an approximate set of coordinates, but it may prove to be impossible to refine the model properly so that it conforms to known values of atomic parameters as well as have the symmetry demanded by the diffraction pattern.

The helical molecule of polyadenylic acid consists of two polynucleotide chains organized about a twofold rotation axis. Figure 4 is a schematic view of the molecule in which the flat ribbons represent the ribose-phosphate backbone chains and the disks

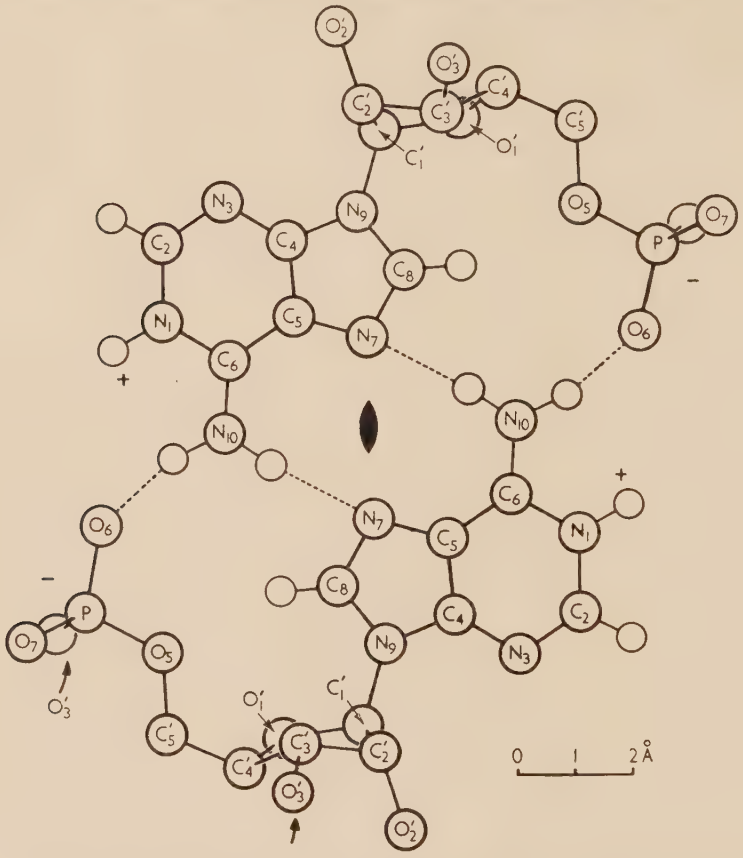

FIG. 5. The two-stranded molecule of polyadenylic acid as viewed down the fiber axis. Each adenine residue forms three hydrogen bonds. An extra O_3' atom is shown to indicate the backbone connections. For clarity the hydrogen atoms on the sugar have been omitted.

represent the adenine residues. Successive residues are related by a translation of 3·8 Å and a rotation of 45°. Both backbone chains are parallel to each other, as shown by arrows. This is in contrast to the two-stranded molecule of deoxyribonucleic acid in which the twofold rotation axes are perpendicular to the fiber axis, and the two backbone chains are anti-parallel. The adenine rings are tilted about 10° from the horizontal, but this is not shown in Fig. 4. Because of the twofold rotation axis, the two bases which are hydrogen bonded to each other are tipped in opposite directions, much like the blades of a propeller.

Figure 5 shows a view of the molecule as seen down the fiber axis. The hydrogen bonding between the adenine residues is shown, as well as the hydrogen bonding

between the adenine amino group and the phosphate oxygen atom from the opposite chain. Two arrows point to successive O_3 atoms of the ribose ring, and that atom is shown twice in order to show how the backbone chain is connected. Nitrogen 1 of the adenine ring is protonated, with a positive charge on the ring. The reasons for this will be discussed below.

In order to see the molecule in terms of the space which it occupies, we have made a diagram in which the atoms are represented as spheres drawn with their van der Waals radii. Figure 6 shows this view of the molecule. The fiber and molecular axis is

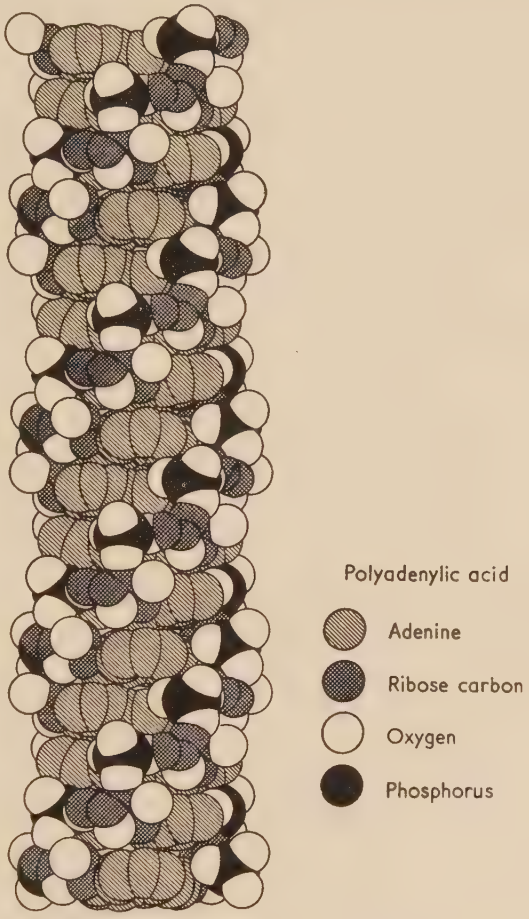

FIG. 6. Van der Waals model of polyadenylic acid. Hydrogen atoms are not represented in this diagram.

vertical, and it can be seen that the adenine bases are slightly tilted. The outstanding feature which this diagram illustrates is the compactness of the molecule. The molecule is a helix, but the helical grooves are not very evident owing to the fact that the phosphate groups are pulled in towards the center of the molecule in order to hydrogen-bond with the adenine amino group.

This compact form is probably responsible for the fact that the helix is intact even under a vacuum. In addition, the rounded outline is probably responsible for randomness in packing, as discussed below.

6. The Density and Space Group of Polyadenylic Acid

To obtain an approximate estimate of the density to be expected we must estimate the number of water molecules that will fit into the unit cell. This can be done approximately by using the partial specific volume of polyadenylic acid in solution, which is known to be in the neighbourhood of 0·54 (R. Haselkorn, personal communication). If we take a tetragonal cell with dimensions $16{\cdot}8 \times 16{\cdot}8 \times 15{\cdot}2$ Å, then calculation shows that there should be room for about eight molecules of water per nucleotide. This gives a density of about 1·47. If the fiber used contained a small amount of sodium ion (which occupies very little volume) this figure might be a little higher, say 1·5.

This is rather lower than the observed value of 1·53 obtained by flotation. This discrepancy can only be explained by assuming that in the fiber there were less crystalline regions with a higher density. As the postulated tetragonal cell is a very open one this is not implausible.

In spite of these uncertainties the density shows clearly that there are two nucleotides for every 3·8 Å in the z direction, since three nucleotides would be an impossibly tight fit (calculated density 1·70) and one nucleotide would give far too low a density (calculated 1·23).

The molecule of polyadenylic acid in the helical form described has a great deal of symmetry. In addition to the twofold rotation axis along the helix axis, there is also an eightfold screw axis, which can be used crystallographically as a fourfold screw axis. Hence the space group may well be $P4_2$ where a c-axis is 15·2 Å and the asymmetric unit consists of two adjoining nucleotides. The helix is covalently linked in a right-handed fashion, but this is not specified by the space group symmetry.

7. Comparison of Calculated and Observed Intensity Data

From the final set of coordinates the continuous Fourier transform was calculated using the computer program already mentioned. This program computes a cylindrically averaged Fourier transform for helical molecules. This is the most appropriate form of comparison to be used for polyadenylic acid since there is little evidence for crystallinity or sampling of the transform with one or two exceptions cited above. The program computes the cylindrically averaged intensity $I(R, l/c)$, where

$$I(R, l/c) = \sum_n \left\{ \left[\sum_j f_j J_n(2\pi r_j R) \cos\left\{ n\left(\frac{\pi}{2} - \phi_j\right) + \frac{2\pi l z_j}{c} \right\} \right]^2 + \left[\sum_j f_j J_n(2\pi r_j R) \sin\left\{ n\left(\frac{\pi}{2} - \phi_j\right) + \frac{2\pi l z_j}{c} \right\} \right]^2 \right\}$$

where j = total number of atoms in the asymmetric unit; r_j, ϕ_j and z_j are the cylindrical polar atom coordinates, n = order of Bessel functions suitable for the helical symmetry. We have used four orders of Bessel function for each layer line; additional contributions could be neglected. In this computation we have not used a temperature factor.

Intensity data were collected from diffraction photographs obtained with the multiple film technique. The intensities of the diffraction maxima were measured with the recording microdensitometer by taking traces which went at right angles to the layer lines as well as along them. This was done because, as a result of the lack of

complete orientation of the fiber molecules, many of the reflexions were arced, with appreciable intensity off the layer lines. Because of this arcing of the reflexions, and because of the limited integrating ability of the recording densitometer, we regard the intensity data obtained as only semi-quantitative. We have, therefore, not considered it worthwhile to correct the recorded intensities for the usual cylindrical and polarization factors. These corrections, if applied, would have the principal effect of reducing the recorded intensities near the meridian.

It was possible to measure the relative intensities of the two reflexions which occur at 1·68 Å and 1·90 Å, but no attempt has been made to relate these accurately to the rest of the diffraction pattern.

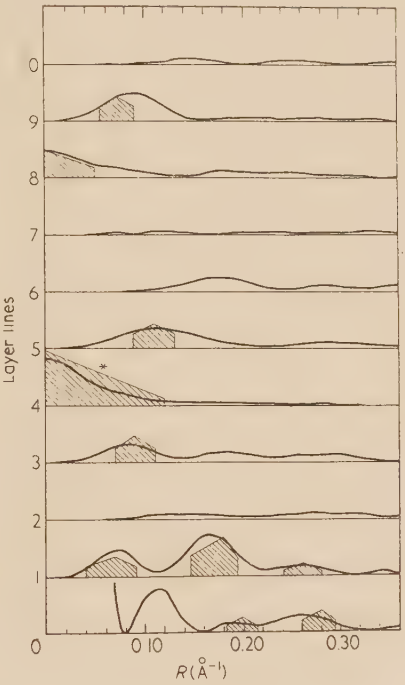

Fig. 7. The observed and calculated intensities for polyadenylic acid. The calculated intensities are indicated by the continuous curves. The observed data are plotted in the shaded areas, the apex indicating the position of maximum intensity. The height of the apex indicates intensity, but the measurements may be in error by as much as 50%. The observed reflexions on layer lines 8 and 9 are not on the same scale as the other observed intensities. *Intensities on this layer line are plotted at one-fifth the actual values.

The observed and calculated intensities on the various layer lines are shown in Fig. 7. It can be seen that there is moderately good but not perfect agreement. Note particularly that the model predicts strong intensity at a spacing of 1·90 Å (second order of 3·8 Å) as well as a strong reflexion at 1·68 Å which should be just off the meridian. This latter reflexion which can be seen in Plate II has an intensity distribution compatible with its being off-meridional.

The observed intensity data are plotted in Fig. 7 in such a way as to indicate its semi-quantitative nature. The most intense part of the diffracted intensity on a layer line was located by projecting the diffraction pattern onto an appropriate Bernal chart. This point was used to determine the position of the apex of the pentagonal

shaded areas which indicate observed intensity. This could be done unambiguously in most cases. However, the medium intense reflexion on the 5th layer line never split into its two off-meridional components. Hence its position on the layer line was determined by assuming that the arc originated on that layer line; this uniquely determines the cylindrical radius R for the reflexion. The same technique was used for the 9th layer line reflexion. The height of the shaded intensity figure was determined by the densitometer tracings, while the width was estimated using both the tracings and visual appraisal. The straight edges on the pentagonal intensity figures do not, of course, represent the shape of the diffracted X-ray beams. In Fig. 7, the observed and calculated intensities for the 4th layer line (3·8 Å) are plotted on a scale 0·2 times that of the rest of the diagram, as indicated by an asterisk. Only the outermost equatorial reflexions are plotted in Fig. 7, since the inner reflexions are discrete and are handled separately.

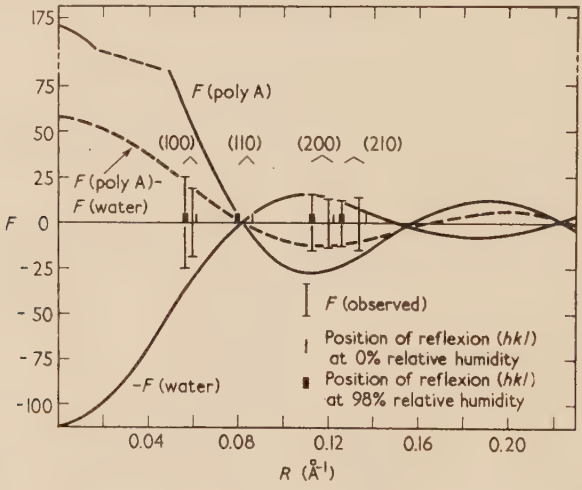

Fig. 8. Observed and calculated structure factors for the equator of polyadenylic acid. The dashed line represents the structure factor for the molecule minus the structure factor for a cylinder of water. The observed data are indicated by vertical lines which cross the horizontal axis. The positions of the reflexions at extreme values of the relative humidity are indicated by short vertical lines.

When considering the agreement between the observed and calculated intensity distributions in Fig. 7 it should be emphasized that no allowance has been made for the effect of bound water molecules on the diffraction pattern. Polyadenylic acid takes up a small amount of water and holds it firmly, and it is quite likely that this water will modify the diffraction pattern slightly.

The water surrounding the molecule may have a substantial effect on the equatorial diffraction pattern. We have accordingly computed the equatorial intensities by taking this water environment into account. This calculation was carried out by assuming that the molecule is cylindrical in outline (cf. Fig. 6), with an outer radius r_0, and is suspended in a sea of water which extends from r_0 to infinity. The equatorial intensities or structure factors are then the difference between the contribution due to the molecule itself and that due to a cylinder of water of radius r_0. Thus, for the equator we have plotted in Fig. 8 the structure factor for the molecule itself, the cylinder of water and the difference between these quantities (dashed line). That is:

$$F = F \text{ (poly A)} - F \text{ (water cylinder)}$$

$$= \sum_j f_j J_o(2\pi r_j R) - \frac{r_o z \rho}{R} J_1(2\pi r_o R)$$

where z = height of the cylinder of water (3·8 Å for 2 nucleotides);
ρ = electron density of water = 0·33 electrons/Å^3;
r_0 = 7·5 Å.

It can be seen that the structure factor passes through zero very near the point at which the 110 reflexion should appear in the square lattice. Hence this accounts for the failure to observe this reflexion. The fact that 210 reflexion is readily observed whereas 200 is frequently very weak may be partially, but not entirely, accounted for by the higher multiplicity of 210. Observed data are plotted in Fig. 8 for the reflexions 100, 200 and 210 at 20% and 98% relative humidity. These structure factor measurements should be regarded as accurate only to approximately ± 30%, due to the diffuseness of the reflexions. However, it can be seen that there is rough agreement with the calculated structure factor curve.

The diffuseness of these equatorial reflexions may arise from several sources. It is quite likely that the molecules tend to crystallize in the tetragonal cell because of the 45° rotation between adjoining nucleotide residues in the chain. However, there are opportunities for various types of randomness. The chains are directional, and so they can be oriented up and down at random. In addition, because the helix is very compact and rounded, rotational disorder can be present. These may have the effect of producing an equatorial packing domain which is small, and leads to broad diffuse equatorial reflexions. This randomness is also responsible for the smeared, non-discrete nature of the off-equatorial reflexions, which come closer to representing the continuous Fourier transform than a sampling at discrete points.

We have spent some time studying the packing between molecules in the tetragonal lattice at various equatorial spacings. There are several possibilities, but we shall not discuss them because the diffraction data are not sufficiently precise.

8. The Model of Morgan & Bear

A paper was recently published by Morgan & Bear (1958) which described two possible structures for the molecule of polyadenylic acid. We believe both of these structures to be incorrect. Since these authors reject their second structure on the grounds that it does not fit the diffraction data, we need not consider it further here. Their structure I is very unusual in that the two polynucleotide chains are wrapped around each other in anti-parallel fashion with each chain containing four residues per turn. The ribose-phosphate chains are located in the center of the molecule with the adenine residues projecting out radially from the center core. The two chains are related by dyad axes, perpendicular to the fiber axis, going through each pair of hydrogen-bonded ribose rings. Although it has some provocative features, this model can be ruled out for several reasons which we shall proceed to outline.

In the first place it is not clear to us that the structure can be built satisfactorily along the lines the authors have described. Whereas most of the bond distances in their model are acceptable, many of the angles are not. In Table 2 we list the bond angles that occur in their structure together with the standard values. It can be seen that distortions are present as large as 20° to 30°, and these are quite unallowable. Furthermore, the authors have neglected to consider some of the unfavorable van der

Waals contacts between various units. Thus, they have the two charged phosphate groups "in contact" with each other. However, the phosphorus atoms are 3·89 Å apart and the oxygens are 2·46 Å apart, both of these values being considerably below the accepted values. We think it is unlikely that these coordinates can be refined to standard values. This is probably an example of the situation discussed above, in that a preliminary and uncritical examination of a potential molecular configuration looks promising but, on closer examination, it turns out that the model is not feasible stereochemically.

TABLE 2

Bond angles in the model of Morgan & Bear

Angle	Value in structure I	Standard value	Distortion
$O_1'C_4'C_5'$	139°	110°	29°
$N_9C_1'O_1'$	132°	110°	22°
$C_2'C_3'O_3'$	124°	110°	14°
$C_1'C_2'O_2'$	120°	110°	9°
$PO_5'C_5'$	102°	about 120°	about 18°
$O_3'PO_7$	77°	110°	33°

Secondly, the structure looks energetically unfavorable. It is held together by one weak hydrogen bond between the sugars, and furthermore, the negatively charged phosphate groups are brought close together so that the molecule would tend to fly apart in solution, whereas it has been shown experimentally by Fresco (1959) that polyadenylic acid retains its helical configuration in solution.

It has been established by Fresco & Doty (1957) that the helical form of polyadenylic acid is stable at pH 5, but not at pH 7. The structure of Morgan & Bear does not explain this. Nor does it explain in a natural way the spacing of 3·8 Å between the bases.

Further support for models having the bases on the inside arises from chemical work concerning the action of concentrated nitrous acid on the adenine residue in ribonucleotide chains. In 4 M-$NaNO_2$ at pH 4·3 adenine residues are usually oxidized to hypoxanthine, since the amino group is replaced by an oxygen. However, polyadenylic acid does not react under these conditions when left at room temperature for four days. (A. Bendich & H. Rosenkranz, personal communication.) This result would not be understandable if the adenine residues project away from the molecular axis into the solution; however, it is naturally explained by the fact that the adenine residues are buried in the center of the molecule and are hence unreactive to nitrous acid.

Finally, it should be mentioned that a cylindrically averaged transform calculation carried out with the Morgan-Bear coordinates does not yield a diffraction pattern in agreement with the observed data. The second strongest reflexion on the calculated pattern is on the 3rd layer line, while the near-meridional part of the 2nd layer line is more intense than the contribution further out. In short, we feel there is very little chance that this model is correct.

9. Discussion

We arrived at our interpretation for the structure of polyadenylic acid before the effect of hydrogen ion concentration was noted. Beers & Steiner (1957) pointed out that an abrupt shift occurred in the ultraviolet absorption spectrum of polyadenylic acid when the pH was lowered to about pH 5. They correlated the shift in the spectrum with the absorption of one proton per nucleotide base. Shortly after that, Fresco & Doty (1957) showed that, at the lowered pH, the molecule had a rigid form composed of variable numbers of polyadenylic acid molecules in contrast to the flexible randomly coiled form which it exhibited at pH 7. Thus we were faced with the question of how the additional proton was absorbed in polyadenylic acid. The answer to this question is quite clear in the case of adenine hydrochloride in crystalline form. Cochran (1951) has made a detailed analysis of the crystal structure of the protonated adenine residue and his results show that the additional hydrogen is located on N_1 of the purine ring. We therefore considered the effects of adding a proton at this position on the structure which we had postulated for polyadenylic acid. The results are shown in Fig. 5 where a positive charge is shown on N_1 in close proximity to the negatively charged phosphate group of the opposite ribose-phosphate backbone. In this position it is clear that the additional charge on the adenine residue stabilizes the molecule electrostatically. This might be described as an "inner salt," since the polymer no longer has an overall charge, even though there are isolated charges on different parts of the helix.

In this form the molecule has considerable stability. It has been shown by Fresco & Klemperer (1959) that the "melting temperature," T_m (the mean of the temperature range over which the material changes from a helical to a random coil form) of a solution of polyadenylic acid at pH 4·25 and ionic strength 0·15 is about 90°C. This is roughly the same as the T_m of calf thymus DNA at pH 7·0 and similar ionic strength, and is considerably higher than the T_m's of polyinosinic acid, polyinosinic *plus* polycytidylic acid and polyadenylic *plus* polyuridylic acid (Doty, Boedtker, Fresco, Haselkorn & Litt, 1959).

Polyadenylic acid, in addition to combining with itself to form this two-stranded molecule, can also combine with polyuridylic acid to form two- and three-stranded structures (Rich & Davies, 1956; Felsenfeld, Davies & Rich, 1957). Similar structures are formed with polyinosinic acid (Rich, 1957*a*) and with polyribothymidylic acid (A. Rich, unpublished results). It should be noted that these structures are all formed at neutral pH where polyadenylic acid exists as a flexible single chain. All of these structures exhibit diffraction patterns that are quite different from that shown in Plate I. However they all have in common a configuration in which the charged ribose-phosphate chains are helically arranged on the outside of the molecule surrounding the hydrogen bonded purine or pyrimidine residues.

We would like to acknowledge assistance by Leslie Barnett, and also by Dr. S. Benzer in obtaining the final coordinates.

REFERENCES

Beers, R. F., Jr. & Steiner, R. F. (1957). *Nature*, **179**, 1076.
Broomhead, J. (1948). *Acta Cryst.* **1**, 324.
Cochran, W. (1951). *Acta Cryst.* **4**, 81.

Crick, F. H. C. (1957). In *Cellular Biology, Nucleic Acids and Viruses*, Special Publication of the New York Academy of Sciences, V, p. 173.
Davies, D. R. & Rich, A. (1959). *Acta Cryst.* **12**, 97.
Doty, P., Boedtker, H., Fresco, J. R., Haselkorn, R. & Litt, M. (1959). *Proc. Nat. Acad. Sci., Wash.* **45**, 482.
Felsenfeld, G., Davies, D. R. & Rich, A. (1957). *J. Amer. Chem. Soc.* **79**, 2023.
Fresco, J. R. (1959). *J. Mol. Biol.* **1**, 106.
Fresco, J. R. & Doty, P. (1957). *J. Amer. Chem. Soc.* **79**, 3928.
Fresco, J. R. & Klemperer, E. (1959). *Ann. N.Y. Acad. Sci.* **81**, 730.
Fuller, W. (1959). *J. Phys. Chem.* **63**, 1705.
Grunberg-Manago, M., Ortiz, P. J. & Ochoa, S. (1955). *Science*, **122**, 907.
Morgan, R. S. & Bear, R. S. (1958). *Science*, **127**, 80.
Rich, A. (1957*a*). In *Cellular Biology, Nucleic Acids and Viruses*, Special Publication of the New York Academy of Sciences, V, p. 186.
Rich, A. (1957*b*). In *Chemical Basis of Heredity*, ed. by W. D. McElroy & B. Glass, p. 557. Baltimore: Johns Hopkins Press.
Rich, A. & Davies, D. R. (1956). *J. Amer. Chem. Soc.* **78**, 3548.
Rich, A. & Watson, J. D. (1954). *Proc. Nat. Acad. Sci., Wash.* **40**, 759.
Spencer, M. (1959). *Acta Cryst.* **12**, 59 and 66.
Watson, J. D. (1957). In *The Chemical Basis of Heredity*, ed. by W. D. McElroy & B. Glass, p. 505. Baltimore: Johns Hopkins Press.

J. Mol. Biol. (1961) **3**, 87–100

X-Ray Diffraction Studies on Ribosomes from Various Sources

A. Klug, K. C. Holmes and J. T. Finch

Birkbeck College Crystallography Laboratory, London W.C.1, England

(*Received 4 October 1960*)

X-ray diffraction studies have been made of u noriented specimens of preparations of ribosomes from rat liver, yeast and *E. coli*. Comparative photographs have also been taken of isolated RNA, some proteins, and two small spherical viruses.

Wet gels of particles from all three sources give clear indications of an RNA pattern. After drying or freeze-drying, the diffraction patterns bear no resemblance to that of dried, isolated RNA but are protein-like in character. They are identical in all three cases, indicating a very similar type of protein configuration in particles from different sources. On re-wetting, the original wet gel pattern is recovered, and this effect is reversible. The difference between the patterns in the dry and wet state can be accounted for by the large decrease in scattering power of RNA, relative to that of protein, on drying.

We conclude that the structure of the RNA in the ribosomal particles from all three sources is very similar to that of extracted RNA. Structural studies on isolated RNA are therefore relevant to the problem of whether or not there is a well-defined *in vivo* structure for RNA, and this question is discussed. The X-ray evidence is strongly suggestive of a structure in which two backbone strands run roughly parallel to one another with a separation of the order of 12 Å, but which is not perfectly regular.

1. Introduction

During the last few years we have, at various times, made X-ray diffraction studies on ribosomes extracted from different types of cells. Samples of ribosomes from rat liver, yeast, and *Escherichia coli* have been sent to us by a number of workers in different laboratories. These particles contain as major components only protein and RNA, and also bear a superficial resemblance to the small spherical viruses which we have been studying in this laboratory. Accordingly we set out to investigate any possible structural similarities between them.

Since no one has succeeded in crystallizing ribosomes, nor any component part, our studies have necessarily been confined to taking "powder" photographs of unoriented specimens, in the form of an amorphous mass or wet gel of particles. Our aim was, first, to see whether one could obtain information on the overall particle size and shape from the low-angle part of the X-ray diagrams; and, secondly, to get a general idea of the internal structure by comparing the broad features of the moderate- and high-angle diffraction pattern with the corresponding regions of X-ray diagrams of isolated RNA, of pure proteins and of viruses.

Our preliminary conclusions (Franklin, Klug, Finch & Holmes, 1958), drawn from the first results on ribosomes from rat liver and yeast, need revision. The reason for this lies in an error of interpretation of our early observations that the X-ray diagrams

of dry and wet ribosomes are very different (see below), the former being protein-like in character and the latter strongly resembling that of isolated RNA. The samples as supplied to us were usually lyophilized, and, in view of the considerable instability of unlyophilized material that had been reported (Petermann & Hamilton, 1955; Roth, 1958) we took this to mean that the results on the dry preparations were the more reliable, and that in the wetted preparations the RNA was segregating in some way from the protein. In this paper we report further work that shows this not to be the case, and that the observations on the wetted ribosomes reflect the *in vivo* state of the RNA.

We were stimulated to reconsider the interpretation of our observations by the appearance of a paper of Wilkins, Zubay & Wilson (1959), which showed that a similar situation obtained in respect of the dry and wet states of nucleohistone. In this case, at 98% relative humidity, the X-ray diagrams show the characteristic diffraction from DNA, whereas at low humidity the DNA pattern fades and the diagram is due to the protein. Our consideration of these matters has also been encouraged by a prior communication by Zubay & Wilkins (1960) of the results of their X-ray diffraction studies on ribosomes from *E. coli*. A brief account of our work has already been reported (Faraday Society Informal Discussion, March 1960).

2. Materials and Methods

(a) *Materials*

Rat liver ribosomes

(a) Lyophilized samples of microsomal particles from rat liver were supplied by Dr. Mary Petermann of the Sloan-Kettering Foundation, New York. The material was kept at about 0°C in transit and, when necessary, stored at temperatures below 0°C. It was generally found that the X-ray pattern did not change after storage below 0°C for several months.

Depending on the method of isolation originally used, wet gels were prepared either by adding various dilutions of calf-liver extract (Petermann & Hamilton, 1957), or, in the case of later samples prepared in phosphate-$MgCl_2$ buffer (Petermann, Hamilton, Balis, Samarth, & Pecora, 1958), by simply adding distilled water. The mixing to form a stiff gel was accelerated by low-speed centrifuging in a capillary tube.

In one experiment, a capillary tube containing wet gel was re-opened after photography, the same specimen lyophilized and re-photographed.

Analysis of the material (Petermann, private communication) gave 0·2% of lipid phosphorus, pointing to the presence of 5% phospholipid.

(b) Samples of freshly made ultracentrifuge pellets of rat liver ribosomes, prepared according to the procedure of Palade & Siekevitz (1956), were supplied by Dr. J. L. Simkin of the National Institute for Medical Research, London. Subsequently, a preparation was also made without using the deoxycholate treatment.

These samples (at 0°C) were photographed within hours of their preparation.

Yeast ribosomes

Ribonucleoprotein particles from yeast (Chao & Schachman, 1956; Chao, 1957) were supplied in lyophilized form by Drs. Schachman and Stenesch of the Virus Laboratory, Berkeley. Since $MgCl_2$ or $CaCl_2$ was initially present in addition to the phosphate buffer, wet gel was prepared by simply adding distilled water. Samples were kept cold as for the rat liver microsomes. In addition, a sample of fresh ultracentrifuge pellets was also supplied and this was examined within a week of its preparation.

E. coli *ribosomes*

A fresh ultracentrifuge pellet prepared by the method of Tissières & Watson (1958; see also Tissières, Watson, Schlessinger & Hollingworth, 1959) was supplied by Dr. J. D.

Watson of Harvard University. The solution originally contained 0·01 M-Mg^{2+} and 0·01 M-tris (2-amino-2-hydroxymethylpropane-1:3-diol) buffer (pH 7·4), so that the preparation consisted essentially of 70 S particles and their dimers.

Specimens were always kept at about 0°C during storage and photography.

Some of the material was lyophilized for X-ray photographs of the dry state, and the same specimen was re-wetted and re-photographed.

Ribonucleic acid

RNA from turnip yellow mosaic virus was supplied by Dr. R. Markham of the A.R.C. Virus Research Unit, Cambridge.

RNA extracted by the phenol method from *E. coli* protoplasts (Littauer & Eisenberg, 1959) was supplied by Dr. U. Z. Littauer of the Weizmann Institute, Rehovoth, Israel.

RNA prepared from previously extracted 70 S ribosomes of *E. coli* (see Kurland, 1960) was supplied by Dr. J. D. Watson.

Viruses

The samples of turnip yellow mosaic virus, and of the associated top component used, were originally supplied to this laboratory by Dr. R. Markham, and the tomato bushy stunt virus by Messrs. F. C. Bawden and N. W. Pirie of Rothamsted Experimental Station.

Proteins

Ribonuclease and lysozyme were obtained commercially.

Haemoglobin was supplied by Dr. D. W. Green of the Royal Institution, London.

(b) *Experimental*

X-ray photographs of the specimens, contained in either glass or quartz capillary tubes of about 1 mm diameter, were taken with monochromatic CuKα radiation on a 12 cm diameter evacuated Guinier focusing camera equipped with a bent quartz crystal. A demountable Beaudouin semi-microfocus X-ray tube was used. For the moderate angle photographs (spacings less than about 30 Å) the defining slit at the specimen was usually about 2 mm high and 0·5 mm wide, but for the low-angle work the slit was made shorter and narrower. The specimen holder was kept cool to a temperature of about 2°C during exposures, except in the case of the dry RNA specimens where this was unnecessary. The concentration of the wet gels used was generally of the order of 20 to 30%, but no attempt was made to control this. The dry materials (at air humidity) were packed fairly tightly into the capillary tubes with the aid of a fine glass rod.

Under these conditions, exposure times to give moderately strong photographs of comparable average intensity over the 20 Å to 4 Å region were typically as follows: wet ribosomes, 30 hr; dry ribosomes, 60 hr; wet RNA 25 hr; dry RNA, 120 hr; wet proteins, 25 hr; dry proteins, 50 hr. These figures are only very roughly approximate ones and are intended to illustrate the large differences in scattering power (for the moderate angle region) of the various materials. In comparing times for the wet and dry states of the same material, it should be remembered that, in terms of the amount of dry material present, the differences in scattering power may be even greater than the above times would suggest, since in the wet specimen there is probably less material present per unit volume than in the dry specimens.

Microdensitometer traces of the intensity distribution along the equator of the films were made using a Joyce-Loebl Walker microdensitometer. No attempt was made to correct for any non-uniformity in background, and in nearly all cases the intensity, I, was measured relative to that of clear film behind the backstop. However, in the case of dry RNA, which scatters most weakly of all, a correction had to be made for the scattering from the walls of the quartz capillary tube by subtracting the intensity distribution obtained from a blank run on an empty capillary tube. Fused quartz scatters fairly strongly in the 4 Å region, and despite the thinness of the capillary walls, this background scattering is not negligible when very weak scatterers are examined. (The effect can even be seen in the (uncorrected) intensity curves for dry proteins (Fig. 4) where the maximum

at 4·5 Å characteristic of the wet proteins appears to have moved to a spacing of 4 Å.) In the case of the wet gel specimens, no correction could be made for the background scattering of the liquid water, since the concentration was not known accurately. All intensity curves for wet specimens therefore show a strong peak at, or very close to, a spacing of 3·1 Å, the first maximum for water.

3. Results

(a) *Low-angle scattering*

The low-angle diffraction pattern from wet gels of ribosomes shows central scattering, but no additional subsidiary maxima characteristic of spheres of uniform density

TABLE 1

Low-angle scattering from ribosome gels (spacings $>$ 30 Å†)

Source	Spacing in Å	
Rat liver		
	*c.*90	weak, sharp
Freeze-dried preparation wetted	50	weak, sharp
	?40	very weak, sharp
Fresh ultracentrifuge pellet	120	fairly strong, sharp
	85	fairly strong, sharp
	50	medium, fairly broad
	?40	very weak
Yeast		
	90	medium, sharp
	46	weak, fairly broad
E. Coli		
‡	300	strong, sharp
‡	118	medium, sharp
‡	77	medium, sharp
	43	strong, sharp

† The lower limit chosen for this Table corresponds to the upper limit of the spacings of peaks on the RNA diffraction pattern.

‡ These spacings were kindly checked and measured accurately by Mr. A. W. Longley, using a low-angle camera with a specimen to film distance of 25 cm.

such as are produced by the small spherical viruses (Leonard, Anderegg, Shulman, Kaesberg & Beeman, 1953). We have not attempted to determine the radius of gyration of the ribosomal particles, since we understand this is being done by others (private communications from J. W. Anderegg, U. W. Arndt & W. W. Beeman, and H. M. Dintzis & W. Dibble), but the central darkening present on our photographs is compatible with particles of linear extension of the order of 200 Å.

All photographs show, in addition, a number of weak maxima corresponding to rather high spacings. These are not all developed to the same extent for different specimens, and those spacings that have been observed more than once are given in Table 1. The list is not exhaustive, as we have not made a thorough investigation in

this range. Although we cannot give a structural interpretation, the spacings observed at about 120 Å, 90 Å, 50 Å (and possibly 40 Å) do seem to be characteristic of some common structural organization in the ribosomes, since they are found in different species. The maximum at about 40 Å observed in the case of the rat liver ribosomes could possibly be due to the presence of lipid (see above, under Materials), since this is the only maximum (at 42 Å) also clearly observed in photographs from dry specimens. On the other hand, since a similar spacing is also shown by the *E. coli* ribosomes, which are presumably free from lipid, this spacing may also be characteristic of the particle structure of the rat liver ribosomes.

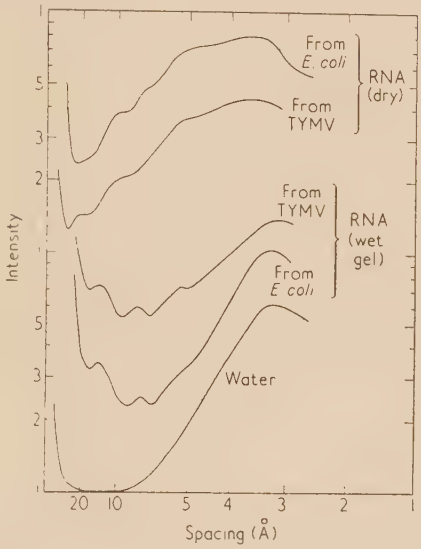

FIG. 1. Scattering curves of wet and dry RNA from two different sources.

The curves shown are logarithmic plots of the intensity distribution measured from microdensitometer traces of the X-ray photographs. In the case of the dry RNA, these have been corrected for the scattering by the walls of the capillary tubes in which the specimens are contained. Note that the peak near 3 Å in the RNA wet gel curve is displaced to a slightly higher spacing than that in the water scattering curve, shown for comparison. The RNA peak at about a spacing of 28 Å cannot be clearly shown on the scale used here (see Table 2).

The maximum at 300 Å produced by the *E. coli* ribosomes does not appear to be a secondary maximum of the single particle scattering, since the spacing is too large. It may be due to interparticle scattering such as would be produced by some kind of aggregation or even loose association of 100 s particles in the medium.

(b) *Moderate-angle scattering* (*spacings* < 30 Å)

The experimental results are given in the form of plots of the logarithm of the scattered intensity against the Bragg spacing (Figs. 1 to 5). The spacings of the maxima are also summarized in Table 2 in terms of an idealized RNA pattern consisting of six bands. In presenting the results on the ribosomes, we have arbitrarily set an upper limit of 30 Å to the spacings under discussion here, since this is the highest spacing shown by isolated RNA. Maxima observed at spacings greater than 30 Å in the ribosome photographs have been listed in Table 1.

(i) *RNA* (Fig. 1, Table 2)

The photographs we have obtained of RNA from *E. coli* and from turnip yellow mosaic virus are very similar to one another and also appear to be essentially in-

TABLE 2

Moderate-angle scattering (*spacings* 30 Å *to* 3 Å)

Spacings measured on microdensitometer traces
(In some cases, two values are given in order to show range of variability)

	Spacings of peaks (in Å)					
RNA: wet gel						
—from TYMV	*c.* 30	12·4	7·5	5·5	—	(3·2)
—from *E. coli*	28 medium, fairly sharp	12·8 strong	7·7 medium	5·9 weak	—	(3·3) displaced w.r.t. water maximum
RNA: dry						
—from TYMV	*c.* 22	10·6	? *c.* 7·0	5·2	3·5	
—from *E. coli*	— weak, sharp	10·5 strong	7·2 weak	5·2 medium	3·5 very strong, very broad (? 3·8 + 3·3 bands)	
Ribosomes: wet gel						
Rat liver	27 medium, fairly sharp	11·5 strong, broad	7·5 7·2 weak, broad	5·5 weak, broad	? 3·7 very weak	water peak
Yeast	29 medium, sharp	11·5 strong, broad	8·0 medium, broad	5·5 weak (+ hint of shoulder at 4·7 Å)	? 3·7 very weak weak broad peak with max. at about 3·5 Å	water peak
E. coli	28 strong, sharp	12·0 12·5 strong, fairly broad	7·5 medium, broad	5·5 weak, broad	—	(3·3) displaced w.r.t. water maximum
Ribosomes: freeze-dried						
Rat liver	25–28 weak, broad		10 strong, broad		3·8 strong, broad	
Yeast	—		10		3·8	
E. coli	—		10		3·8	

distinguishable from those reported for RNA from a variety of sources by Rich & Watson (1954*a*).

The pattern obtained from wet gels of RNA consists of four rings at spacings of about 30 Å, 12·5 Å, 7·5 Å, 5·5 Å, and a strong maximum at about 3 Å, which is

largely due to the scattering by water which is, of course, present in much greater concentrations than RNA in the specimen tube. Careful measurements of the position of this maximum on the microdensitometer traces show it to occur at a spacing of 3·2 Å or 3·3 Å and thus definitely displaced from the spacing of 3·1 Å produced by pure water. Moreover, in some cases, the peak shape is seen to be sharper than that given by water alone. We therefore have good evidence for relatively strong RNA scattering in this region superimposed on the water scattering, and can reasonably attribute this RNA contribution to the maxima at 3·3 Å and 3·8 Å reported by Rich & Watson (1954*a*,*b*) for RNA fibres. It is perhaps worthwhile noting that the reason that these effects are detectable at all above the water background in scattering by gels containing relatively low concentrations of RNA, is that, in our X-ray technique, the diffraction patterns are recorded with high resolution by the use of focused monochromatic radiation.

The dry RNA pattern consists, in idealized form, of the same six bands as in wet RNA, but with decreases in the larger spacings (Rich & Watson, 1954*a*). This is essentially what we have observed, but different specimens do not always show all these lines equally well developed. This may be due to variations in the relative humidity and hence water content during the preparation of the specimens. The occurrence of weak bands at 22 Å and 7 Å is variable, the constant features being the strong bands at 10·5 Å and 5·2 Å and the very broad maximum centred at a spacing of about 3·5 Å. Only rarely have we been able to detect a hint of the latter being made up of the two bands at 3·3 and 3·8 Å reported by Rich & Watson (1954*a*,*b*). In one instance a dry preparation of *E. coli* RNA, originally provided by Watson, which had been stored for several months, appeared to be anomalous in that it gave a weak broad band at a spacing of 16 to 18 Å and a stronger band at 12 Å. On the other hand, the *E. coli* RNA originally provided by Littauer gave the usual pattern even after storage for over a year. We cannot say whether or not these observations reflect a difference in the stability of the RNA prepared by different methods, due, say, to different degrees of contamination by enzyme.

(ii) *Proteins* (Fig. 2)

For comparison purposes, we have also taken X-ray photographs on the same camera of a number of proteins both in the air-dried state and as wet gels. Results for two basic proteins are shown in Fig. 2. The scattering, in all cases, is typically (see, for instance, Arndt & Riley, 1955) concentrated in the 10 Å and 4·5 Å regions in both the wet and dry state, though different proteins give distinguishable curves and there are marked changes in the 10 Å region in the wet-dry transition. In our photographs, the broad maximum at 4·5 Å appears to be displaced to a mean spacing of about 4 Å for the dry specimens, probably because of the decrease in protein scattering on drying relative to the strong background in this region produced by the glass walls of the capillary tubes. No correction was made for this effect in Fig. 2.

(iii) *Spherical viruses* (Fig. 3)

The scattering curves of turnip yellow mosaic virus (TYMV), which contains 40% RNA (Markham, 1959), and of the associated nucleic-acid free protein particle, the so-called top component, both in the wet state, have been discussed elsewhere (Klug & Finch, 1960). Most of the intensity is concentrated in the 10 Å and 4 Å regions associated with protein scattering, but both curves show modulations of high period

($\sim 1/60$ Å^{-1}) due to the regular substructure of the protein shell. The main difference between the two curves is that the very broad maximum in the virus curve at a spacing of about 30 Å is not found in the top component. There are smaller changes

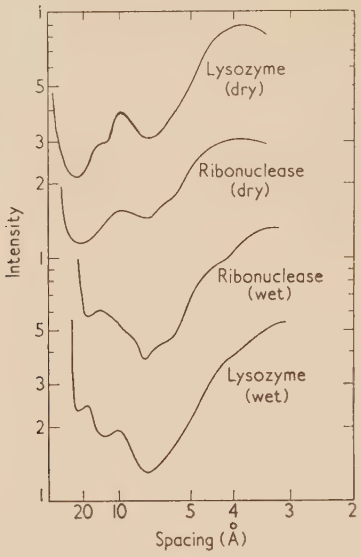

Fig. 2. Scattering curves of two proteins in the wet and dry states.
No correction has been made for the scattering by the walls of the capillary tubes.

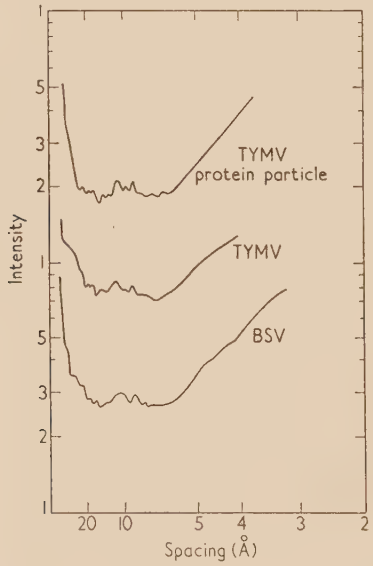

Fig. 3. Scattering curves from a sludge of small crystals of tomato bushy stunt virus (BSV), of turnip yellow mosaic virus (TYMV), and of the RNA-free, non-infectious, protein top component associated with turnip yellow mosaic virus (Markham, 1959).

in the neighbourhood of the 10 Å region, where the intensity of the virus scattering increases near a spacing of 11·5 Å, decreases at 9·6 Å and increases at about 5 Å, relative to that of the top component. While the differences near 30 Å, 12 Å and 5 Å.

are all found in regions where the isolated RNA shows diffraction bands, the scattering curve does not appear to be simply the sum of the top component curve plus that of 40% free RNA. Thus it seems that a proportion of the RNA in the virus particle has a structure different from that of isolated RNA and presumably one imposed upon it by the virus protein. It should also be noted that the scattering curve of TYMV does not have particularly stronger RNA characteristics than that of tomato bushy stunt virus, which contains only 17% RNA.

The scattering from dry TYMV gives diffuse protein rings at 4·5 Å and 9·0 Å, the fine structure being completely lost (Zubay & Wilkins, 1960).

(iv) *Ribosomes*

The main features of the diffraction patterns of freeze-dried ribosomes from rat liver, yeast and *E. coli* are two broad bands at 10 Å and at 3·8 Å (Fig. 4). The curves for the ribosomes from these three different sources are identical with one another.

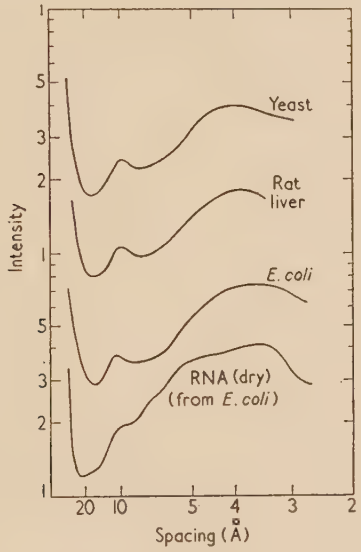

Fig. 4. Scattering curves of freeze-dried preparations of ribosomes from three different sources, compared with that of dry RNA.

The patterns are essentially protein-like in character, as can be seen by a comparison with the scattering curves for the proteins ribonuclease and lysozyme (Fig. 2). They bear little resemblance to the pattern produced by dry RNA, except insofar as the preparations of rat liver ribosomes showed a weak band at a spacing of 25 to 28 Å and inasmuch as the maximum in the 4 Å region is found at 3·8 Å rather than at 4 Å as in the proteins.

The scattering curves from wetted ribosomes of the three species examined are shown in Fig. 5. The patterns strongly resemble one another, the differences in relative heights of corresponding peaks in Fig. 5 arising from the fact that the ribosome concentration in the wet gels was not controlled. The *positions* of the maxima are all the same, and are very close to those found for wet gels of RNA. As can be seen from the summary in Table 2, nearly all the characteristic RNA bands can be identified, and, in the case of the *E. coli* ribosome pattern, the displacement of the water peak at 3·1 Å

to a slightly higher spacing is detectable, just as for isolated RNA (see above). Such slight differences as are found from the diffraction pattern of isolated RNA, notably the displacement of the 12·5 Å band of RNA to lower spacings (11·5 to 12·0 Å) in the ribosome photographs, can be accounted for by the presence of protein.

As explained in the Introduction, the very marked contrast between the photographs of dry and wet ribosomes was originally taken to mean that the RNA configuration in the dry particles was determined by the protein of the ribosomes (Franklin *et al.*, 1958), but that the RNA was segregating from the protein in the wetted ribosomes. Several lines of evidence now point to the fact that this state of structural segregation of the RNA from the protein, observed in the wet state, is characteristic of the native particles:

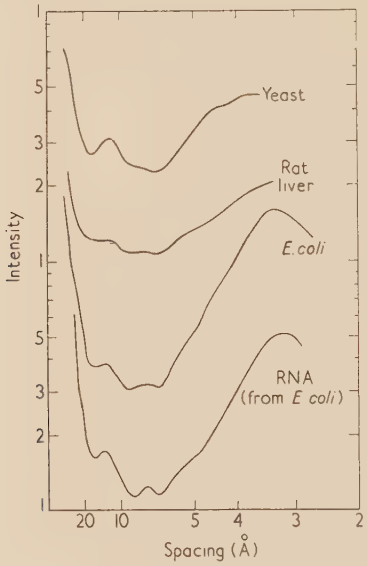

FIG. 5. Scattering curves of wet gels of ribosomes from the sources shown compared with that of a gel of RNA.

The concentrations in the various specimens have not been controlled, and the water background (see Fig. 1) cannot therefore be subtracted: no significance can therefore be attached to differences in heights of corresponding peaks on different curves.

Peaks at spacings higher than 28 Å are listed in Table 1.

(i) The protein-like character of the curves obtained from the dry ribosomes, despite the very large proportion of RNA contained in them ($\sim 50\%$) can be accounted for by the very weak scattering power of dry RNA relative to that of protein. A comparison of exposure times (see 2(b), page 89) shows that dry RNA scatters about one third as strongly as dry protein. Thus the sum of scattering from more or less equal amounts of dry RNA and dry protein, not in structural dependence on one another, would nevertheless appear to be protein-like in character. This was confirmed by an experiment in which an X-ray photograph was taken of a 1 : 1 mixture of dry RNA and dry lysozyme. The pattern obtained was almost indistinguishable from that of pure dry lysozyme.

(ii) The change in the X-ray pattern between the wet and dry states of the ribosomes is reversible. This was demonstrated by two different experiments. In the first,

a wetted preparation of freeze-dried rat liver ribosomes, which gave an RNA-like pattern, was re-freeze-dried and photographed. The X-ray pattern obtained was the same as if the particles had not been wetted. In the second, a fresh wet gel of *E. coli* ribosomes was freeze-dried and gave the usual protein-like pattern; but, on re-wetting, the original RNA-like pattern was recovered.

(iii) Electron micrographs of a preparation of rat liver ribosomes, which had been exposed to X-rays during photography in the wet state, were kindly taken for us by Dr. Robley C. Williams. These showed no evidence of any degradation of the particles nor of any release of fibrous material from them.

(iv) In all cases, weak exposures of fresh preparations of dilute gels of ribosomes (in the form of ultracentrifuge pellets), photographed, at times, within a few hours after preparation, showed the band at 12 Å which is the strongest in the RNA pattern.

4. Discussion

The behaviour of ribosomes with respect to water content is very similar to that of nucleohistone (Wilkins *et al.*, 1959): at high humidity the diffraction pattern is largely due to nucleic acid and at low humidity to protein. The reason for this must lie in the large change in the relative scattering powers of protein and nucleic acid on drying. The main protein diffraction rings at 10 Å and 4·5 Å are thought to correspond respectively to the lateral separation between adjacent segments of polypeptide chains and to the repeat distance along the chains. These overall structural features are presumably retained on drying, so that, although a protein pattern becomes weaker and more diffuse, it is not radically changed. On the other hand, the innermost peaks of the RNA pattern are all reduced in spacing on drying, indicating a transverse shrinking of the RNA molecules; and presumably the RNA molecules also crumple up more irregularly on drying so that the diffraction pattern is severely weakened as well.

The fact that diffraction patterns of dry ribosomes are produced largely by their protein enables us to compare—in a very general way—the protein structures of different species. The curves for rat liver, yeast and *E. coli* ribosomes in Fig. 4 are indistinguishable from one another, indicating a very similar structural organization of the protein. It would not be surprising if this structural similarity was the reflection of very similar amino acid compositions, such as have been observed in the cases of ribosomal protein from rabbit reticulocytes, pea seedlings and rat liver by T'so, Bonner & Dintzis (1958).

The strong resemblance of the diffraction patterns of wet ribosomes from all three sources examined to that of gels of isolated RNA is a good indication that the structure of the RNA in the ribosomes is very similar to that of extracted RNA. The fact that our conclusion holds for ribosomes from three such widely differing species as rat liver, yeast and *E. coli* suggests that there is a common type of structural organization for the ribosomes of all organisms.

Our results and conclusions on all three species are entirely in accord with those of Zubay & Wilkins (1960) on *E. coli* ribosomes. These workers found that the X-ray diffraction patterns of ribosomes with sedimentation coefficients of 100 s, 70 s, and 50 s (Tissières & Watson, 1958) show no obvious difference. Under the conditions of our experiments the ribosomes were likely to be present mainly in the form of 70 s particles (for *E. coli*) or 80 s particles (for rat liver and yeast) and their dimers. The

results of Zubay & Wilkins (1960) show that the general conclusions probably hold for the smaller components as well.

Further evidence that RNA configuration in solution is basically the same as in the ribosomes comes from the demonstration by Schlessinger (1960) of the identical hypochromicity (both total and configurational) of *E. coli* ribosomes and their isolated RNA. Similar results on the total hypochromic effect were obtained for *E. coli* ribosomes by Zubay & Wilkins (1960), who also showed that the absolute extinction coefficients of the RNA in the ribosomes is about the same as that of free RNA in 0·1 M-phosphate buffer. Earlier, Hall & Doty (1959) found that rat liver ribosomes also show a hypochromic effect, similar to that shown by free RNA.

These results mean that structural studies on isolated RNA (and on related model compounds) are relevant to the problem of the secondary structure of the RNA within the ribosomes.

To assign a structural meaning to the spacings observed in powder diagrams of RNA it is necessary to have a diffraction pattern of an oriented fibre. Unfortunately the best patterns so far obtained (Rich & Watson 1954*b*) are rather poor, but suggestive of a rather disordered DNA-like or double helical configuration. More information on this point has come from the studies of Rich (1957, 1959) on synthetic polyribonucleotides. In particular, the RNA pattern resembles that given by a mixed polynucleotide polymer containing either only adenine and uracil bases, or, alternatively, all four bases, in more or less random sequence (Rich, 1957). Furthermore, the moderately well-oriented diffraction pattern of fibres of a 1 : 1 complex formed between polyinosinic acid and polycytidylic acid is said to resemble that of RNA (Davies & Rich, 1958).

It seems clear that the 28 Å spacing of wet RNA corresponds to a superposition of the equatorial and first layer-line reflections of an oriented double-helical pattern, the 12·5 Å spacing to a strong second layer-line, and the 3·3 and 3·8 Å spacings to the separation between neighbouring bases. In the case of a double-helical model, the second layer-line has a contribution from a second-order Bessel function, and the spacing of the reflections therefore corresponds roughly to the lateral separation of the two strands. It is significant that the strongest band observed in the ribosomal diffraction patterns from all three sources as well as from RNA (see Fig. 5) is the 12·5 Å spacing. This is strongly suggestive of a structure in which two chains run roughly parallel to one another with a separation of this order, but which is otherwise irregular. A model of this kind with occasional base-pairing has been discussed by Crick (1957), and recent physico-chemical studies of RNA in salt solutions at moderate temperatures suggest that it has a partial helical structure (Doty, Boedtker, Fresco, Haselkorn & Litt, 1959*b*) containing hydrogen-bonded regions. (See also Cox & Littauer, 1959.)

Within this general class of two-strand structures a number of more specific models are possible: e.g., imperfect hairpin-like helices having a DNA-like character and united by flexible unstructured regions (Doty, Boedtker, Fresco, Hall & Haselkorn, 1959*a*), or a double helix-with-loops as proposed by Fresco & Alberts (1960) to account for the complex formed between the synthetic polymers poly-U and poly-AU. The nature of the present X-ray evidence, based essentially on recording the dominant spacings that occur, is such that we cannot tell these models apart. An important step forward, has, however, been recently taken by Luzzati, who has made *absolute* measurements of the low-angle X-ray scattering from dilute RNA solutions. From these, it seems that the average mass per unit length along the RNA molecules is the

same as that for DNA (Timasheff & Luzzati, 1960). If correct, this would imply that the bulk of the RNA is in a double-helical configuration and that limits could be set to the degree of irregularity and/or looping.

It is too early to say whether there is any biological significance in the secondary structure of the RNA that is found in the ribosomes as well as in isolated RNA. It should be borne in mind that in the tobacco mosaic virus (TMV) particle the RNA is in the form of a single chain (Franklin unpublished, see Franklin, Caspar & Klug, 1959), yet after extraction it appears to coil up (Boedtker, 1959; Haschemeyer, Singer & Fraenkel-Conrat, 1959) to form a secondary structure of one of the types just discussed. This presumably happens by random hydrogen-bond formation between bases. This TMV RNA gives an X-ray pattern very similar to that of RNA from other sources (Rich & Watson, 1954*a*,*b*), in particular to ribosomal RNA, and its physico-chemical properties in solution are also very similar to that of other RNA's (Doty *et al.*, 1959*a*). It thus appears to be extremely difficult to distinguish by methods of this kind the characteristics of a possibly inherently well-defined configuration (ribosomal RNA, say) from one that apparently arises in a haphazard fashion (TMV RNA, say).

The investigations reported here were originally begun together with our colleague, the late Dr. Rosalind Franklin, to whose memory we should like to pay tribute here.

We wish to thank Drs. Mary Petermann, H. K. Schachman, J. L. Simkin, and J. D. Watson, for supplying preparations of ribosomal particles for these investigations; Drs. R. Markham and U. Z. Littauer for supplying RNA, and Dr. D. W. Green for supplying haemoglobin; and Drs. G. Zubay and M. H. F. Wilkins for access to their unpublished data and for discussion.

The work was supported by the Agricultural Research Council and by a research grant no. E-1772 from the National Institute of Allergy and Infectious Diseases, U.S. Public Health Service.

REFERENCES

Arndt, U. W. & Riley, D. P. (1955). *Phil. Trans.* A **247**, 409.
Boedtker, H. (1959). *Biochim. biophys. Acta*, **32**, 519.
Chao, F.-C. (1957). *Arch. Biochem. Biophys.* **70**, 426.
Chao, F.-C. & Schachman, H. K. (1956). *Arch. Biochem. Biophys.* **61**, 220.
Cox, R. A. & Littauer, U.Z. (1959). *Nature*, **184**, 818.
Crick, F. H. C. (1957). *Spec. Pub. N.Y. Acad. Sci.* **5**, 173.
Davies, D. R. & Rich, A. (1958). *J. Amer. Chem. Soc.* **80**, 1003.
Doty, P., Boedtker, H., Fresco, J. R., Hall, B. D. & Haselkorn, R. (1959*a*). *Ann. N. Y. Acad. Sci.* **81**, 693.
Doty, P., Boedtker, H., Fresco, J. R., Haselkorn, R. & Litt, M. (1959*b*). *Proc. Nat. Acad. Sci., Wash.* **45**, 482.
Franklin, R. E., Caspar, D. L. D. & Klug, A. (1959). In *Plant Pathology: Problems and Progress, 1908–1958*, ed. by C. S. Holton p. 447. Madison: University of Wisconsin Press.
Franklin, R. E., Klug, A., Finch, J. T. & Holmes, K. C. (1958). *Disc. Faraday Soc.* **25**, 197.
Fresco, J. R. & Alberts, B. M. (1960). *Proc. Nat. Acad. Sci., Wash.* **46**, 311.
Hall, B. D. & Doty, P. (1959). *J. Mol. Biol.* **1**, 111.
Haschemeyer, R., Singer, B. & Fraenkel-Conrat, H. (1959). *Proc. Nat. Acad. Sci., Wash.* **45**, 313.
Klug, A. & Finch, J. T. (1960). *J. Mol. Biol.* **2**, 201.
Kurland, C. G. (1960). *J. Mol. Biol.* **2**, 83.

Leonard, B. R., Anderegg, J. W., Shulman, S., Kaesberg, P. & Beeman, W. W. (1953). *Biochim. biophys. Acta*, **12**, 499.
Littauer, U. Z. & Eisenberg, H. (1959). *Biochim. biophys. Acta*, **32**, 336.
Markham, R. (1959). In *The Viruses*, ed. by F. M. Burnet & W. M. Stanley, Vol. II, p. 33. New York: Academic Press.
Palade, G. E. & Siekevitz, P. (1956). *J. Biophys. Biochem. Cytol.* **2**, 176.
Petermann, M. L. & Hamilton, M. G. (1955). *J. Biophys. Biochem. Cytol.* **1**, 469.
Petermann, M. L. & Hamilton, M. G. (1957). *J. Biol. Chem.* **224**, 725.
Petermann, M. L., Hamilton, M. G., Balis, E., Samarth, K. & Pecora, P. (1958). In *Symposium on Microsomal Particles and Protein Synthesis*, ed. by R. B. Roberts, p. 70. Washington, D.C., Acad. of Sciences. (Distributed by Pergamon Press.)
Rich, A. (1957). *Spec. Pub. N.Y. Acad. Sci.* **5**, 186.
Rich, A. (1959). In *A Symposium on Molecular Biology*, ed. by R. E. Zirkle, p. 47. University of Chicago Press.
Rich, A. & Watson, J. D. (1954*a*). *Nature*, **173**, 995.
Rich, A. & Watson, J. D. (1954*b*). *Proc. Nat. Acad. Sci., Wash.* **40**, 759.
Roth, J. S. (1958). *Arch. Biochem. Biophys.* **74**, 277.
Schlessinger, D. (1960). *J. Mol. Biol.* **2**, 92.
Timasheff, S. N. & Luzzati, V. (1960). *Biochem. J.* **76**, 56P.
Tissières, A. & Watson, J. D. (1958). *Nature*, **182**, 778.
Tissières, A., Watson, J. D., Schlessinger, D. & Hollingworth, B. (1959). *J. Mol. Biol.* **1**, 221.
T'so, P. O. P., Bonner, J. & Dintzis, H. M. (1958). *Arch. Biochem. Biophys.* **76**, 225.
Wilkins, M. H. F., Zubay, G. & Wilson, H. R. (1959). *J. Mol. Biol.* **1**, 179.
Zubay, G. & Wilkins, M. H. F. (1960). *J. Mol. Biol.* **2**, 105.

J. Mol. Biol. (1961) **3**, 101–109

Transfer of DNA from Parent to Progeny in a Tissue Culture Line of Human Carcinoma of the Cervix (Strain HeLa)†‡

Edward H. Simon

California Institute of Technology, Pasadena, California, U.S.A.§

(*Received 18 August 1960, and in revised form 8 October 1960*)

5-bromodeoxyuridine was used to label the DNA of HeLa cells. The density of the DNA from cells kept in the presence of the analogue for one and two divisions was examined by means of density gradient centrifugation. After the first division, all the DNA was found to be half-labeled; after the second, both half and fully labeled material was found. These results are consistent with a semiconservative mechanism of DNA replication.

1. Introduction

According to the generally accepted model of DNA structure proposed by Watson & Crick (1953), the molecule is a double helix consisting of two complementary chains

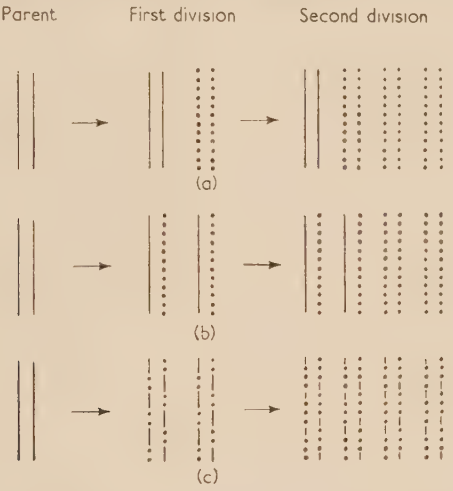

Fig. 1. Models of DNA replication. Predictions for the distribution of parental material between the daughter duplexes for the first and second division according to the three models of replication: (a) conservative, (b) semiconservative, and (c) dispersive.

of nitrogenous bases connected by sugar-phosphate backbones. The complementarity is introduced by the selection rule that adenine pairs only with thymine, and guanine only with cytosine. These bases, however, can be replaced by analogues having the same hydrogen-bonding properties as the original. Figure 1 illustrates the three

† Part of this investigation was carried out during the tenure of a Predoctoral Fellowship from the National Cancer Institute, United States Public Health Service.

‡ Submitted to the California Institute of Technology in partial fulfilment of the requirements for the degree of Doctor of Philosophy.

§ Present address: Department of Biological Sciences, Purdue University, Lafayette, Indiana.

general schemes by which the molecule may duplicate (Delbrück & Stent, 1957). Conservative models imply that the original parental strands remain intact and do not separate (Block, 1955). Semiconservative models imply that the strands separate but that each individual strand remains intact (Watson & Crick, 1953), and dispersive models imply that the parental material is more or less equally distributed among the daughter strands (Delbrück, 1954). By giving the progeny and parental DNA different density labels and applying the density gradient technique developed by Meselson, Stahl & Vinograd (1957), it is possible to distinguish among these models of replication.

Meselson & Stahl (1958) labeled the DNA of *E. coli* with ^{15}N and obtained results consistent with the semiconservative model. Sueoka (1960), with the same methods, obtained similar results for the replication of DNA in *Chlamydomonas*.

In the present work, 5-bromodeoxyuridine (BDU) has been employed as the label for investigating the transfer of DNA from parental to progeny HeLa (human carcinoma of the cervix) cells. BDU has the advantage of making the density difference between normal and half-labeled DNA about four times greater than in the Meselson & Stahl experiments. Furthermore, it can be used to label cells grown in complex media whereas ^{15}N cannot. It will be shown that the replication of HeLa cell DNA is consistent with the semiconservative model.

2. Materials and Methods

(a) *Cell growth studies*

The cells were derived from a clonal line of HeLa S3, stem 1 cells originally isolated by Gey (Scherer, Syverton & Gey, 1953), and later cloned by Puck (Puck & Fisher, 1956), who designated it S3, and then recloned by Vogt (1958), who designated it stem 1. Cells were grown in 50 mm petri dishes with 5 ml. of modified Eagle's medium, as described in Temin & Rubin (1958), plus 15% horse and 15% human serum. Stock lines of cells were transferred by trypsinization every 3 to 4 days and new stock plates seeded with 2 to 3×10^5 cells. Cultures were kept in a humidified CO_2 incubator at 37 to 38°C. Medium changes were usually made every two days.

The growth rate of the culture was determined by drawing two circles, each about 5 mm in diameter, on the bottom of a petri dish and adding 5×10^4 to $1{\cdot}5 \times 10^5$ cells in 5 ml. of medium. The cells within the circles were counted 12 to 24 hr after plating, and on successive days thereafter. In general, 2 plates were used for each determination, the counts from both circles on each plate being added. The low cell densities minimized overcrowding and the consequent slowing down of cell multiplication.

(b) *Analogues*

The 5-bromodeoxyuridine was obtained from the Cyclo Chemical Co. of Los Angeles, and aminopterin through the courtesy of the Lederle Research Laboratories, Pearl River, New York.

(c) *Labeling procedure*

Cultures containing 1 to 3×10^6 cells per petri dish were trypsinized, and 5×10^4 to 3×10^5 cells were transferred into 5 ml. of medium supplemented with 5-bromodeoxyuridine (BDU). In some cases, aminopterin was also added to the medium to inhibit endogenous thymidylic acid synthesis (Simon, 1960).

(d) *Preparation of DNA*

The DNA was isolated by two methods; its density distribution was the same in both cases. The first, or direct, method had the advantages of speed, efficiency, gentleness of treatment and economy of material. Between 0·5 and 2×10^6 cells were removed by

trypsinization, centrifuged and resuspended in 1 ml. of 0·9% NaCl to 0·01 M-Na citrate, then subjected to three rapid freeze-thaw cycles and centrifuged again at 4°C. The sediment was suspended in 0·1 to 0·3 ml. citrate saline, and a suitable portion placed in concentrated CsCl for subsequent examination in the analytical ultracentrifuge. It was possible to have the preparation in the ultracentrifuge within 1·5 hr after removing the cells from the plate. Since the cells were either kept below 4°C or in concentrated CsCl the entire time, there was little chance for DNase to act or for artifacts of preparation to occur. This method has the disadvantage that little material is removed; as a result the sample contains a considerable amount of non-DNA u.v.-absorbing material, and accurate density measurements are difficult to make.

This problem was alleviated by the second, or phenol, method as modified from Kirby (1957), which was used to confirm results obtained by the direct method. Ten to thirty million cells were removed as described above and immediately suspended in 1·5 ml. fresh neutral (pH 6·8 to 7·2) trichloroacetate and 1·5 ml. purified phenol. The cells were ground with a mechanically driven Teflon grinder, transferred to a centrifuge tube, and spun at 10,000 rev/min for 1 min at 4°C. The aqueous phase was removed, treated again with phenol, and extracted several times with ether. The nucleic acid was precipitated with 2 vol cold ethanol, dissolved in 1 ml. 0·04 M-NaCl, and reprecipitated. After redissolving in citrate-saline, a sample was run in the ultracentrifuge. By saving only the material that precipitated in the first 30 sec, after the addition of the ethanol, a partial separation of the DNA from the RNA was achieved.

(e) *Density measurements*

From 2 to 5 μg of DNA were placed in 1 ml. of purified CsCl (optical density at 2600 Å less than 0·1). The density of the solution was adjusted to 1·75 and 0·7 ml. was placed in the ultracentrifuge cell and centrifuged for about 15 hr at 44,770 rev/min. Preliminary experiments showed that this time sufficed for the bands to reach their equilibrium position. The density of the resultant band could be calculated directly from the initial density of the CsCl solution, the velocity of the centrifuge run, and the distance of the band from the center of the fluid column (Meselson *et al.*, 1957). In this way it was shown that normal HeLa DNA has a density of 1·70. A more convenient method is to run a marker DNA of given density with each sample. The resulting picture may then be traced with a densitometer (the Joyce-Loebl double beam microdensitometer was used) and the distance between peaks measured directly (Sueoka, 1960). In these experiments, normal HeLa DNA is assumed to have a density of 1·700, and the other densities are given relative to this standard. One unit is defined as equal to 1 mm on the trace, and is approximately equal to $2/3 \times 10^{-3}$ density units. The results will be given in terms of this parameter, assuming normal DNA to be at zero units.

3. Results

(a) *Normal cells*

The doubling time of the HeLa cell cultures in these experiments was 17 to 24 hr. Since Vogt, working with microdrops, had shown that no cells divide until at least 12 hr after plating, the "zero" cell count was made at that time.

DNA from a normal, exponentially growing culture of HeLa cells prepared by the phenol method is shown in the left-hand band of Fig. 3. Note that the band is decidedly skewed towards the heavy side. A similar result has been found with DNA isolated from calf thymus (Meselson *et al.*, 1957).

(b) *Effects of one division in BDU*

Two methods were employed to demonstrate the effects of one division in the presence of BDU on cellular DNA.

In the first, cells were plated at a concentration of $1{\cdot}5 \times 10^5$ per plate into medium containing either 12 or 20 μg BDU/ml. Both concentrations yielded similar results. Counts made 12 and 36 hr after plating showed that both control and treated cultures had approximately doubled in that interval (Table 1). Figure 2 shows a photometer

TABLE 1

Growth of cells for 36 hr in 20 μg/ml. BDU

	Hours after plating			
	Experiment A		Experiment B	
	12	36	12	36
Control	77†	175	155†	332
	195	369	135	286
	58	107	118	229
Total	330	651	408	847
BDU	130	267	162	390
	127	230	129	294
	120	298	86	155
Total	377	795	377	839

† Number of cells/2 circles/plate. Cells were plated into normal medium and medium containing 20 μg/ml. BDU. First count made 12 hr, second count 36 hr, after plating.

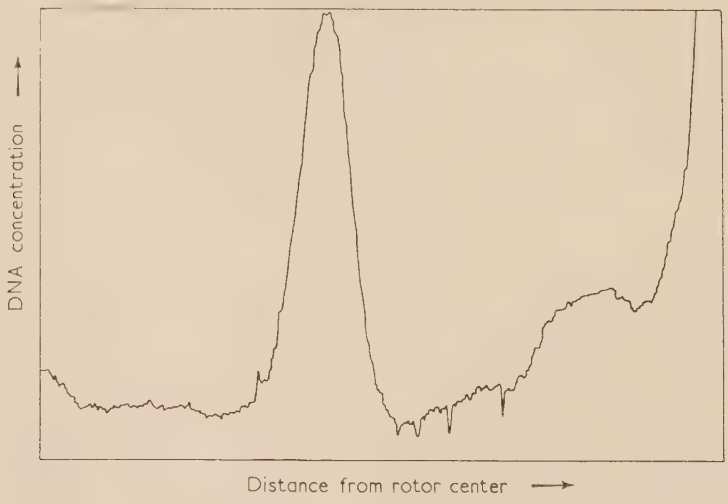

FIG. 2. Densitometer trace of DNA from HeLa cells after one division in BDU. Cells were harvested 36 hr (one division) after being plated into medium containing 20 μg/ml. Their DNA was isolated by the direct method, as described in the text, and banded in a CsCl density gradient at a speed of 44,770 rev/min. The features of the band are independent of how the DNA was isolated. The hump to the right of the band is an artifact probably caused by a drop of oil on the lens of the ultracentrifuge (see Fig. 3).

trace of DNA isolated from cells in an experiment of this type. Note that there is no heavier or lighter band (the "hump" 85 units from the DNA is an artifact—see Fig. 3) and that the band is relatively symmetrical. Figure 3, representing the same pre-

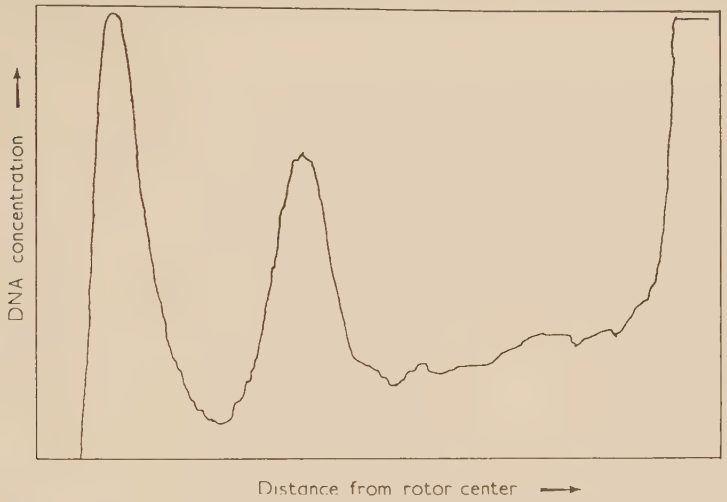

FIG. 3. Densitometer trace of normal and half-substituted DNA from HeLa cells. Normal cells were added to the centrifuge cell containing the material of Fig. 2. Their DNA was isolated by the direct method and banded at a speed of 44,770 rev/min. The trace permits ready comparison of the differences between the two bands. Note that there is no trace of material to the right of the half-substituted band.

paration with marker DNA added, permits ready comparison of the differences between the two bands.

The second method was based on the observations that the folic acid analogue aminopterin prevents cell division and that in the presence of aminopterin and BDU (A + B) HeLa cells divide only once (Simon, 1960). Aminopterin was made a specific

TABLE 2

Growth of cells in aminopterin + BDU

	Days after plating					
	1	2	3	4	5	6
	138†	238	—	300	—	287
	126	189	—	270	—	263
Total	264	427	—	570	—	550

† Number of cells/2 circles/plate. Cells were plated in usual manner into medium containing 5 μg/ml. aminopterin, 20 μg/ml. BDU, 40 μg/ml. adenosine and 40 μg/ml. glycine. First count was made about 15 hr after plating.

inhibitor of thymidylic acid synthesis by the addition of adenosine and glycine to the medium (Hakala, 1957; Simon, 1960). Under these conditions, maximum BDU incorporation would be expected. Samples of 4×10^5 cells were placed in plates containing

medium supplemented with 5 μg aminopterin/ml., 20 μg BDU/ml., 40 μg adenosine/ml., and 40 μg glycine/ml. For counting purposes, 1×10^5 cells were plated into an identical medium. The DNA of the cells of the first group was banded 4 days after plating, at which time the control cells had approximately doubled (Table 2). Again, a single, sharp, substituted band was found.

(c) *Effects of two divisions in BDU*

Preliminary experiments showed that although the first division of HeLa cells in BDU was completed within 36 hr after plating, it took several days for the number of cells to double again. Therefore, it was impossible to attain a population of cells which had divided exactly twice in the presence of BDU, and it was necessary to determine a time that would allow an appreciable number of the cells to divide twice but none to divide a third time. Fifty to fifty-five hours proved to be adequate.

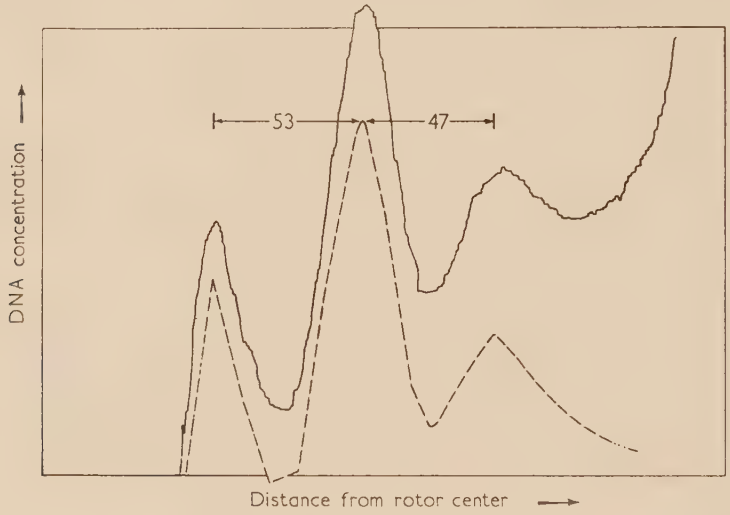

FIG. 4. Densitometer trace of DNA from HeLa cells after two divisions in BDU. Cells were harvested 51 hr after being plated into medium containing 12 μg/ml. 5-bromodeoxyuridine. At this time all the cells had divided once, and some twice. Normal cells grown at the same time were mixed with the treated ones in a ratio of 1 : 4 and the DNA was isolated by the phenol method described in the text. The broken line shows the same run after absorption due to the CsCl is subtracted. The distances are given in "units." One unit is defined as equal to 1 mm on the densitometer trace and is approximately equal to $2/3 \times 10^{-3}$ density units.

In order to ascertain more precisely the relative densities of the bands appearing at these times, in some experiments, control cells (grown at the same time) were added to the test cells and the DNA isolation carried out on the pooled material. The results were the same as when independently isolated DNA was added as the marker.

The experiment was performed three times under slightly different conditions, with quantitatively identical results. In the experiment illustrated (Fig. 4) the cells were grown in the presence of 12 μg/ml. BDU, their medium replaced 24 hr after plating, and the cells removed for assay 17 hr later. The sample was mixed with a portion of normal cells grown at the same time at a ratio of 4 : 1 and the DNA was isolated by the phenol method.

The observed densities of approximately 1·735 and 1·77 correspond respectively to about 35% and 70% replacement of thymine with BDU (Meselson *et al.*, 1957). It should be noted that the conversion of density to per cent replacement is uncertain and may be in error by as much as 50%.

4. Discussion

Each of the models of DNA duplication predicts a specific distribution of parental DNA among the progeny (Fig. 1). The conservative model predicts that after the first division both old and new DNA will be present. Since after one division in BDU only new DNA is found (Fig. 2), the conservative model is unequivocally excluded.

It remains to distinguish between the semiconservative and dispersive models. After two divisions, the semiconservative model predicts two bands, one hybrid and one fully substituted, whereas the dispersive model predicts a single three-quarter substituted band. Unfortunately, it was not possible to obtain cultures in which all the cells had divided twice in the presence of the analogue. The dispersive model, therefore, cannot be excluded merely because two substituted bands are found. We can exclude it for other reasons, however. To do so, we must consider the genesis of the heavy DNA recovered from cells kept 51 hr in BDU.

The first possibility is that this DNA resulted from two divisions in BDU. According to the semiconservative model, the band should have a density of 106 units—twice the density of the hybrid band (Fig. 4). According to the dispersive model, the density should be 80 units (53 + 53/2). The observed density is 100 units.† The slight discrepancy between the observed value and the value expected according to the semiconservative model will be discussed later. The much greater difference between the value predicted by the dispersive model and the one observed would have to be explained by a very strong selection of heavily incorporated molecules. The detrimental effect of incorporation of BDU into DNA (Simon, 1960) makes such an interpretation appear extremely unlikely.

The second possibility is that the DNA of the heavy band had replicated more than twice. HeLa cells, under our best conditions, have a division time of 17 hr; therefore, no more than three divisions could have occurred in the 51 hr that elapsed between their plating and harvesting. We can proceed to show that in fact only two divisions occurred. The DNA of cells collected 36 hr after plating gave rise to a single band. This means that virtually all the molecules had divided once and only once, a natural conclusion of the semiconservative model. The band could not have been the result of two dispersive divisions; if it had, the half-substituted material would have had a density of 35·3, and no material heavier than 71 units could have been found.‡ Figure 4 shows that this was not the case. Accordingly, if the heavy DNA had undergone three divisions, two of them would have had to occur between 36 and 51 hr; but as shown above, this is impossible. Furthermore, no trace of a band between the hybrid and heavy DNA was seen in any of the experiments with cells taken 48 to 55 hr after plating. Such a band, made up of DNA which had replicated twice, would be expected because of the asynchrony of the culture. These findings essentially rule out the dispersive model for DNA replication.

† The effect of the nonlinearity of the CsCl gradient and the compression of the CsCl solution on the relative positions of the bands were considered and found to be negligible. Both corrections would tend to equalize the distances between the bands.

‡ These numbers were derived as follows: 35·3 + 35·3/2 = 53, the observed density after the postulated two divisions; 71 = 2 × 35·3, or twice the half-substituted material.

The relative lightness of the fully substituted band is probably due to selection of special molecules. They can arise by two methods. One is the presence in the culture of cells able to restrict incorporation of BDU. Such cells would probably be the ones most likely to divide first. The other is heterogeneity with regard to BDU incorporation among molecules within individual cells. This would possibly be related to their guanine-cytosine content (see below). The selection hypothesis is based on the observation that DNA synthesized in the presence of aminopterin and BDU, and therefore maximally substituted, is incapable of further multiplication (Simon, 1960). In the absence of aminopterin, submaximal levels of incorporation are possible and heavily substituted molecules would tend to be selected against.

A distribution of guanine-cytosine content among the DNA molecules is suggested by the asymmetry of the band formed by normal HeLa DNA. The band has a pronouncedly heavy tail, an indication that not all of its molecules are of equal density. Rolfe & Meselson (1959) have shown that the density of DNA increases with increasing guanine-to-adenine ratio. Accordingly, the heavy tail may consist of molecules rich in cytosine and poor in thymine. Sueoka, Marmur & Doty (1959) have shown that this is the explanation of the similar tail observed in thymus DNA.

The hybrid band, on the contrary, is nearly symmetrical. This finding would be a consequence of the assumed guanine-cytosine distribution, since the molecules of the tail, which are rich in cytosine, can incorporate less BDU than the others, and therefore have a smaller increment in density. The difference in incorporation would tend to offset the original difference in density and reduce the tail in the half-substituted band. After a second division in BDU, these molecules would be lighter than the majority; if they tend to be the first molecules to divide, that would explain the observed density of the heavy band.

The reported distribution of DNA between parent and progeny cells does not in itself prove that the conserved subunit is the single polynucleotide strand predicted by Watson & Crick (1953). Meselson & Stahl (1958) have shown that when hybrid DNA is heated the two subunits separate. The identity of these subunits has been the subject of several investigations (Cavalieri, Rosenberg & Deutsch, 1959; Marmur & Lane, 1960; Doty, Marmur, Eigner & Schildkraut, 1960). Cavalieri *et al.* have presented evidence indicating that the subunits are double helices, while the Doty group has suggested somewhat more convincingly that the subunits are indeed two single polynucleotide strands. This latter conclusion, combined with the work of Sueoka (1960) on *Chlamydomonas* and the present work on HeLa cells, makes it appear likely that DNA from most sources multiplies according to the semiconservative model suggested by Watson & Crick (1953). The matter, however, remains open.

The author is indebted to Dr. Renato Dulbecco for his guidance and encouragement throughout the course of this work, and to Dr. R. L. Sinsheimer and Dr. J. Vinograd for the use of the ultracentrifuge and for many helpful discussions. Financial assistance was received from a National Science Foundation graduate training grant G-3438 and, in the form of a predoctoral research fellowship, from the National Institutes of Health, United States Public Health Service. In addition, the author held an Arthur McCallum Fellowship during the summer of 1957.

REFERENCES

Block, D. P. B. (1955). *Proc. Nat. Acad. Sci., Wash.* **41**, 1058.

Cavalieri, L. F., Rosenberg, B. H. & Deutsch, J. F. (1959). *Biochem. Biophys. Res. Comm.* **1**, 124.

Delbrück, M. (1954). *Proc. Nat. Acad. Sci., Wash.* **40**, 783.
Delbrück, M. & Stent, G. S. (1957). In *The Chemical Basis of Heredity*, ed. by W. D. McElroy & B. Glass, p. 699. Baltimore: Johns Hopkins Press.
Doty, P., Marmur, J., Eigner, J. & Schildkraut, C. (1960). *Proc. Nat. Acad. Sci., Wash.* **46**, 461.
Hakala, M. T. (1957). *Science*, **126**, 255.
Kirby, K. S. (1957). *Biochem. J.* **66**, 495.
Marmur, J. & Lane, D. (1960). *Proc. Nat. Acad. Sci., Wash.* **46**, 453.
Meselson, M. & Stahl, F. W. (1958). *Proc. Nat. Acad. Sci., Wash.* **44**, 671.
Meselson, M., Stahl, F. W. & Vinograd, J. (1957). *Proc. Nat. Acad. Sci., Wash.* **43**, 581.
Puck, T. T. & Fisher, H. W. (1956). *J. Exp. Med.* **104**, 427.
Rolfe, R. & Meselson, M. (1959). *Proc. Nat. Acad. Sci., Wash.* **45**, 1039.
Scherer, W. F., Syverton, J. T. & Gey, G. O. (1953). *J. Exp. Med.* **97**, 695.
Simon, E. H. (1960). Ph.D. Thesis, California Institute of Technology.
Sueoka, N. (1960). *Proc. Nat. Acad. Sci., Wash.* **46**, 83.
Sueoka, N., Marmur, J. & Doty, P. (1959). *Nature*, **183**, 1429.
Temin, H. M. & Rubin, H. (1958). *Virology*, **6**, 669.
Vogt, M. (1958). *J. Cell. Comp. Physiol.* **52**, suppl. 1, p. 271.
Watson, J. D. & Crick, F. H. C. (1953). *Cold Spr. Harb. Symp. Quant. Biol.* **21**, 91.

J. Mol. Biol. (1961) **3**, 110–111

Letters to the Editor

A New Crystalline Form of Mercuripapain

Drenth & Jansonius (1959) have reported on the unit cell of mercuripapain crystallized from 70% aqueous ethanol. The crystals appeared to be monoclinic with space group P_2. A crystalline suspension of mercuripapain has also been prepared from aqueous NaCl solution (Kimmel & Smith, 1954), but the crystals were reported to be submicroscopic in size. I have recently succeeded in growing crystals from this medium which are suitable for study by X-ray crystallography.

The crystals grew at room temperature in the dark in approximately two weeks. Single crystals were mounted in sealed capillary tubes in equilibrium with their mother liquor. Precession photographs ($\mu = 11°$) were obtained with CuKα radiation from the rotating anode X-ray tube designed by Mr. D. A. G. Broad. The crystals were orthorhombic with space group $C222_1$; $a = 44$ Å; $b = 66$ Å; $c = 124$ Å. For this space group there are 8 equivalent positions per unit cell. Since the molecular weight of papain is accurately known, the number of molecules per asymmetric unit can be calculated within an accuracy of about 30% by using density data derived from other proteins. For a number of crystalline proteins in equilibrium with their mother liquor, it is found that there are from 0·35 to 0·51 protein molecular weight units per Å^3 (Blow, 1957; Drenth & Jansonius, 1959; Kendrew & Parrish, 1956; Steinrauf, 1959). Assuming that these crystals have a similar protein content, the protein weight in the unit cell must be between 126,000 and 184,000 molecular weight units. On the basis of a molecular weight of papain of 20,600 (Hill & Smith, 1960), there is only one molecule of papain per asymmetric unit. If there were two, the protein molecular weight per unit cell would be 330,000 which is well outside this range. The electrophoretic and ultracentrifugal studies of Smith, Kimmel & Brown (1954), showed that mercuripapain crystallized as a mixture of monomer and a heavy complex with approximately six times the molecular weight of papain. Thus it appears that the crystals photographed are of the monomeric form of mercuripapain and should be suitable for more detailed studies by X-ray diffraction.

I am indebted to Dr. David Blow for encouragement and for assistance in interpreting the X-ray photographs and to Drs. Emil Smith and J. R. Kimmel for a generous gift of mercuripapain. This investigation has been aided by a grant from The Jane Coffin Childs Memorial Fund for Medical Research.

Medical Research Council Unit for
Molecular Biology
Cavendish Laboratory
Cambridge, England

Anne Stockell†

Received 10 November 1960

† Fellow of the Jane Coffin Childs Memorial Fund for Medical Research. Now at Dept. of Biochemistry, University of Cambridge, Cambridge, England.

REFERENCES

Blow, D. M. (1957). Ph.D. Thesis, University of Cambridge.
Drenth, J. & Jansonius, J. N. (1959). *Nature*, **184**, 1718.
Hill, R. L. & Smith, E. L. (1960). *J. Biol. Chem.* **235**, 2332.
Kendrew, J. C. & Parrish, R. G. (1956). *Proc. Roy. Soc.* A, **238**, 305.
Kimmel, J. R. & Smith, E. L. (1954). *J. Biol. Chem.* **207**, 515.
Smith, E. L., Kimmel, J. R. & Brown, D. M. (1954). *J. Biol. Chem.* **207**, 533.
Steinrauf, L. K. (1959). *Acta Cryst.* **12**, 77.

J. Mol. Biol. (1961) **3**, 112–116

A Comparison of Adult and Foetal Horse Haemoglobins

The foetal haemoglobins of several species have been shown to differ from adult haemoglobins. Resistance to alkali denaturation, oxygen dissociation curves, electrophoretic mobility, chromatographic behaviour and *iso*leucine content have been most often used as criteria for distinguishing between adult and foetal haemoglobins of a given species (Huisman, van der Helm, Visser & van Vliet, 1959). In addition the "fingerprint" method of Ingram (1958) has been used in comparing foetal and adult human haemoglobins (Hunt, 1959).

Adult horse haemoglobin has been studied by X-ray analysis in this laboratory, and the question arose whether foetal horse haemoglobin differed in structure from the adult form. To answer it, we have used the methods of chromatography on carboxymethylcellulose, rate of alkali denaturation, "fingerprinting," and X-ray crystallography, but observed no differences.

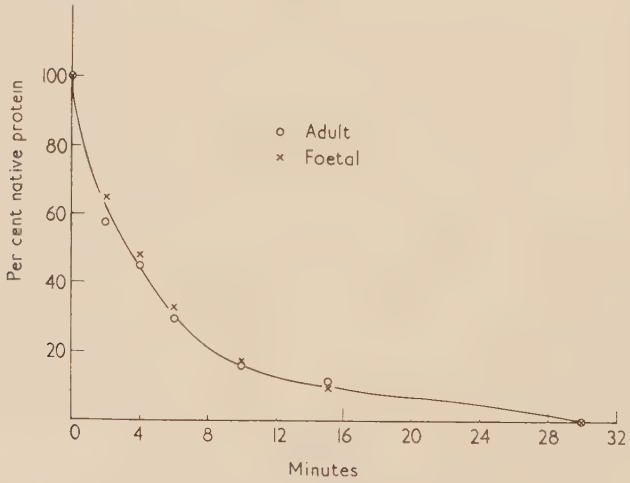

FIG. 1. Rates of denaturation of adult and foetal horse haemoglobins determined spectrophotometrically at pH 11·8.

Blood was obtained from a foetal horse at approximately 3 to 4 months gestation. Haemoglobin was prepared as described by Ingram (1955) and crystallized from 2 M-ammonium sulphate for examination by X-rays. No significant differences could be detected between the unit cell dimensions or the intensities of the X-ray reflexions when foetal and adult horse haemoglobin crystal were compared.

The absorption spectrum of horse haemoglobin denatured with alkali and reduced with $Na_2S_2O_4$ showed a peak at 559 mμ. The rate of alkali denaturation was determined on 3 ml. samples of protein diluted with 0·01 M-$NaHCO_3$ and reduced with $Na_2S_2O_4$. After an initial reading at 559 mμ, 0·02 ml. of 10 N-NaOH were added to

the haemoglobin solutions and the optical density measured as a function of time. The pH of the solutions measured with a glass electrode was 11·8. Under these conditions there is no significant difference in the rate of denaturation of the foetal and adult haemoglobins (Fig. 1).

Separation of the components of foetal horse haemoglobin on a column of carboxymethylcellulose was attempted using the system described previously (Perutz, Steinrauf, Stockell & Bangham, 1959) for adult horse haemoglobin. A "fast" and a "slow" fraction were obtained under the same conditions as for the adult protein. Of the protein recovered from the column approximately 23% emerged in the "fast" fraction and 77% in the "slow" fraction.

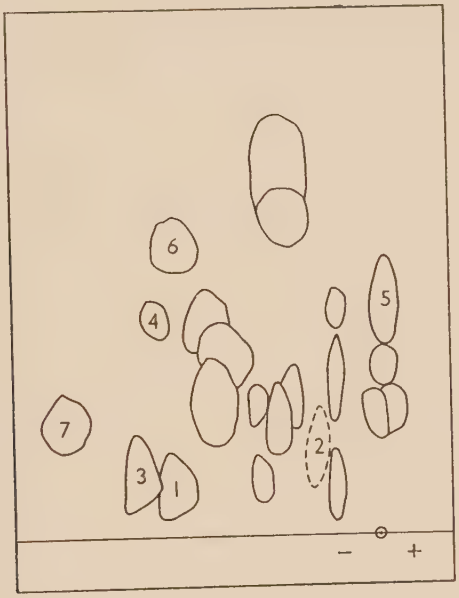

Fig. 2. Tracing of a "fingerprint" of a tryptic digest of globin from the "fast" fraction of horse haemoglobin. Peptide 2 occurs only in the "slow" fraction and is inserted in dotted lines to show its relative position on the fingerprint.

Globin prepared from each fraction was digested with trypsin and "fingerprinted" as described previously (Ingram, 1958). Comparison of the "fingerprints" of the adult and foetal species showed that the two "fast" fractions had identical patterns, as did the two "slow" fractions. In addition, specific tests for peptides containing sulphur, arginine, histidine, tyrosine and tryptophan† gave identical patterns when comparing corresponding fractions. Chymotryptic digests of the trypsin-resistant cores of each fraction followed by "fingerprinting" (Hunt & Ingram, 1958) gave patterns that were identical for all four proteins.

† The colour reactions specific for various amino acids were carried out as described by Block, Durrum & Zweig (1958) under the following authors:

ninhydrin—Toennies & Kolb, 1951.
sulphur—Toennies & Kolb, 1951.
histidine—Karler, 1952; Baldridge & Lewis, 1953.
arginine—Jepson & Smith, 1953.
tyrosine—Acher & Crocker, 1952.
tryptophan—Smith, 1953.

Amino acid analyses of the numbered tryptic peptides shown in Fig. 2 were carried out on each of the four haemoglobin fractions. In order to obtain sufficient material, each peptide was eluted with 20% acetic acid from four fingerprints of each fraction. In those fractions in which peptide 1 or 2 was missing, the area of the paper where it would be expected to appear was cut out and eluted. After removal of the solvent the peptides were hydrolysed in 6 N-HCl at 110°C for 15 hr. The amino acids were analysed by the Redfield (1953) method as modified by Hunt & Ingram (1960). The results are given in Table 1. The only differences observed were those described earlier for the

Table 1

Tryptic peptides of horse haemoglobin

Peptide	Amino acids present	Haemoglobin species			
		adult fast	adult slow	foetal fast	foetal slow
1	glu, gly, ala, his, lys	+	○	+	○
2	asp, glu, gly, val, ala, leu, his, pro, lys	○	+	○	+
3	his, gly, ala, lys	+	+	+	+
4	val, lys	+	+	+	+
5	asp, glu, gly, ser, ala, val, met, leu, phe, pro, lys	+	+	+	+
6	asp. leu, arg	+	+	+	+
7	lys	+	+	+	+

+ indicates presence of peptide
○ indicates absence of peptide

adult fractions; i.e. presence of peptide 1 and absence of peptide 2 in the "fast" fractions and absence of peptide 1 and presence of peptide 2 in the "slow" fractions. The difference between the two fractions cannot at present be explained by the substitution of one amino acid in the "fast" fraction by another in the "slow" fraction as is the case in different types of human haemoglobin (Ingram, 1959). Instead it appears that the "slow" fractions contain a peptide with at least four more amino acids than the corresponding peptide of the "fast" fractions. However, the possibility exists that peptide 2 of the "slow" fraction is present in the "fast" fraction as two peptides, one of which has not been detected on the "fingerprint." More intensive chemical studies of the fractions will be necessary to determine whether or not this is the only chemical difference between the "fast" and "slow" fractions. At any rate, in the present study no chemical differences have been observed between corresponding fractions of adult and foetal horse haemoglobins.

The finding that adult and foetal horse haemoglobins are identical was unexpected, since foetal haemoglobin is different from the adult pigment in a great variety of species, as shown, for instance, by the oxygen dissociation curves of foetal (or newly hatched) and adult haemoglobins in man, rabbit, goat, sheep, cow, chicken, frog (cited

by Barcroft, 1946), terrapin (McCutcheon, 1947) and a teleost fish (Manwell, 1957). However, a search of the literature has provided two possible exceptions. In six different species of the primitive vertebrate *Chondrichthyes* no difference was observed between oxygen dissociation curves of foetal and adult haemoglobins (McCutcheon, 1947). A study of the alkaline resistance and spreading velocity of foetal and adult types of mammalian haemoglobin showed no differences between these haemoglobins in the cat (Brinkman & Jonxis, 1936). In the mammal, transfer of oxygen from mother to foetus is not dependent solely on molecular differences in their haemoglobins, but various other factors, including haemoglobin concentration; placental circulation and blood pH are contributory (Barcroft, 1946). Thus it may be that in the horse, and possibly in other mammals as well, other factors permit the efficient transfer of oxygen from mother to foetus so that there is no need for a specific foetal haemoglobin. However the present study does not eliminate the possibility of the existence of a specific foetal horse haemoglobin prior to three months gestation.

We wish to thank Miss Eileen Blincoe for her skilful technical assistance and Dr. Roger Short, School of Veterinary Medicine, Cambridge for obtaining the foetal horse blood used in this work. This investigation has been aided by a grant from The Jane Coffin Childs Memorial Fund for Medical Research.

Medical Research Council
Unit for Molecular Biology
Cavendish Laboratory
University of Cambridge, England

Anne Stockell†
M. F. Perutz
Hilary Muirhead
Stanley C. Glauser‡

Received 10 November 1960

† Fellow of the Jane Coffin Childs Memorial Fund for Medical Research. Now at Department of Biochemistry, University of Cambridge, Cambridge, England.

‡ Postdoctoral Fellow of the National Science Foundation. Now at Department of Biology, Massachusetts Institute of Technology, Cambridge, Massachusetts, U.S.A.

REFERENCES

Acher, R. & Crocker, C. (1952). *Biochim. biophys. Acta*, **9**, 704.
Baldridge, R. C. & Lewis, H. B. (1953). *J. Biol. Chem.* **202**, 169.
Barcroft, J. (1946). *Researches on Pre-natal Life.* Vol. I, Oxford: Blackwell Scientific Publications.
Block, R. J., Durrum, E. L. & Zweig, G. (1958). *Paper Chromatography and Paper Electrophoresis.* New York: Academic Press.
Brinkman, R. & Jonxis, J. H. P. (1936). *J. Physiol.* **88**, 162.
Huisman, T. H. J., van der Helm, H. J., Visser, H. K. A. & van Vliet, G. (1959). *Abnormal Haemoglobins*, ed. by J. H. P. Jonxis & J. F. Delafresnaye, p. 181. Oxford: Blackwell Scientific Publications.
Hunt, J. A. (1959). *Nature*, **183**, 1373.
Hunt, J. A. & Ingram, V. M. (1958). *Biochim. biophys. Acta*, **28**, 546.
Hunt, J. A. & Ingram, V. M. (1960). *Biochim. biophys. Acta*, **42**, 409.
Ingram, V. M. (1955). *Biochem. J.* **59**, 653.
Ingram, V. M. (1958). *Biochim. biophys. Acta*, **28**, 539.
Ingram, V. M. (1959). *Brit. Med. Bull.* **15**, 27.
Jepson, J. B. & Smith, I. (1953). *Nature*, **172**, 1100.
Karler, A. (1952). *U.S. Atomic Energy Comm.* UCRL-1838, May 29.

McCutcheon, F. H. (1947), *J. Cell. Comp. Physiol.* **29**, 333.
Manwell, C. (1957). *Science*, **126**, 1175.
Perutz, M. F., Steinrauf, L. K., Stockell, A. & Bangham, A. D. (1959). *J. Mol. Biol.* **1**, 402.
Redfield, R. R. (1953). *Biochim. biophys. Acta*, **10**, 344.
Smith, I. (1953). *Nature*, **171**, 43.
Toennies, G. & Kolb, J. J. (1951). *Analyt. Chem.* **23**, 823.

J. Mol. Biol. (1961) **3**, 117–120

The Protein Subunit of Turnip Yellow Mosaic Virus

Turnip yellow mosaic virus (TYMV), which was isolated in crystalline form by Markham & Smith (1949), is a "spherical" ribonucleoprotein virus containing 63% protein and 37% RNA. Physico-chemical (Markham, 1951), X-ray diffraction (Klug & Finch, 1960) and electron microscope (Cosentino, Paigen & Steere, 1956; Huxley & Zubay, 1960; Nixon & Gibbs, 1960) studies have shown that the virus particle has a sedimentation coefficient of 106 s, a particle molecular weight of $5{\cdot}0 \times 10^6$ and that it consists of a "core" of RNA surrounded by a spherical shell of protein which is built up from a symmetrical assembly of structural subunits.

The present communication summarizes our results on the isolation and chemical characterization of the protein monomer which forms the structural subunit of the virus.

Isolation

The protein moiety of the virus was dissociated from the RNA, and isolated in quantitative yield by means of 67% acetic acid, as described for tobacco mosaic virus (TMV) by Fraenkel-Conrat (1957). The protein prepared in this manner proved to be an insoluble aggregate which, after oxidation with performic acid or reduction with SO_3^{2-} in 8 M-urea, gave a water soluble monomer of low molecular weight. It was subsequently found that the "native" monomer contained 4 free SH groups and that their high susceptibility to oxidation caused the protein to aggregate through the formation of intermolecular S-S linkages. This aggregation can be prevented if the cysteine residues are converted into carboxymethylcysteine residues (by reaction of the virus with iodoacetic acid in 8 M-urea at pH 8·2, *cf.* Moore, Cole, Gundlach & Stein, 1958) before proceeding with the isolation of the protein by the acetic acid method.

Characterization

The oxidized, reduced, and carboxymethylated (CM) forms of the virus protein have been examined by a variety of analytical procedures, and were found to behave as homogeneous proteins according to the following criteria:

1. The oxidized and reduced forms gave single symmetrical peaks (both with a sedimentation coefficient of 1·8 s) in the analytical ultracentrifuge and in moving boundary electrophoresis at pH's of 4·0 and 8·5. Similarly each protein gave rise to only one component when it was submitted to zone electrophoresis on starch and to chromatographic analysis on DEAE cellulose, respectively.

2. No free N-terminal amino acids were detected when the various forms of the protein were submitted to N-terminal group analysis (*cf.* Fraenkel-Conrat, Harris & Levy, 1955) by the fluorodinitrobenzene and phenyl *isc*thiocyanate methods. The absence of even trace amounts of end-group showed that the virus protein had not suffered any detectable degradation under the various conditions employed for its isolation, and that it was not contaminated to any significant extent with plant protein.

3. No free amino acids were produced when the intact virus was treated with carboxypeptidase. With the isolated protein, on the other hand, 4 different amino acids, threonine, serine, valine and aspartic acid, were released. From quantitative rate studies the C-terminal sequence of the virus protein was shown to be —Asp.Val. Thr.Ser.Thr—OH. The minimum molecular weight of the protein chain calculated from the yield of C-terminal threonine was 21,300 ± 500 (*cf.* TMV, Harris & Knight, 1952, 1955).

4. The oxidized and carboxymethylated proteins were both analysed for constituent amino acids as described by Spackman, Stein & Moore (1958), and the following amino acid composition (given to the nearest whole number of residues per mole, 21,300 g, of protein) was found: aspartic acid (12), threonine (26 to 27), serine (18), glutamic acid (15), proline (19 to 20), glycine (8), alanine (16), cysteine (as cysteic acid from oxidized protein; as carboxymethylcysteine from CM-protein) (4), valine (14 to 15), methionine (4), *iso*leucine (15), leucine (18), tyrosine (3), phenylalanine (5), tryptophan (2), lysine (8), histidine (3), arginine (3). Tyrosine and tryptophan were estimated directly in a sample of the reduced protein by a spectrophotometric method (Goodwin & Morton, 1946). The amino acid composition of the isolated virus protein agrees fairly closely with values obtained previously (M. W. Rees, unpublished results) for the whole virus. It should be noted, however, that the minimum molecular weight based on tryptophan content alone (i.e. assuming one residue of tryptophan per mole of protein) would be of the order of 10,000 rather than 20,000, but the content of arginine, histidine and tyrosine fits in well with the value of 21,300 ± 500 derived from the results of C-terminal group analysis.

Further studies, involving the characterization of peptide fragments derived from the virus protein by the action of trypsin and chymotrypsin (for example there are three unique sequences containing arginine), support the validity of the above conclusions concerning the molecular size of the protein subunit. In addition they provide the most conclusive evidence of all to support the view that all the protein subunits in the virus are *chemically* very similar, if not identical.

N-terminal sequence

The peptide pattern obtained when the soluble peptides derived from the virus protein by the action of trypsin are submitted to ionophoresis on paper at pH 6·5 is shown in Plate I. When a sample of the same peptide mixture was pre-treated with aminopeptidase (Spackman, Smith & Brown, 1955) only the acidic peptide (T_1) was found to be unchanged. T_1 was found to contain 12 amino acids in the following proportions: Asp (2), Glu (3), Ala (1), Met (1), Ileu (1), Leu (2), Arg (1), Lys (1); its resistance to aminopeptidase suggested that it did not possess a free α-NH_2 group and that consequently it might be the N-terminal peptide in the virus protein. This prediction was confirmed when experiments involving limited proteolysis with trypsin (carried out in a pH-stat and terminated when 1·0 to 1·2 μmoles of base had been consumed per μmole, 21 mg, of protein) revealed that T_1 was the only major product of reaction. The residual protein fraction was found to contain N-terminal threonine in amount corresponding to a chain weight of about 20,000, a value which is consistent with the loss of peptide T_1 from the N-terminus of the parent protein.

Peptide T_1 was broken down into smaller peptide fragments by means of chymotrypsin and pepsin, respectively, and its amino acid sequence has been provisionally

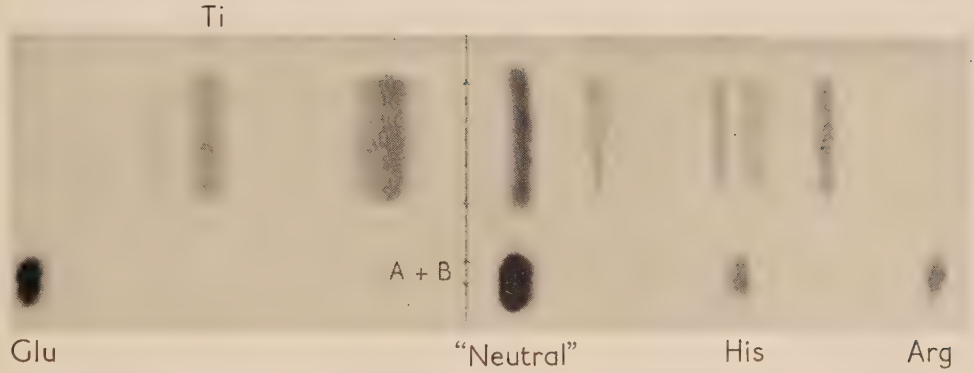

PLATE I. The peptide pattern obtained by paper ionophoresis (pyridine-acetic acid buffer, pH 6·5, 35 v/cm for 2 hr) of the pH 5 soluble fraction of a trypsin digest of TYMV protein.

[*To face page* 118

established, as shown in Fig. 1. It should be noted that the Lys.Glu bond is not hydrolysed by trypsin: presumably enzyme action is inhibited by the side chain carboxyl groups on the adjacent aspartic acid and glutamic acid residues. The presence of the N-terminal acetyl group was established when acetylhydrazide was identified among the products of hydrazinolysis of a dipeptide containing methionine and glutamic acid, isolated from a pepsin digest of T_1. In this respect TYMV resembles TMV (Narita, 1958) and cucumber-4 virus (Narita, 1959).

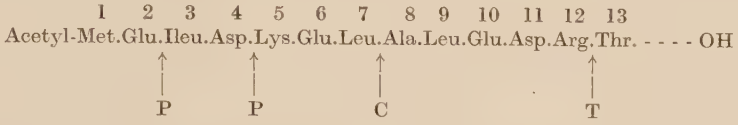

Fig. 1. The N-terminal amino acid sequence in TYMV protein. Arrows indicate points of cleavage by trypsin (T), chymotrypsin (C) and pepsin (P).

Conclusion

The structural subunit in the protein shell of TYMV has thus been shown to be a single-chain protein containing approximately 200 amino acid residues with a molecular weight of 21,300 $\pm$ 500. It seems clear, therefore, that the substructures revealed in the electron microscope and by X-ray diffraction are morphological aggregates of the chemical subunit which we have described. The results of X-ray analysis (Klug & Finch, 1960) suggest that the protein shell of the virus consists of 60 structurally equivalent subunits; and on the assumption that each of these substructures contains more than one chemical subunit it was postulated that the virus particle contains either 120 or 180 protein subunits. Electron microscope studies, on the other hand (Huxley & Zubay, 1960; Nixon & Gibbs, 1960), reveal the presence of 32 substructures, which fall into two separate groups, of 12 and of 20 structurally equivalent units respectively. This picture of the virus structure can be reconciled with the X-ray results if it is assumed that each of the 32 substructures consists of identical chemical subunits arranged either in 12 groups of 5 and 20 groups of 3, to account for a 120 unit structure, or in 12 groups of 5 and 20 groups of 6 to fit in with a 180 unit structure. Other alternative arrangements are also possible, and if, for example, the substructures seen in the electron microscope were to represent two distinct types of structural aggregates of 5 protein molecules (i.e. 20 groups of 5 assembled in one particular way, and 12 groups of 5 in another different way), then a structure composed of 160 protein subunits could also be envisaged.

On the basis of the available chemical evidence (that is, assuming a particle molecular weight of $5{\cdot}0 \times 10^6$, a protein content of 63% and a protein subunit of 21,300) it may be calculated that the virus particle contains approximately 150 protein subunits; in order to accommodate 160 or 180 subunits, the virus particle would have to possess a molecular weight of the order of $5{\cdot}3 \times 10^6$ or $6{\cdot}0 \times 10^6$ respectively. Thus, although the chemical evidence is entirely consistent with the view that the protein moiety of the virus particle consists of a regular assembly of protein molecules which are identical, at least as regards *primary* structure, further work will be necessary before the exact number of subunits can be unequivocally established.

Studies on the primary structure of the protein subunit of TYMV are being continued and will be reported in greater detail in future publications.

We are greatly indebted to Dr. R. Markham, F.R.S. for his generous co-operation in supplying us with turnip yellow mosaic virus. We also wish to thank Mr. M. W. Rees and Miss B. D. Worboys for carrying out the original amino acid analysis of the oxidized virus protein, and Mr. R. J. A. Turner for valuable technical assistance.

Department of Biochemistry
University of Cambridge
England

J. Ieuan Harris †
John Hindley ‡

Received 13 December 1960

† Member of the Scientific Staff of the Medical Research Council.
‡ Imperial Chemical Industries Fellow.

REFERENCES

Cosentino, V., Paigen, K. & Steere, R. L. (1956). *Virology*, **2**, 139.
Fraenkel-Conrat, H. (1957). *Virology*, **4**, 1.
Fraenkel-Conrat, H., Harris, J. I. & Levy, A. L. (1955). In *Methods of Biochemical Analysis*, ed. by D. Glick, vol. 2, pp. 359–425. New York: Interscience.
Goodwin, T. W. & Morton, R. A. (1946). *Biochem. J.* **40**, 628.
Harris, J. I. & Knight, C. A. (1952). *Nature*, **170**, 613.
Harris, J. I. & Knight, C. A. (1955). *J. Biol. Chem.* **214**, 215.
Huxley, H. E. & Zubay, G. (1960). *J. Mol. Biol.* **2**, 189.
Klug, A. & Finch, J. T. (1960). *J. Mol. Biol.* **2**, 201.
Markham, R. (1951). *Disc. Faraday Soc.* **11**, 221.
Markham, R. & Smith, K. M. (1949). *Parasitology*, **39**, 360.
Moore, S., Cole, R. D., Gundlach, H. G. & Stein, W. H. (1958). *Proc. IVth Int. Congress Biochem.*, ed. by H. Neurath & H. Tuppy, Symposium VIII, 52. London: Pergamon Press.
Narita, K. (1958). *Biochim. biophys. Acta*, **30**, 352.
Narita, K. (1959). *Biochim. biophys. Acta*, **31**, 372.
Nixon, H. L. & Gibbs, A. J. (1960). *J. Mol. Biol.* **2**, 197.
Spackman, D. H., Smith, E. L. & Brown, D. M. (1955). *J. Biol. Chem.* **212**, 255.
Spackman, D. H., Stein, W. H. & Moore, S. (1958). *Analyt. Chem.* **30**, 1190.

J. Mol. Biol. (1961) **3**, 121–124

The Theory of Mutagenesis

In this preliminary note we wish to express our doubts about the detailed theory of mutagenesis put forward by Freese (1959*b*), and to suggest an alternative.

Freese (1959*b*) has produced evidence that shows that for the r_{II} locus of phage T4 there are two mutually exclusive classes of mutation and we have confirmed and extended his work (Orgel & Brenner, in manuscript). The technique used is to start with a standard wild type and make a series of mutants from it with a particular mutagen. Each mutant is then tested with various mutagens to see which of them will back-mutate it to wild type.

It is found that the mutations fall into two classes. The first, which we shall call the base analogue class, is typically produced by 5-bromodeoxyuridine (BD) and the second, which we shall call the acridine class, is typically produced by proflavin (PF). In general a mutant made with BD can be reverted by BD, and a mutant made with PF can be reverted by PF. A few of the PF mutants do not appear to revert with either mutagen, but the strong result is that no mutant has been found which reverts identically with both classes of mutagens, and that (with a few possible exceptions) mutants produced by one class cannot be reverted by the other.

Freese also showed that 2-aminopurine falls into the base analogue class, and that most (85%) spontaneous mutants at the r_{II} locus were not of the base analogue type. We have confirmed this and shown that they are in fact revertible by acridines. We have also shown that a number of other acridines, and in particular 5-aminoacridine, act like proflavin (Orgel & Brenner, in manuscript).

Freese has produced an ingenious explanation of these results, which should be consulted in the original for fuller details. In brief he postulated that the base analogue class of mutagens act by altering an A—T base-pair on the DNA (A = adenine, T = thymine) into a G—C pair, or *vice versa* (G = guanine, C = cytosine, or, in the T even phages, hydroxymethylcytosine). The fact that BD, which replaces thymine, could act both ways (from A—T to G—C or from G—C to A—T) was accounted for (Freese, 1959*a*) by assuming that in the latter case there was an error in pairing of the BD (such that it accidentally paired with guanine) while *entering* the DNA, and in the former case after it was already in the DNA.

Such alterations only change a purine into another purine, or a pyrimidine into another pyrimidine. Freese (1959*b*) has called these "transitions." He suggested that other conceivable changes, which he called "transversions" (such as, for example, from A—T to C—G) which change a purine into a pyrimidine and *vice versa*, occurred during mutagenesis by proflavin. This would neatly account for the two mutually exclusive classes of mutagens, since it is easy to see that a transition cannot be reversed by a transversion, and *vice versa*.

We have been led to doubt this explanation for the following reasons.

Our suspicions were first aroused by the curious fact that a comparison between the *sites* of mutation for one set of mutants made with BD and another set made with PF (Brenner, Benzer & Barnett, 1958) showed there were no sites in the r_{II} gene, among the samples studied, common to both groups.

Now this result alone need not be incompatible with Freese's theory of mutagenesis, since we have no good explanation for "hot spots" and this confuses quantitative argument. However it led us to the following hypothesis:

that acridines act as mutagens because they cause the insertion or the deletion of a base-pair.

This idea springs rather naturally from the views of Lerman (1960) and Luzzati (in preparation) that acridines are bound to DNA by sliding *between* adjacent base-pairs, thus forcing them 6·8 Å apart, rather than 3·4 Å. If this occasionally happened between the bases on *one* chain of the DNA, but not the other, during replication, it might easily lead to the addition or subtraction of a base.

Such a possible mechanism leads to a prediction. We know practically nothing about coding (Crick, 1959) but on most theories (except overlapping codes which are discredited because of criticism by Brenner (1957)) the deletion or the addition of a base-pair is likely to cause not the substitution of just one amino acid for another, but a much more substantial alteration, such as a break in the polypeptide chain, a considerable alteration of the amino acid sequence, or the production of no protein at all.

Thus one would not be surprised to find on these ideas that mutants produced by acridines were not capable of producing a slightly modified protein, but usually produced either no protein at all or a grossly altered one.

Somewhat to our surprise we find we already have data from two separate genes supporting this hypothesis.

(1) The *o* locus of phage T4 (resistance to osmotic shock) is believed to control a protein of the finished phage, possibly the head protein, because it shows phenotypic mixing (Brenner, unpublished). Using various base analogues we have produced mutants of this gene, though these map at only a small number of sites. We have failed on several occasions to produce any *o* mutants with proflavin. On another occasion two mutants were produced; one never reverted to wild type, while the other corresponded in position and spontaneous reversion rate to a base analogue site. We suspect therefore that these two mutants were not really produced by proflavin, but were the rarer sort of spontaneous mutant (Brenner & Barnett, unpublished).

(2) We have also studied mutation at the *h* locus in T2L, which controls a protein of the finished phage concerned with attachment to the host (Streisinger & Franklin, 1956).

Of the six different spontaneous h^+ mutants tested, all were easily induced to revert to *h* with 5-bromouracil (BU)†. This is especially significant when it is recalled that 85% of the spontaneous r_{II} mutants could not be reverted with base analogues (Freese, 1959*b*).

We have also shown (Brenner & Barnett, unpublished) that it is difficult to produce h^+ mutants from *h* by proflavin, though relatively easy with BU. The production of *r* mutants was used as a control.

It can be seen from Table 1 that if the production of h^+ mutants by BU and proflavin were similar to the production of *r* mutants we would expect to have obtained $\frac{57 \times 26}{108} = 13 h^+$ mutants with proflavin, whereas in fact we only found 1, and this may be spontaneous background.

† (Added in proof.) Five of these have now been tested and have been shown not to revert with proflavin.

Let us underline the difference between the *r* loci and the *o* and *h* loci. The former appear to produce proteins which are probably *not* part of the finished phage. For both the *o* and the *h* locus, however, the protein concerned forms part of the finished phage, which presumably would not be viable without it, so that a mutant can be picked up only if it forms an *altered* protein. A mutant which deleted the protein could not be studied.

TABLE 1

	r	h^+
BU	108	57
Proflavin	26	1

It is clear that further work must be done before our generalization—that acridine mutants usually give no protein, rather than a slightly modified one—can be accepted. But if it turns out to be true it would support our hypothesis of the mutagenic action of the acridines, and this may have serious consequences for the naïve theory of mutagenesis, for the following reason.

It has always been a theoretical possibility that the reversions to wild type were not true reversions but were due to the action of "suppressors" (within the gene), possibly very closely linked suppressors. The most telling evidence against this was the existence of the two mutually exclusive classes of mutagens, together with Freese's explanation.

For clearly if the forward mutation could be made at one base-pair and the reverse one at a different base-pair, we should expect, on Freese's hypothesis, exceptions to the rule about the two classes of mutagens. Since these were not found it was concluded that even close suppressors were very rare.

Unfortunately our new hypothesis for the action of acridines destroys this argument. Under this new theory an alteration of a base-pair at one place *could* be reversed by an alteration at a different base-pair, and indeed from what we know (or guess) of the structure of proteins and the dependence of structure on amino acid sequence, we should be surprised if this did not occur.

It is all too easy to conceive, for example, that at a certain point on the polypeptide chain at which there is a glutamic residue in the wild type, and at which the mutation substituted a proline, a further mutation might alter the proline to aspartic acid and that this might appear to restore the wild phenotype, at least as far as could be judged by the rather crude biological tests available. If several base-pairs are needed to code for one amino acid the reverse mutation might occur at a base-pair close to but not identical with the one originally changed.

On our hypothesis this could happen, and yet one would still obtain the two classes of mutagens. The one, typified by base analogues, would produce the substitution of one base for another, and the other, typically produced by acridines, would lead to the addition or subtraction of a base-pair. Consequently the mutants produced by one class could not be easily reversed by the mutagens of the other class.

Thus our new hypothesis reopens in an acute form the question: which back-mutations to wild type are truly to the original wild type, and which only appear to be

so? And on the answers to this question depend our interpretation of all experiments on back-mutation.

We suspect that this problem can most easily be approached by work on systems for which the amino acid sequence of the protein can be studied, such as the phage lysozyme of Dreyer, Anfinsen & Streisinger (personal communications) or the phosphatase from *E. coli* of Levinthal, Garen & Rothman (Garen, 1960). Meanwhile we are continuing our genetic studies to fill out and extend the preliminary results reported here.

Medical Research Council Unit
for Molecular Biology
Cavendish Laboratory

Pathology Laboratory
both of Cambridge University
England

S. Brenner
Leslie Barnett
F. H. C. Crick

Alice Orgel

Received 16 December 1960

REFERENCES

Brenner, S. (1957). *Proc. Nat. Acad. Sci., Wash.* **43**, 687.
Brenner, S., Benzer, S. & Barnett, L. (1958). *Nature*, **182**, 983.
Crick, F. H. C. (1959). In *Brookhaven Symposia in Biology*, **12**, 35.
Freese, E. (1959*a*). *J. Mol. Biol.* **1**, 87.
Freese, E. (1959*b*). *Proc. Nat. Acad. Sci., Wash.* **45**, 622.
Garen, A. (1960). 10th Symposium *Soc. Gen. Microbiol.*, London, 239.
Lerman, L. (1961). *J. Mol. Biol.* **3**, 18.
Streisinger, G. & Franklin, N. C. (1956). In *Cold Spr. Harb. Sym. Quant. Biol.* **21**, 103.

INSTRUCTIONS TO AUTHORS

1. The *Journal of Molecular Biology* will publish papers on the nature, production and replication of biological structure at the molecular level, and its relation to function. Suitable subjects are sub-cellular organization: molecular genetics: structure and replication of viruses: molecular structure of muscle, nerve and other tissues: structure of proteins, nucleic acids, carbohydrates, lipids, etc., and their synthetic analogues, as investigated by X-rays, light absorption and other methods: problems of inter- and intra-molecular energy transfer. The Journal will not as a rule publish papers when the subject matter is outside the fields defined above; however, when the subject matter borders on molecular biology and is of special interest in relation to molecular biology such papers may be published when space permits.

2. The Journal will also publish Letters to the Editor (averaging 1000 words), and occasional review articles dealing with a more restricted or immediately topical field than those in review journals. (The Editor should be consulted in advance by anyone who considers submitting such a review.)

3. Communications will often describe results obtained by specialized techniques (for example, those of X-ray crystallography and of genetics), and it is most important that technical terms should be avoided or be clearly defined; in any event the actual results obtained and their implications should be described in a way which does not demand from the reader specialized knowledge of a particular technique.

Papers should contain the maximum density of information compatible with clarity, and every sentence should be scrutinized to ensure that its presence is essential. Authors should include enough experimental details to enable others to repeat the work (these may be printed in small type). Careful preparation of manuscript will aid prompt publication; carelessness will cause delay.

4. *Submission of Manuscripts.* Manuscripts should be sent to Dr. J. C. Kendrew, Peterhouse, Cambridge, England, or to any member of the Editorial Board. The submission of manuscript will be taken to imply that the material is original, and that no similar paper has been or will be submitted for publication elsewhere.

Papers will normally be published in English. Manuscripts in French or German will also be accepted, though the use of these languages may cause delay in publication.

5. *Copy.* Papers should be typewritten in double spacing *throughout* (including tables, legends and footnotes), on one side of quarto paper, with a margin of 1 inch all round. The position of tables and illustrations should be indicated in the text; tables and legends for illustrations should be typed separately at the end of the manuscript. All pages should be numbered serially and securely fastened together. Two copies of each manuscript should be submitted, together with three copies of the summary (see § 6) and four copies of the abstract (see § 9).

A short running title of not more than 40 characters (including spaces), suitable for page headings, should be indicated if the full title is longer than this.

The name of the laboratory where the work has been done should be indicated on the title page. All typescript (including the references) should be carefully checked for errors.

6. *Summary.* A summary will be printed at the head of all papers (excluding Letters to the Editor); this should generally not exceed 300 words, and should be intelligible to the general reader without reference to the main text. Abbreviations should be avoided. Summaries of papers to be printed in French or German will be in English, and should be longer (up to 1000 words) for the benefit of readers not familiar with these languages.

7. *Conventions.* The conventions used in current issues of the Journal for headings, references, etc., should be followed in preparing manuscripts. References should be listed alphabetically at the end of the paper, and abbreviated according to the *World List of Scientific Periodicals*, except that for periodicals with English names capital initial letters should be used throughout. Citations in the text should read thus: Smith, Brown & Robinson (1957), or (Smith, Brown & Robinson, 1957). When a citation has more than two authors, the names of all of them should be given at the first citation (except for more than five authors), and on subsequent citations thus: (Smith *et al.*, 1957). The conventions (Brown, 1957*a*), (Brown, 1957*b*) should be used where more than one paper by the same author(s) has appeared in one year. Volume number should be indicated in the typescript thus: **35.**

Footnotes should be avoided whenever possible. Essential footnotes should be indicated by superscript figures in the text and collected on a single page placed at the end of the manuscript.

Customary abbreviations will be used; authors may refer to *Chemical Abstracts*, to the *Biochemical Journal*, **66**, 8 (1957), and to *Notes on the preparation of papers to be communicated to the Royal Society* (1951). Certain non-standard abbreviations of chemical substances are convenient, and those listed in the *Journal of Biological Chemistry* may be used without further definition (e.g. DNA, ATP). Any other abbreviations of this kind should be used sparingly, and must be defined in a footnote at the point in each manuscript where the first such abbreviation occurs.

8. *Illustrations.* It is often convenient to make a *drawing* two or three times larger than it will appear in the Journal, but very large drawings should be avoided and it will be helpful if drawings and illustrations are submitted on quarto (or 8½ by 11 inch) sheets. Drawings should be made in Indian ink on tracing linen, Bristol board, or faintly blue-lined graph paper; the originals should always be submitted with the manuscript, since photo-prints of drawings often cannot be reproduced satisfactorily. Explanations should, as far as possible, be placed in the legend; the drawing itself should contain a minimum of lettering, and this should be inserted lightly in *blue pencil*, in lower case except for proper names, when a capital should be used. It should be remembered that drawings will be reduced to a size not exceeding 8 by 5 inches, and that the final thickness of the lines should be 0·25 to 0·3 mm. If a curve is given merely for illustrative purposes no cross-lines are needed, but the axes should be graduated at intervals, and the diagram should be boxed in. Where possible, related diagrams should be grouped to form a single figure, and should be prepared uniformly and *on the same scale.* Where appropriate and possible a scale should be included in the illustration itself; the magnification may be noted in the legend and adjusted after reduction by the blockmaker.

Whenever possible *photographs* should be supplied the same size as they are to appear in the Journal. The page area available for a plate is 5 by 7 inches or, at the most, 6 by 8 inches.

Line drawings will be referred to as Figure 1, Figure 2, etc., and half-tone blocks as Plate I, Plate II, etc. The name(s) of the author(s) and the number should be written on all illustrations, together with the indication "Top" if necessary. Besides the original illustrations *one* duplicate set must accompany the second copy of the manuscript; these may be photo-prints, and need not be of the same quality as the originals but must be clear and legible. If *oversize* original drawings are submitted (bigger than 8½ by 11 inches) they must be accompanied by *two* sets of small photo-prints.

9. *Abstracts.* Authors should send with their manuscripts *four copies* (typewritten in double spacing) of an abstract, in about 100 words, suitable for inclusion in biological abstracting journals. This abstract will not appear in the *Journal of Molecular Biology* but will be scrutinized by the Editors before being passed for publication. The abstract should outline as briefly as possible the results and definitive conclusions of the work. Details of methods are generally not required.

The abstract should be headed as follows: title of paper; name(s) of author(s); *J. Mol. Biol.*, followed by space for the year, volume and page references; abbreviated postal address (including country of origin) to which applications for reprints may be sent. For example: The isolation and properties of deoxyribonucleoprotein particles containing single nucleic acid molecules. G. Zubay & P. Doty. J. Mol. Biol. . . . . (Dept. of Chem., Harvard Univ., Cambridge, Mass., U.S.A.). —text of abstract follows.

10. *Reprints.* Fifty reprints of each paper will be supplied free of charge; additional copies may be purchased.

COMPARATIVE BIOCHEMISTRY

A Comprehensive Treatise

Edited by **Marcel Florkin,** *University of Liège, Belgium*
and **Howard S. Mason,** *University of Oregon Medical School*

In 6 volumes. **Comparative Biochemistry** provides a sound, critical and provocative summary of present knowledge in the field. It presents a systematic comparison of the biochemical phenomena of life throughout the phylogenetic scale. Most of the chapters, each of them by an expert, are pioneering efforts in the field.

Subscription Prices on orders for the complete set

Volume 1 Sources of Free Energy

1960, 590 pp., illus., $18.00, 128s. 6d. Subscription Price: $16.00, 115s. 8d.

A Guide to the Nomenclature and Classification of Organisms, by HELEN A. STAFFORD
An Introduction to Comparative Biochemistry, by MARCEL FLORKIN and HOWARD S. MASON
Thermodynamics of Living Systems, by HENRY EYRING, RICHARD P. BOYCE, and JOHN D. SPIKES
Comparative Mechanisms for Fatty Acid Oxidation, by P. K. STUMPF and G. A. BARBER
Phosphoric Acid Anhydrides and Other Energy-Rich Compounds, by F. M. HUENNEKENS and H. R. WHITELEY
Onium Compounds and Their Biological Significance, by G. L. CANTONI
Phototropism and Phototaxis, by KENNETH V. THIMANN and GEORGE M. CURRY
The Distribution and Evolution of Visual Systems, by GEORGE WALD
Aerobic and Anaerobic Reactions of Inorganic Substances, by CLAUDE FROMAGEOT and JACQUES C. SENEZ
Comparative Biochemistry of Glycolysis, by ERNEST BUEDING and EMMANUEL FARBER
Comparative Biochemistry of Electron Transport and Oxidative Phosphorylation, by ERIC E. CONN
Utilization of Thermal Energy by Living Organisms, by MARY BELLE ALLEN
AUTHOR INDEX—SUBJECT INDEX.

Volume 2 Free Energy and Biological Function

1960, 685 pp., illus., $20.00, 143s. Subscription Price: $18.00, 128s. 6d.

Free Energy and the Biosynthesis of Phosphates, by M. R. ATKINSON and R. K. MORTON
Utilization of Free Energy for the Biosynthesis of Saccharides, by LUIS F. LELOIR, CARLOS E. CARDINI, and ENRICO CABIB
Comparative Biochemistry of Free Energy Utilization for the Biosynthesis of Peptides and Proteins, by H. CHANTRENNE
Ammonia Metabolism and Urea Biosynthesis, by PHILIP P. COHEN and GEORGE W. BROWN, JR.
Muscular Contraction, by S. V. PERRY
Other Mechanisms Producing Movements, by HARTMUT HOFFMANN-BERLING
Active Transport, by B. ANDERSEN and H. H. USSING
Balance of Water, Electrolytes and Nonelectrolytes, by FREDA BROWN and W. D. STEIN
The Mechanisms of Osmoregulation, by J. SHAW
Nerve Conduction and Electrical Discharge, by MICHEL A. GEREBTZOFF and ERNEST SCHOFFENIELS
Bioluminescence, by E. NEWTON HARVEY
AUTHOR INDEX—SUBJECT INDEX.

Volumes 3 and 4: Constituents of Life

Volumes 5 and 6: Cells and Organisms

Detailed information available upon request

ACADEMIC PRESS, New York and London

INTRODUCTION TO A

Submolecular Biology

by **Albert Szent-Györgyi**

The Institute for Muscle Research at the Marine Biological Laboratory
Woods Hole, Massachusetts

1960, 135 pp., illus. (including one colour plate), $5.00, 40s.

CONTENTS

Part 1: General Considerations

Introduction

Why Submolecular Biology? The Problem Is Stated

The Energy Cycle of Life

Units and Measures: Redox Potentials. Ionization Potentials and Electron Affinities. Orbital Energies

Electronic Mobility: Electromagnetic Coupling. Resonance Transfer of Energy. Semiconduction. Charge Transfer

Problems of Charge Transfer

Three Examples of Charge Transfer: Quinone-Hydroquinone. Riboflavine (FMN) and Serotonin. Cortisone I_2

Miscellaneous Remarks: Water. Ions. Metachromasia

Part 2: Problems and Approaches

On the Mechanism of Drug Action

On ATP

On the Chemistry of the Thymus Gland

The Living State.

"*. . . Szent-Györgyi's work has throughout been marked by its bold advances, by its intuitions which, seeming rash at the time, are afterwards found to be verified.*"
—NATURE

"*Every three or four years Albert Szent-Györgyi puts out a little book, full of theories, experiments, and speculations about the nature of biological processes as they currently seem to him. These books are invariably entertaining and stimulating, for no one is quicker than Szent-Györgyi to invent a new theory, or more spritely than he is in presenting it.*"

—JOURNAL OF CHEMICAL EDUCATION

ACADEMIC PRESS, *New York and London*
111 Fifth Avenue, New York 3, New York
17 Old Queen Street, London, S.W.1

In 2 Volumes

Mechanisms in Radiobiology

Edited by **MAURICE ERRERA**

Faculté des Sciences, Université Libre de Bruxelles

and **ARNE FORSSBERG**

Radiobiologiska Institutionen, Karolinska Institutet, Stockholm

THESE two volumes cover the principles of radiobiology, including allied areas in radiation physics and radiation chemistry. The treatise presents a comprehensive treatment of the field, with major emphasis upon those subjects for which review articles are not readily available elsewhere.

Each author is actively engaged in research within the particular field of his contribution. The co-operation of these scientists has produced a work useful as a handbook for the student and as a reference work for the advanced research worker.

Volume 1: GENERAL PRINCIPLES

Spring 1961, about 500 pp., illus., approx. $15.00, 107s. 6d.

Physical principles of Radiation Action
By F. HUTCHINSON and E. POLLARD, Yale University

Target Theory and Radiation Effects on Biological Molecules
By F. HUTCHINSON and E. POLLARD, Yale University

Radiation Chemistry
By EDWIN J. HART and ROBERT L. PLATZMAN
Argonne National Laboratory

The Biochemical Lesion *in Vivo* and *in Vitro*
By M. G. ORD and L. A. STOCKEN
University of Oxford

Cytological Effects
By THEODORE N. TAHMISIAN, Argonne National Laboratory

Effects on Subcellular Units and Free-Living Cells
By TIKVAH ALPER, Hammersmith Hospital, London

Radiation Genetics
By SHELDON WOLFF, Oak Ridge National Laboratory

The Induction of Mutations as a Method in Plant Breeding
By ÅKE GUSTAFSSON, Forest Research Institute, Stockholm

AUTHOR INDEX—SUBJECT INDEX.

Volume 2: MULTICELLULAR ORGANISMS

1960, 395 pp., illus., $13.00, 93s.

General Biology: Gametes, the Developing Embryo, and Cellular Differentiations
By ROBERTS RUGH, College of Physicians and Surgeons, Columbia University

General Biology: The Adult Organism
By CARL-JOHAN CLEMEDSON, University of Göteborg, and ARNE NELSON, The Research Institute of National Defense, Stockholm

Immunology
By MILAN HAŠEK and ALENA LENGEROVÁ, Institute of Biology, Czechoslovak Academy of Sciences, Prague

Mechanisms of Protective and Sensitizing Action
By LORENTZ ELDJARN and ALEXANDER PIHL, The Norwegian Radium Hospital, Oslo

Recovery and Therapy of the Irradiated Organism
By D. W. VAN BEKKUM, Medical Biological Laboratory of the National Defense Research Council T.N.O., Rijswijk (Z.H.), The Netherlands

AUTHOR INDEX—SUBJECT INDEX.

ACADEMIC PRESS, New York and London

ED IN STACKS
18 APR '63 F
1 May 61R 225
9 MAY 63F
28 JUN 61R
20 Feb 64F
26Feb64F
1640
1 Dec 64F
14 MAY 65F
6 May '65F

CONTENTS

PARK, R. B. and PON, N. G., Correlation of Structure with Function in *Spinacea oleracea* Chloroplasts 1

FREDERICQ, E., OTH, A. and FONTAINE, F., The Ultraviolet Spectrum of Deoxyribonucleic Acids and their Constituents 11

LERMAN, L. S., Structural Considerations in the Interaction of DNA and Acridines 18

SUEOKA, N., Variation and Heterogeneity of Base Composition of Deoxyribonucleic Acids: A Compilation of Old and New Data . . . 31

ELLIOTT, G. F. and LOWY, J., Low-Angle X-Ray Reflections from Living Molluscan Muscles 41

GROSSMAN, L., LEVINE, S. S. and ALLISON, W. S., The Reaction of Formaldehyde with Nucleotides and T2 Bacteriophage DNA . . 47

SYMONDS, N. and RITCHIE, D. A., Multiplicity Reactivation after the Decay of Incorporated Radioactive Phosphorus in Phage T4 61

RICH, A., DAVIES, D. R., CRICK, F. H. C. and WATSON, J. D., The Molecular Structure of Polyadenylic Acid 71

KLUG, A., HOLMES, K. C. and FINCH, J. T., X-Ray Diffraction Studies on Ribosomes from Various Sources 87

SIMON, E. H., Transfer of DNA from Parent to Progeny in a Tissue Culture Line of Human Carcinoma of the Cervix (Strain He La) 101

Letters to the Editor—

A New Crystalline Form of Mercuripapain, A. STOCKELL . . . 110

A Comparison of Adult and Foetal Horse Haemoglobins, A. STOCKELL, M. F. PERUTZ, H. MUIRHEAD and S. C. GLAUSER . . . 112

The Protein Subunit of Turnip Yellow Mosaic Virus, J. I. HARRIS and J. HINDLEY 117

The Theory of Mutagenesis, S. BRENNER, L. BARNETT, F. H. C. CRICK and A. ORGEL 121

Printed in Great Britain at the Aberdeen University Press